CHARACTERISATION OF HEART AND DIAPHRAGM MOTION: IMPLICATIONS FOR TREATMENT PLANNING AND DELIVERY OF RADIOTHERAPY FOR VENTRICULAR TACHYCARDIA

A thesis submitted to the University of Manchester for the degree of

Doctor of Clinical Science

in the Faculty of Biology, Medicine and Health

2021

JAMES M. DANIEL

SCHOOL OF MEDICAL SCIENCES

Contents

Word count: 28479

Glossary

AAD Anti-Arrythmic Drug.

AP Anterior-Posterior (anatomical direction).

AV Atrioventricular.

CBCT Cone-Beam CT.

CoD Centre of Displacement.

cpm cycles per minute.

CT Computed Tomography.

DIBH Deep Inspiration Breath Hold.

DICOM Digital Imaging and COmmunications in Medicine.

EAM Electroanatomical Mapping.

ECG Electrocardiogram.

ECGI Electrocardiographic Imaging.

EM Electromagnetic.

EP Electrophysiology.

ES Electrical Storm.

FFT Fast Fourier Transform.

GTV Gross Tumour (or Target) Volume.

ICD Implantable Cardioverter Device.

IDE Investigations Device Exemption.

ITV Internal Target Volume.

LAD Left Anterior Descending (artery).

LR Left-Right (anatomical direction).

LV Left Ventricle.

LVEF Left Ventricular Ejection Fraction.

MDT Multi-Disciplinary Team.

MI Myocardial Infarction.

MLC Multi-Leaf Collimator.

MRI Magnetic Resonance Imaging.

OAR Organ At Risk.

PET Positron Emission Tomography.

PORV Planning Organ at Risk Volume.

PTV Planning Target Volume.

RF Radio-Frequency.

SABR Stereotactic Ablative Radiotherapy.

SAE Serious Adverse Event.

SBRT Stereotactic Body Radiotherapy.

SCD Sudden Cardiac Death.

SGRT Surface Guided Radiotherapy.

SI Superior-Inferior (anatomical direction).

SPECT Single Photon Emission CT.

STAR STereotactic Arrhythmia Radioablation.

US Ultrasound.

VA Ventricular Arrhythmia.

VT Ventricular Tachycardia.

Abstract

A novel use of radiotherapy to treat ventricular tachycardia (VT) delivers large doses of high energy x-rays to the VT substrate: STereotactic Arrhythmia Radioablation (STAR). This treatment has only recently been developed for the clinic and characterisation of cardiac and respiratory motion in radiotherapy is of interest but is not yet generally achieved.

This thesis examines the feasibility and utility of tracking both the distal electrode (pacing lead tip) of implantable cardioverter defibrillators (ICD) and the diaphragm in STAR patients. Lead tip and diaphragm positions are identified in kV planar images of the patient, acquired on a linear accelerator before radiotherapy treatment planning and immediately prior to treatment, and tracked across the image sequence. A coding toolkit was constructed for this purpose and was shown to track both objects to within 0.5 mm. The toolkit was able to identify the pacing lead tip and diaphragm in 84.9% and 94.4% of tested frames respectively. Data from 3 patients treated at South Tees NHS Hospitals Foundation Trust showed full amplitude lead tip displacements of 7.7 $\pm$ 1.4, 9.7 $\pm$ 1.9 and 11.8 $\pm$ 2.3 mm in left-right, ant-post and sup-inf directions respectively. Average diaphragm displacement amplitudes were reported between 8.5 and 22.3 mm.

The utility of the data was shown to be twofold: (1) providing quantitative information useful for informing target volume dimensions, and (2) providing quality assurance at the point of delivery; ensuring that cardiac and respiratory cycles are the same when delivering radiotherapy as when it was planned. This work provides a method for assessing cardiac and respiratory motion in STAR patients, and discusses the implications of those measured data. This methodology may be applicable to other treatment sites such as lung tumours.

Declaration

No portion of the work referred to in this thesis has been submitted in support of an application for another degree or qualification of this or any other university or other institute of learning.

Copyright statement

Dedication and acknowledgements

Dedications

This work is firstly a grateful response to God: Soli Deo gloria. He created all thing, including the human heart.

Second, my family. My wife, Hannah, who has put up with more than she should have had to. You have made this possible and you deserve a lot of the credit for it. My wonderful children Abigail and Rebecca and their HSST counterparts, Molly and Joel: thanks for being there and making me smile while I was so busy.

Third, my colleagues. A lot of my work has been covered by a number of you. Thank you for your kind support and encouragement.

My supervisors: Kevin Burke and Phil Whitehurst. Thank you for your ideas and discussions throughout this process. Thanks to the consultants: Clive Peedell, Matt Bates and Andy Thornley for your time and energy and getting me involved in a thoroughly interesting and exciting new treatment technique.

Acknowledgements

Thanks to Tony Alton for help with producing figures and for the work on the moving platforms which were used to validate this work. Thanks to Darren Thompson for your help making it all work.

Thanks to the Center for Noninvasive Cardiac Radioablation (CNCR) at Washington University in St. Louis. Your support in helping us begin treating this exciting technique and the advice and support you have provided to me in producing this thesis is much appreciated.

Thanks also to everyone who has read and commented on this thesis and given feedback. Special thanks to my Dad and my colleagues Dan Johnson and Helen Curtis in this regard.

The author

Academic Qualifications

- MSc in Medical Physics, *University of Leeds*, 2007
- MSci in Theoretical Physics, *Durham University*, 2005

Publication history

1. Wood, A., Aynsley, E., Kumar, G. and others, Long term overall survival outcomes in patients with early stage, peripherally located Non-Small Cell Lung Cancer, treated with Stereotactic Ablative Radiotherapy (SABR) in a non-academic cancer centre, *Clinical Oncology*, 2020
2. Daniel, J & Tudor, GST 'Tomotherapy' chapter in 'Physical aspects of quality control in radiotherapy – 2nd edition', 2018, *IPEM*
3. Richmond N.D., Daniel J.M., Whitbourn J.R., Greenhalgh A.D. Dosimetric characteristics of brass mesh as bolus under megavoltage photon irradiation. 2016 *British Journal of Radiology*, 89
4. Richmond, N., Allen, V., Daniel, J., Dacey, R., & Walker, C. A comparison of phantom scatter from flattened and flattening filter free high-energy photon beams. 2015 *Medical Dosimetry*, 40(1), 58-63
5. Daniel, J. & Tudor, GST Tomotherapy quality assurance survey in the UK. 2014 *Scope*, June (p16-20)

Conference attendance

During the production of this work, the author attended and the Symposium for Non-invasive Radioablation (SNORAD) in 2018 and presented work at SNORAD 2019. The

author also attended the European Society for Radiotherapy and Oncology (ESTRO) meeting in 2019.

Research and clinical work

This work was completed during a 2 year period of time throughout which the author continued to work as a consultant clinical scientist in Radiotherapy Treatment Planning and Brachytherapy at South Tees Hospitals NHS Foundation Trust and introduced the cardiac SABR (STAR) treatment technique into use. 3 patients were treated for VT with STAR during this time.

Authorship

The author of this thesis was first author on both papers presented here. Patient data was gathered during the introduction of STAR at South Tees Hospitals NHS Foundation Trust which was proposed and implemented by the cardiology and oncology specialists with support from radiographers and clinical scientists including the author. All data gathering and analysis was done by the author in the workplace with supervisory support and comment.

Rationale for journal format

This thesis is submitted in journal format. The papers included in this thesis have been prepared for publication but, at the time of thesis submission, they have not yet been sent to journals for acceptance. Some aspects of the journal articles have been removed for the thesis such as the acknowledgements specific to the papers (now included in the 'Dedication and acknowledgements' section of this thesis) and references have been combined for the whole thesis in one section. Referencing has been made consistent throughout the thesis.

Journal format was approved by the thesis supervisors on the basis that the research was suited to being separated into publishable sections focused on firstly the technical elements of the work and subsequently their application to clinical work. This thesis was prepared as part of the Higher Specialist Scientist Training (HSST) scheme, run by the National School for Healthcare Science (NSHCS), which aimed for clinical scientists to participate actively in research and publish data. Journal format is therefore also appropriate from the perspective of making the research ready for publication.

A section is included at the end of the thesis to provide space outside of publication for critical analysis of the work; to comment on the success or otherwise of the methods used and what research opportunities might follow from this work.

Thesis overview

Over the last decade, an entirely new approach to treating ventricular tachycardia has been developed using high energy x-rays delivered by the same treatment platforms commonly used to treat cancers. The heart is rarely targeted for radiotherapy: little work has so far been done to control for its motion during treatment. Image guidance is frequently used to ensure that patients are positioned correctly for treatment and often to ensure that internal motion is consistent and accounted for in radiotherapy treatment plans. As yet, x-ray image guidance, used to create cone beam CT images of the patient on c-arm linear accelerators, has not been exploited to observe the motion of the metal components of pacemaker devices as a surrogate for cardiac motion. This thesis explores the possibility of such an approach and reports the experience of a three patient group, treated at South Tees Hospitals NHS Foundation Trust.

The first section of the thesis describes the disease and the development of the novel use of radiotherapy to treat it. The research in this thesis is contextualised through discussion of the technical elements of delivering radiotherapy to the heart. Subsequently, comparison is given of this work with other publications which have used imaging technology to extract motion data in the heart and other organs for radiotherapy treatment. The research aims are stated at the conclusion of the first chapter.

Two papers prepared for journal submission are then presented. The first describes the work done to create a methodology for extracting cardiac and respiratory motion data from linear accelerator image guidance data. The second analyses the data from three patients and discusses the implications of these data for radiotherapy treatment. Finally, the work is critically analysed with discussion on what other research opportunities are created through this work.

Two appendices are included. The first provides an overview of the code written by the author of this thesis to facilitate its methodology. The second lists the modules which are combined with this thesis for the completion of the DClinSci.

1 Literature review and research context

1.1 Introduction

1.1.1 Ventricular tachycardia

Ventricular arrhythmias (VA) contribute to between 30 - 75% of all sudden cardiac deaths[1] which total more than 100,000 per year in the UK, according to the British Heart Foundation[2]. Ventricular tachycardia (VT) is one such VA and can be caused by cardiomyopathy, structural or ischaemic heart disease, heart failure and some genetic conditions. VT is most commonly produced by electrical signals being misdirected through diseased tissue (re-entrant circuits), as well as by triggered activity and automatic activation of the muscle[3]. Its symptoms include dizziness, fainting and chest pain and the condition frequently leads to cardiac arrest and death. Management options include pharmacotherapies (such as beta-blockers, anti-arrhythmia drugs and electrolytes), device therapy including implantable cardioverter defibrillators (ICDs), catheter ablation (normally of cardiac scar tissue) or less frequently, anti-arrhythmic surgery[4].

Patients who suffer from VT are at risk of death and are likely to encounter mobility issues and some socially restrictive impacts of having the disease[5]. They will typically experience a number of approaches to treating and managing the condition and, in general, do not have multiple decades of life expectancy remaining. However, if the condition can be effectively treated with the patients less reliant on drugs and ICD shocks, quality of life can be improved[6].

Current standards of care for VT include catheter ablation procedures. Numbers of these procedures are increasing but have poor rates of completely eradicating the condition (around 50 to 60%)[7][8]. Importantly, VT episodes and the number of ICD shocks needed by the patients are associated with progression of heart failure and increased mortality[9]. Whether these events cause mortality or just degrade quality of life, treatment options are important to these patients.

1.1.2 Heart function and VT pathology

The heart is the organ responsible for pumping blood through the circulatory system. It comprises 4 chambers: the left and right atria, and the left and right ventricles (see figure 1). Blood is taken from the body and directed into the lungs for re-oxygenation. The re-oxygenated blood is then returned to the body via the left ventricle which is the largest and most muscular of the 4 chambers.

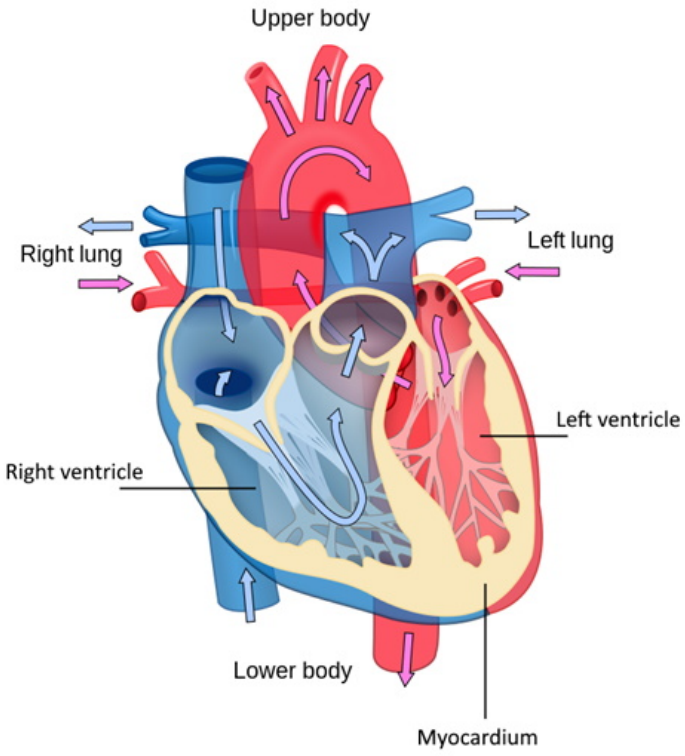

Figure 1: Basic anatomy of the heart. Image taken from https://commons.wikimedia.org/wiki/File:Heart_diagram_blood_flow_en.svg with additional annotation by the author of this work

The walls of the ventricles consist of a series of layers: the epicardium (outer wall), myocardium (muscle) and endocardium (inner wall). The myocardium is the muscle which provides the action by which blood is moved through the heart and body and contains the conduction pathways for the electrical signals to create the correct order of contractions for cardiac function. Electrical signals, generated in the sino-atrial (SA)

node in the wall of the right atrium pass through the atria and into the ventricles via the bundle of His. Signals then proceed to the heart's apex and round to the remainder of the ventricular walls.

In patients with ventricular tachycardia, the myocardial conduction pathways are altered in some way, via previous myocardial infarction or some other damage. For example, scarred tissue can create errant electrical pathways in which the signals 're-enter' causing the tissues to contract too quickly; electrical signals no longer proceed along the correct paths and the ventricle does not effectively push blood out of the heart.

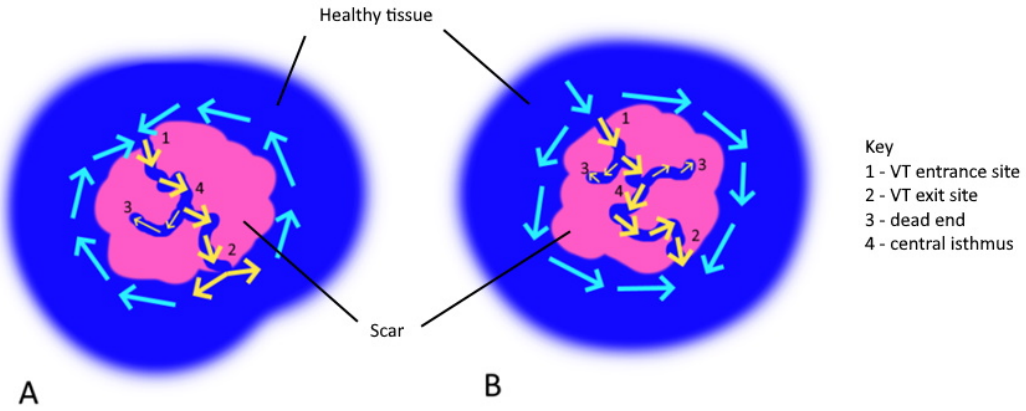

Figure 2: two examples of VT originating from scar tissue. Background blue represents healthy myocardium. Pink is scar tissue with conducting channels running through it. Turqoise arrows show conduction around the scar and yellow arrows show conduction in the scar. In the first case (A) the signal exiting the scar loops back to the entrance point creating a re-entrant circuit. In the second (B), the electrical signal processes through the central isthmus of the scar, arriving later than the signal processing around the scar and causing late activation which is seen as late potentials in the ECG. Image based on personal communication with Matthew Bates and Geoff Lee[10].

VT circuits are complicated and contain multiple entrance and exit points and dead ends[11]. Figure 2 shows 2 examples of VT caused by scar tissue in the myocardium. The application of energy via heat, radiation or chemical methods can alter these errant

pathways sufficiently to disrupt these circuits, allowing for the correct conduction of electrical pathways.

1.1.3 Radiotherapy as a treatment option

A recent clinical development in this field is to use high energy x-rays delivered by linear accelerators, commonly used to treat cancers, in order to modify tissues in which re-entrant circuits occur as an alternative to catheter ablation: STereotactic Arrhythmia Radioablation (STAR)[12]. This concept, sometimes referred to as cardiac SABR[i] (stereotactic ablative radiotherapy), was endorsed to the cardiology and oncology global communities in 2017 with a publication in which 5 patients were treated with STAR and followed up for 12 months[13]. The advantages of using radiotherapy to treat cardiac arrhythmias are that it is both non-invasive and able to treat more deeply than catheter ablation; it has the potential to achieve superior control of the condition.

Radiotherapy is used to treat other, non-oncological indications, for example: "trigeminal neuralgia, arteriovenous malformations, seizures and psychiatric disorders in the brain ... renal artery hypertension [and] back pain"[14]. Radiotherapy delivered via radioactive sources is also used in treating coronary arteries to prevent recurrent restenosis following stenting procedures for heart disease[15]. However, for radiotherapy delivered using high energy x-rays at a distance, the heart is generally regarded as an avoidance structure[16], except in the case of cardiac sarcomas which are relatively rare. The range of toxicities encountered with using radiation to treat disease could possibly make STAR, on balance, an unsuitable approach to improve quality of life in certain patient groups. On that basis, the global community has approached the idea of using STAR tentatively and with great deliberation. At the time of writing, approximately 100 patients have been reported to have received treatment worldwide.

In general, STAR is currently only used for patients who have not responded to

[i]SABR refers to radiotherapy treatments which are generally to small volumes and constructed of fewer fractions with a larger dose per fraction than conventional radiotherapy. STAR has begun development at a time when single fraction lung SABR has also begun to develop general interest in the radiotherapy community.

pharmacotherapies and are limited in their treatment options[17] or are experiencing significant and potentially life-threatening impact from their VT[7,18]. As it is not yet a commissioned part of healthcare services, where it is used it is seen as an experimental treatment with the aim of improving quality of life. Clinical trial data is needed to demonstrate short- and long-term clinical benefit and risk to patients before STAR would be a feasible tool for general use in the population of those patients with VT.

1.1.4 Purpose of this literature review

This review contextualises and rationalises the research presented in this thesis. As the field of STAR is relatively nascent, it was possible to include a majority of publications on the subject in an historical timeline of the field (section 1.2) which sets out the context in which this research has been undertaken. Section 1.3 includes technical aspects of treatment planning for STAR and section 1.4 includes previous research on relevant topics and highlights the novel elements of this thesis.

1.2 Technique development

1.2.1 Technique origins

In 2010, the results of a novel study were reported by a research group in California who had hypothesised that mapping cardiac anatomy could lead to new approaches to treating arrythmias using radiotherapy[19]. Sharma et al. used Harford-Sinclair mini-swine without arrythmias in that study in order to determine whether precisely delivered radiotherapy could generate lesions in the pigs' myocardia. The study was able to demonstrate electrical block[ii] produced near the cavotriscuspid isthmus and AV node leading the authors to conclude that radiotherapy delivery might open up avenues of treatment for various arrythmias including ventricular tachycardia. The study was performed using CyberKnife (Accuray, CA) and made reference to the Synchrony res-

[ii] 'Block' in this context refers to prevention of the electrical signal being carried through that part of the tissue

piratory gating system which was used to compensate for the breathing cycle of the test animals. Cardiac motion was identified as an issue; an 'integrated target volume' (ITV) was used based on a cardiac gated computed tomography (CT) image acquired prior to planning which ensured that all the specified heart tissue would be treated even while it moved.

Among others, this study helped set up an entirely new paradigm for creating an effect in the heart; an original idea which has lead to much interest globally and phase II trials being set up within a decade. Themes were identified in this work which have propagated to the rest of the literature on the subject of radiotherapy to electrically modify the heart: *motion tracking*, *treatment dose* and *planning techniques*. These topics are covered through the remainder of this review.

Further work has been carried out in swine models. Blanck et al.[20] demonstrated in 9 mini-pigs that radiation doses above 32.5 Gy can induce transmural scarring in cardiac muscle; analogous with catheter ablation techniques. More recently, Refaat et al.[21] demonstrated feasibility for CT guided AV radioablation. They used doses of 35 Gy in 3 pigs and 40 Gy in 2 pigs. Each pig eventually developed complete AV block with timings of between 55 and 235 days following treatment but no effect was seen in any pig immediately after ablation. They found no evidence of any toxicity in any of the pigs prior to euthanasia.

Relevant questions which this research raises are:

1. Do human hearts scar at the same radiation levels found in pigs?

2. At what dose level is the desired effect generated? What dose is required to create electrical block and prevent VT from occuring?

These questions have yet to be fully answered.

1.2.2 Initial experiences in humans

Just 2 years after the publication of Sharma et al.[19], the first reported in-man use of STAR was performed at Stanford, CA with the CyberKnife delivery platform[12,22]. A 71 year old man who had had various interventions since cardiac bypass grafting in 2000 was consented for treatment with radiotherapy under a 'compassionate-use' agreement from the FDA and was treated in October 2012. A temporary pacing wire was placed in his right ventricular apex as an imaging marker for tracking of the target with respiratory and cardiac motion. The prescribed dose was 25 Gy to the 75% isodose line, resulting in a maximal dose of 33 Gy to parts of the scar. After treatment, the patient experienced a ten-fold reduction in the number of VT events (as reported by the patient's ICD). A reduction in adjacent medication was attempted but failed.

In addition to the study by Loo et al.[12], another centre also produced single-patient case studies for STAR but in the Czech Republic. Cvek et al.[23] published a case study of a 72 year old female patient who was treated with 25 Gy, again using CyberKnife (Accuray, CA). The patient had exhausted all other forms of treatment and catheter ablations had failed because of the thickness of her myocardial wall. The patient was diagnosed with ventricular tachycardia and the treatment volume was on the base of the left ventricular wall. After 120 days of follow-up, the patient had no recorded episodes of arrhythmia on their ICD and no toxicities were recorded except for a slightly elevated troponin T serum level (an indicator of cardiac damage) after 10 days.

1.2.3 CyberHeart

An early development was the creation of CyberHeart Inc. which owns the intellectual property for a piece of planning software (CardioPlan) and was initially concerned with facilitating STAR treatment using CyberKnife. CyberHeart contributed to a number of early studies noted here and has recently (in 2019) been purchased by Varian, one of the 2 main global linac providers[24]. It is not yet clear how the purchase of CyberHeart by Varian will impact STAR treatments globally, but a large scale trial is currently

being set up with Varian sponsorship.

The first-in-man reported use of radiotherapy for an arrhythmia in the atria (atrial fibrillation (AF)) was reported in 2016 in the form of a poster at ASTRO (American Society for Radiation Oncology) by a group which included members affiliated with CyberHeart Inc., Christus Muguerza (Mexico) and Stanford University (CA, USA)[25]. Using a process similar to that reported in Loo et al.[12], the 59 year old male patient had fiducial-guided motion tracked (Synchrony) CyberKnife treatment with 25 Gy prescribed to the 75% isodose. The patient was discharged a day after treatment and was said to experience no complications of treatment alongside an improved quality of life. In an abstract for the CARDIOSTIM conference in 2017, the same patient was reported to have recurred for AF between 6 and 12 months following treatment and "elected to continue a medical rhythm control strategy"[26].

This later abstract[26] described the CyberHeart group's experience with 5 patients receiving treatment under investigational device exemption (IDE) rules from the FDA and with ethical approval (4 with VT and the previously described AF patient). One patient could not have a tracking fiducial implanted and so could not be treated. While this abstract represents the work by CyberHeart who were affiliated with Accuray and made sole use of Accuray's CyberKnife system, they make a point of saying "A variety of radiosurgery platforms can be used" in the introduction. In earlier publications, CyberKnife was more frequently cited as the tool of choice[12,23,27] largely because of its respiratory motion tracking system. More recently, the field has included CyberKnife and c-arm linear accelerator (linac) approaches alike[13,28]. Data is being gathered by several phase II trials at the time of writing (see section 1.2.8 for details), one specifically set up by the CyberHeart group, and it will be of interest to see whether there are differences between them in terms of patient outcomes.

1.2.4 New England Journal of Medicine article

Initial positive experiences with STAR contributed to the first multi-patient study published in the *New England Journal of Medicine*[13] which presented the first data from a non-CyberKnife centre delivering radiation to treat (only) VT and also included the largest follow up of any published data at that time (12 months). Patients were treated between April and November 2015 and were included in the study if they had experienced at least 3 episodes of ICD-treated VT in the previous 3 months, were on antiarrhythmia medication and had had at least one previous ablation attempt with a catheter. Patients that had undergone placement of a left ventricular assist device were excluded. Treatment was delivered on TrueBeam (Varian) linacs: the first study not to use respiratory tracking and so the treatment volumes were based on a combination of cardiac and respiratory motion.

Results from the 5 patient study showed a 99.9% reduction in VT burden across the patient group considering the number of events experienced by all patients in the 3 months prior to ablation and the number of events recorded during the next year. The year long follow up excluded an initial 6-week 'blanking period' determined to be sufficient to allow the treatment impact of the radiation to be developed in patients' hearts. These figures can be represented as events per patient week and then taken as a ratio of each other to get the reported figures. The reported 99.9% figure might be reconsidered as one patient died 3 weeks after treatment and was the greatest contributor of VT events prior to treatment (>4000 in the 3 months before treatment) and potentially could have been excluded from the results. Also included is the patient who experienced the second greatest number of VT events before ablation (>2000 in the 3 months before treatment) who required re-ablation with a catheter only 4 weeks post radioablation. If both of these patients are removed from the figures, the reduction in VT burden is 98.6% after the blanking period for the 3 patient group. This figure perhaps better reflects the fact that VT events do continue to occur in some patients following STAR. The paper concludes that the treatment was not yet suitable for

clinical use at the time of publication due to its novelty and potential for harm and that a phase I / II trial is being set up (ENCORE-VT) (see later discussion on trials, including updated results from ENCORE-VT) in order to develop the evidence base.

The global impact of the 2017 Cuculich et al.[13] paper was significant. The authors brought together the global community in 2018 at the SNORAD conference (Symposium for Noninvansive Radioablation) at which the details of an upcoming phase II/III trial for STAR were discussed. The paper was also translated into German[29] and was highlighted in Nature[30]. As the technique had now been demonstrated to be feasible with treatment technology more commonly available than CyberKnife, many more centres started to take an interest in this novel approach to treating arrhythmias, including three in the UK at which at least nine patients have now been treated.

1.2.5 Published reviews

Prior to the NEJM article's publication, a review of the use of radiotherapy to treat cardiac arrythmias was published[14]. The paper opens by specifying "a robotic arm mounted delivery system" while later referring to any number of potential radiosurgery platforms. The review was not comprehensive and gave more space to describing radiotherapy to a cardiology audience than the specifics of arrhythmia ablation. The review refers to the small number of patients treated to the date of writing (8 patients by late 2017) and they comment that no radiation-induced complication had yet been observed in the treated patients. In describing the potential for harm, they say that "intracardiac injury may include valvular injury, premature coronary disease, pericardial disease, and rarely intramyocardial injury. Phrenic nerve injury, esophageal injury, and pulmonary injury are also possible"[14].

A subsequent review of the field provides a more comprehensive discussion of the technical approaches and challenges in the field of cardiac radioablation[31]. Published prior to the ENCORE-VT trial result, Sharp et al.[31] describe the results of ten globally treated patients and provide advice on treatment:

- A multi-disciplinary team (MDT) approach should be adopted with care of the patient passing between cardiology and oncology departments
- Electroanatomic mapping (EAM) should be used as a gold standard for targeting
- Non-invasive mapping techniques can be useful as complimentary to other imaging tools for targeting, particularly where single-beat arrhythmias occur

In a review of the year 2018 for cardiology, the NEJM paper was highlighted as opening new doors for therapy and the ENCORE-VT study was also picked out[32].

1.2.6 Further experiences

Following the 2017 publication of Cuculich et al.[13], more clinical and theoretical work has been carried out including:

- A case report on a patient treated for electrical storm (ES)[7]
- MLC tracking for linac based STAR[33]
- In-depth reviews of radioablation sites[34]
- Reported results from trials[5]
- Proof of principle for c-arm linac delivery of radiation gated for cardiac phases[35]

The STAR technique has also started to be mentioned in the wider context of VT treatment. A review on the treatment of VT was presented in *Trends in Cardiovascular Medicine*[36] with a short mention of the potential for VT radioablation and a reference to the Cuculich et al.[13] paper. However, the mention demonstrates the difficulties in communication between EP and oncology: as an example, STAR is referred to as "low dose"[36]. Even in the context of lung SABR doses being ∼50 to 60 Gy, it is a somewhat distorted view to suggest that a 25 Gy single exposure to the heart is "low dose"; the wider cardiology audience is not yet familiar with radiotherapy terminology, something

the SNORAD conference aimed to address. The review references both the Cuculich et al.[13] paper and the ENCORE-VT trial.

The ES case report by Jumeau et al.[7] is built on the success of the NEJM publication[13], citing the 99.9% result previously discussed. Jumeau et al.[7] report that 3 patients were treated at their centre with radioablation to the heart since 2017 treated with a procedure similar to that of Cuculich et al.[13] but focus on the detail of just the first: a patient admitted following ES. The patient was receiving multiple shocks daily and had a catheter ablation procedure which needed to be abandoned due to hypotension. Following the catheter ablation attempt the patient's left ventricular ejection fraction (LVEF), a measure of the percentage of the blood in the left ventricle which is pushed out during one contraction, dropped to 15%. Following radioablation, the patient stopped requiring ICD shocks completely (4 months of follow up reported) and was discharged 2 months after ablation. Extubation was only possible 3 days after ablation and the authors comment that the rapid response of the treatment and the data from Cuculich et al.[13] have contributed towards determining that the mechanisms for STAR are not simply late-induced radiation fibrosis but have a more significant instant component of response. They note that "Some hints might be provided by in vivo data by [Fajardo and Stewart[37]] that showed in experimental models the presence of inflammatory cells in heart tissues within hours after heart irradiation."[7].

An expert opinion piece was published just prior to the Jumeau et al.[7] report in which the statement was made that "the delayed effect of SBRT makes it unsuitable for rapid control of ventricular arrhythmias, such as VT storms."[9]. It is a demonstration of the as-yet unpredictable and nascent characteristics of the field that such a statement was immediately proved incorrect by the first-in-man case of STAR for ES[7] and soon after in a German report[18]. The opinion piece brought the topic to a widely-read and highly rated journal for arrhythmia: *Arrhythmia and electrophysiology review.*

1.2.7 Global efforts

Three hospitals in the UK (Middlesbrough, Sheffield and Newcastle)[38][39] have collectively initiated treatment of patients under compassionate use grounds as the evidence for such treatments to be commissioned by NICE (National Institute for Clinical Excellence) is lacking. In collaboration with each other, they have presented at SNORAD 2019 and the UK SABR consortium 2019.

German groups have recently published their first case studies of patients treated with STAR. The first publication represents the first use of STAR for ventricular fibrillation (VF) storm and one of the youngest patients to receive STAR at 53 year old[18]. The patient needed deep sedation and was refractory to all other treatments but responded well to STAR and was able to be revived, hence the somewhat dramatic title of the paper: "Risen from the dead: Cardiac stereotactic ablative radiotherapy as last rescue in a patient with refractory ventricular fibrillation storm". Another patient, a 78-year old male patient with recurrent episodes of VT who was receiving shocks and anti-tachycardia pacing despite medication, also received 25 Gy in a single fraction to a PTV of 42 cc [28]. While the patient responded to STAR well, he unfortunately died due to complications from a clostridium difficile (c-diff) infection which led to cardiac failure.

An unusual case study was presented by a Chinese group in 2019 of a young (29 year old) patient experiencing VT secondary to a "massive cardiac lipoma (3.5 x 4.0 x 6.5 cm) in the left ventricular wall" [40]. Resection, catheter ablation and medication were attempted but without long term success. A PTV of approximately 71 cc was treated with 24 Gy in 3 fractions with CyberKnife. The authors cite their 'more cautious' dose regime as due to this being the first treatment of its kind (VT secondary to lipoma) and to preserve the function of the left anterior descending artery (LAD). After 4 months of follow up, the patient had been VT free and without complication.

The Princess Margaret hospital in Toronto have treated a case of right ventricular tachycardia[34] and found that 6 days after SABR a reduction of VT burden from 600

events per hour to 0 using a prescription of 25 Gy in a single fraction to a volume of 52 cm^3.

1.2.8 Trials

There have been several trials developed for STAR to date:

- CyberHeart's Cardiac Arrhythmia Ablation Treatment: Patients With Refractory Ventricular Tachycardia[41].
    - Single arm, prospective trial looking at the safety and efficacy of the CyberHeart CardioPlan software in 10 patients. Patient selection includes ages over 60 and with refractory VT. Primary endpoint is safety: measures of SAEs over 30 days and between 31 days and 1 year post treatment. Secondary endpoints include number of shocks and episodes of VT. The estimated primary completion date was December 2018 and the follow up period is 12 months. Results are not yet published.
- ENCORE-VT (Electrophysiology-Guided Noninvasive Cardiac Radioablation for Ventricular Tachycardia)[42]
    - Single arm, phase I/II trial of electrophysiologic guided SABR ablation of the heart in 19 patients. Patient selection includes minimum VT burden requirements and at least one failed catheter ablation. Primary endpoints are safety (number of grade 3 CTCAE v4 (Common terminology criteria for adverse events) or higher SAEs in the first 90 days) and number of participants who experience a reduction in VT burden during the 6 months after treatment. Secondary endpoints include overall survival and a reduction in ICD shocks.
- UCLA's trial[43]

- Single arm, phase I/II trial to determine the maximal tolerated dose to SABR in the heart in 30 patients. Patient selection includes refractory VT. Primary endpoints are shock free survival time and number of patients needing cardiac transplant.

- Germany (RAVENTA, NCT03867747)[44]
  - Single arm trial aiming to show that STAR can be performed safely with no intervention during the first 30 days after treatment in 20 patients. Patients must have myocardial scar and require ICD intervention. Primary endpoint is 30 day adverse event and SAE reports. Secondary endpoints include 12 month SAEs, reduction of VT over 12 months, overall survival and quality of life questionnaires.

- Italy (STRA-MI-VT, NCT04066517)
  - Single arm study looking at 12 month safety and efficacy of STAR in 15 patients. Secondary endpoints include total mortality, quality of life questionnaires and cardiac functional changes. Patients must have refractory VT.

- Canada (STAR VTM, NCT04065802)
  - Single arm study looking at safety and efficacy of STAR in 20 patients, specifically without the use of a multi-electrode vest. Primary endpoints of reduction in VT burden over 6 months and safety endpoint of 90 days after treatment including pericarditis, radiation pneumonitis and changes in cardiac function.

This list is not exhaustive but indicates the level of global interest in this technique.

Initial results of ENCORE-VT were published with a median follow-up time of 13 months for 19 patients[5]. One patient died shortly after ablation but due to an

unrelated accident and was recorded as an 'unlikely' (in terms of the likelihood that it was caused by the treatment) grade 5 SAE. Of the other 18 patients, 4 patients experienced grade 1 or 2 adverse events (nausea, fatigue, hypotension and pneumonitis as examples) which were generally resolved with medication or without intervention. Only one grade 3 SAE was recorded as 'probable' (pericarditis). One other grade 3 SAE was recorded as 'possibly' linked to the treatment (heart failure). 1 year survival was 72% which the authors claim to be similar to the life-expectancy of the patient group without intervention although this was not tested in this single-arm trial.

From the efficacy end-point perspective, a reduction in VT burden was observed in 17 of the 18 patients who survived more than 6 months. The secondary end-points were for a reduction of >50% and >95% in VT episodes and these end-points were achieved by 17 (94%) and 11 (61%) patients respectively. Quality of life was reported by patients to have improved during the 6 months follow up in both "social functioning" and "health change". In the "general health" category, there was no significant difference between baseline and 6 months following treatment[5].

Longer term follow up with the patients in the ENCORE-VT study was published in late 2019[45]. Median follow-up for surviving patients was 24.1 months with 2-year survival reported as 58%. There were no deaths definitively linked to the treatment; 4 deaths were listed as possibly related. It was shown that the effect of treatment persisted in 78% of patients at 2 years post ablation[46]. 2 specific SAEs were noted beyond 2 years post-ablation: a grade 3 pericardial effusion and a grade 4 gastropericardial fistula.

The ENCORE-VT trial has demonstrated that non-invasive radioablation for patients suffering VT who are treatment refractory and have exhausted other treatment options is a potentially safe and effective method to reduce the number of VT events experienced which is known to improve quality of life for these patients. It is now possible to aim for larger, multi-centre trials to grow the body of evidence to potentially demonstrate to regulatory bodies and clinical guidance and commissioning councils

that STAR may be an effective tool for inclusion in the VT treatment toolkit.

A response to the ENCORE-VT trial was included in the same journal issue in which the results were published[47]. This editorial piece describes the success and questions opened up by the study and is cautiously optimistic about the result although the authors comment that "As with any novel therapy, a case report, a small case series, and now a small prospective study are certainly not enough to demonstrate with confidence the safety and efficacy of this novel therapy."[47]. In particular, the editorial is sceptical about the use of the non-invasive mapping procedure used by Robinson et al.[5] for providing targeting of the VT substrate. The authors make the point that the technology is quite untested, as well as the fact that targeting the VT substrate (even when done precisely) may not be the optimal treatment strategy. In previous correspondence, the authors had somewhat presumed CyberKnife technology to be the only viable method of delivery[14] while in the editorial piece in 2019 the focus had shifted to target delineation rather than technical delivery. This gives the sense of how the broadening field was impacting on the cardiology community who were, and still are, learning an entirely new paradigm for treatment.

Finally, the editorial indicates the need for dose-finding studies noting that 25 Gy has been adopted almost universally for this purpose[iii]. Future research should focus on exactly where the dose is being delivered and ask whether there is a required minimum dose level in parts of the tissue that needs to be met in order to generate the treatment effect.

1.2.9 Discussion and conclusions

The field of radioablation for various cardiac arrhythmias has been extant for ten years. Theoretical work has been done in swine, several small scale case reports have been published and now trials are starting to deliver results. It is as yet unclear whether there is a long term future for this technique for several reasons:

[iii] Better reporting of dose-volume data would help as it is not always clear what the minimum and maximum doses received by the target volume are

- Technical challenges and the difficulty in translating good practice between centres with different equipment profiles
- Long term efficacy
- Long term side effects

However, interest in the field is starting to increase with articles seen in the highest level journals such as the *New England Journal of Medicine* and *Nature*. Much more work is likely to be done in the field before conclusions are drawn.

From a technical perspective, it is clear that there is difficulty in removing the common radiotherapy (oncology) language from what is a non-oncological field: for example, unlike in oncology, it is not necessarily a problem to miss part of the target as the desired treatment impact may still be achieved. This is an opportunity for research questions:

- Should the whole scar (or indicated treatment region) be treated or can partial volumes which 'cut' through part of the volume be used to the same effect?
- Covering the whole treatment region is being done according to best radiotherapy practice: adding margins to ensure that a certain percentage of the volume receives a certain percentage of the dose. If partial volumes produce positive results, could margins be reduced to produce the same treatment effect?
- As dose distribution ranges are high with parts of the treatment volume receiving doses in excess of 130% of that prescribed, is 25 Gy enough to have an effect or is it the 30 Gy and above dose that are impacting on the disease? Dose escalation or fractionation studies might be productive in demonstrating the potential for achieving similar outcomes with a reduced risk of negative side-effects.
- Safety is clearly an important issue. As shown by ENCORE-VT, some patients are surviving beyond the 2 year point and can, albeit rarely, experience serious

negative side effects of treatment. How can organs at risk be best protected given the lack of certainty around the geography of treatment volumes?

Significant work in the form of phase II and above trials is required to answer these questions. Various locations around the world are putting such trials together. Speaking a common language between cardiology, oncology and the technical teams (physicists and radiographers) delivering these treatments will be critical to achieve useful results. The team at Washington University at St Louis have begun developing that language at the SNORAD conferences and continual communication will be needed to ensure the field continues to develop.

1.3 Technical elements of STAR

Several authors of case reports and trials have described the techniques used to deliver STAR and there have been a number of specific planning studies published as well. In this section, the techniques are described and details supplied with regard to the following planning parameters:

- Delivery platform and motion management approaches
- Planning technique and target volumes
- Organs at risk and toxicity

1.3.1 Delivery platform

Delivery platforms that have been used to deliver STAR to actual patients are: CyberKnife (Accuray, CA), Elekta Versa linear accelerators (Elekta, SE) and Varian linear accelerators (Truebeam and Edge) (Varian, CA). Other platforms have been proposed for the use but not yet employed, such as the MRI linac[48] and carbon-ion therapy units[49]. No published literature yet exists for proton beam therapies except for a recent study in swine[50]. Planning systems that have been used to develop plans

for cardiac SABR include Eclipse (Varian, CA), Pinnacle (Philips, NL), MultiPlan (Accuray, CA) and TRiP4D (GSI, DL). As yet, no published data is known to exist for Elekta treatment planning systems (OMP, Monaco) (Elekta, SE), Tomotherapy (Hi-Art, Precision) (Accuray, CA) or RayStation (RaySearch, SE).

The CyberKnife platform operates as a linear accelerator mounted on a robotic arm and has the option of either multi-leaf collimators (MLC) (M6 model) or irises of varying diameter (G4 model). Individual beamlets are planned and the beam is directed from a wide range of angles towards the target. The Synchrony tracking system has been used for CyberKnife deliveries of radioablation to the heart[12 19 23]. It works by internally tracking a fiducial marker with x-ray images while simultaneously tracking the patient's surface as a marker for respiratory motion. While of clear benefit, Synchrony, or indeed any motion tracking system is not capable of reducing margins to zero although it has been used to do so in at least one case[7].

A comparison of the abilities of CyberKnife with other treatment units and planning systems is given by Weidlich et al.[51] who conclude that the CyberKnife system presented the best opportunity to spare nearby critical structures and had the advantage of online tracking. The authors, whose conflicts of interest include working for CyberHeart, also used a zero margin for respiratory motion for CyberKnife which is likely to be too small given the work of Fahimian et al.[52] (see section 1.4).

The Varian Truebeam and Edge linear accelerators are not equipped to perform motion tracking in the same way as CyberKnife[iv], although respiratory gating solutions exist which would shut the beam off when the target moves out of field. In general, this leads to wider margins being applied to targets when CyberKnife is not being used[13].

The problem of motion management is far from resolved in STAR and a detailed look at this problem is presented in section 1.4: Motion modelling and tracking.

[iv]However, a group in Australia have been working on MLC tracking of targets and have applied their research to the topic of cardiac arrhythmias[33].

1.3.2 Planning technique and target volumes

In this section, the approaches used for treating the target in the ENCORE-VT trial are noted and the volumes of tissue treated in ENCORE-VT and other publications are compared.

It should be noted that drawing clear conclusions about planning and treatment techniques is not yet possible given the low numbers of patients that have been treated globally. A range of planning and treatment approaches for 4 groups, each of which has recorded 10 or more patient treatments, have been reported[53]. While there appear to be a range of outcomes, the difference in reported timescales and the associated range of different side effects, combined with the small patient numbers, make such an assertion impossible at this early stage in human trials of STAR.

Cuculich et al.[13] used both static field planning approaches and non-coplanar volumetric modulated arc therapy (VMAT) in the Pinnacle planning system; the same approaches were used during the ENCORE-VT trial which has been the only trial yet to report results[5]. Oesophagus, lungs, stomach and spinal cord were included as organs at risk with tolerances set as maximum and near maximum dose limits[42]. Patients were immobilised with BODYFIX 'VacBags' (Elekta, SE) which ensure the patient can be located on the treatment unit in the same position that they were imaged in for treatment planning. The target, identified as the VT exit site and the scar using a number of different imaging modalities, was constructed as a 'Gross Target Volume' (GTV) which was outlined on a free-breathe CT scan and then grown to an 'Internal Target Volume' (ITV) using combined cardiac and respiratory motion from a 4D CT scan. Finally the ITV was grown by 5mm in all directions to create a 'Planning Target Volume' or PTV. Note that the use of 'GTV' is a term adopted from the oncology world and needs some translation into the STAR setting. In cancer treatment, the complete treatment of the GTV is usually associated with intended treatment outcomes. In STAR, however, the entire GTV does not need to be irradiated in order to achieve the desired treatment effect. A STAR GTV will usually include some region of tissue that, if irradiated, will

result in a change to the VT pathology. Due to the inherent uncertainty in defining the VT exit site, the GTV will commonly also include a volume of tissue that does not need to be irradiated to achieve the treatment goal.

Cuculich et al. refer to the 'ablation volume'[13] which has caused some confusion with other authors. Jumeau et al.[7] for example compare ablation volumes from their 3 patient study (19, 21, 35 cc) with the range of ablation volumes from Cuculich et al. (17 to 81 cc) and note that theirs are smaller. However, the difference from a planning perspective is even more significant. It appears that Jumeau et al.[7] are presenting PTV data: they outline the VT substrate and add "no additional margin ... for planning"[7]. Conversely, Cuculich et al.[13] have presented GTV data and this point is clarified in the ENCORE-VT trial report as "median planning target volume was 98.9 cc (range, 60.9 - 298.8)."[5]. These are large differences: volumes are almost 5 times larger and the equivalent ratio of sphere diameters is approximately 1.7. It is assumed that this difference is due in part because CyberKnife was used with target tracking[7], but also must demonstrate a difference in the volume of tissue identified for treatment in each case.

At SNORAD 2019, there was discussion regarding future trials. An exclusionary point was suggested that planning target volumes in excess of 200 cc should be rejected from trials as the evidence suggests that larger treatment volumes might be associated with lower survival rates[54].

There have been significant efforts to apply non-invasive mapping technologies for detecting VTs in patients; invasive cardiac catheter mapping techniques carry inherent risk[55] and it can be a challenge to capture certain arrhythmias which are transient or infrequent[56]. The difficulty with non-invasive methods is in solving the "inverse problem of electrocardiography"[57] as regularisation of the signals can fundamentally change the interpretation of the ECG data[58].

There are at least 2 commercial solutions to implementing multiple-lead ECG technology for non-invasive arrhythmia mapping: the BioSemi 256 lead vest, now owned

by Medtronic and referred to as the CardioInsight vest and the 'View into Ventricular Offset' (VIVO) system which uses 12-lead ECGs. Results of using the CardioInsight vest in-vivo have been published[55]; 'high spatial resolution' is referred to but not quantified[59]. In brief, the technology has been shown to reproduce the in-vivo findings of electrocardiogram (EGMs) that were low voltage and fractionated meaning that scar could be identified and correlated with scars seen on MRI or SPECT images.

From the cardiology perspective, these technologies appear to be useful to localise arrhythmias[59 60] and for risk stratification in ischaemic cardiomyopathy (ICM) patients[61]. From a radiotherapy perspective, the spatial accuracy of the technology may not yet be sufficiently high to contribute to delineation: one source quotes 10 to 43 mm[57], another reports median localisation errors of 10.6 vs 27.3 mm for epicardial mapping and 7.7 vs 17.1 mm for endocardial mapping[62] (comparing 12 lead ECG with a new statistical approach against the BioSemi 120 lead vest).

However, the applicability of surface ECGI for, at least, ischaemic VT has been called into question by a Canadian study[34]. By application of an endocardial balloon with an epicardial sock simultaneously, 9 VTs from 8 patients were measured in-situ to locate the epi-cardial exit sites and mid-diastolic isthmus which would typically be the ablation site during 'conventional' catheter ablation procedures. The study found a median difference of 32 mm between the sites, leading them to conclude that surface ECGI can only be of limited value for locating ablation sites and the authors caution the continued use of the completely non-invasive pathways being established on the basis of multi-lead vest devices.

Clinical trial protocols have left the decision about where to treat in the hands of the clinicians. STRA-MIT-VT recommends the use of electro-anatomical mapping (EAM), CT, cardiac CT and other information to determine the treatment region[63]. ENCORE-VT includes MRI, PET, EAM and other methods to target any scar, inflammation and regions of VT origin[42]. The prescription of 25 Gy in a single fraction has been almost universally applied for STAR except in a small number of cases where 24 Gy in 3#[40]

and 20 Gy in 1#[53] have been used. It has been shown that 32.5 Gy generates electrical block in pigs' hearts[20] but in humans a target dose of 25 Gy to 95% of the target has produced the desired effect[44]. Current trials prescribe 25 Gy in a single fraction to either cover the 95% isodose around the target[44] or for 95% of the target to receive a minimum of 95% of the prescription[42].

On the basis of limited understanding of STAR treatment mechanisms, coverage of the whole delineated substrate should be aimed for; more evidence is needed before volume reduction should be attempted. However, because of the noted uncertainty around localisation of entrance and exit sites, it appears that delivering sufficient energy to *any part* of the scar or circuit might be capable of disturbing the substrate sufficiently to prevent or reduce the arrhythmia. The relevant question then becomes whether treatment volumes are large enough, given the motion of the heart and lungs, to actually deliver specific doses (25 Gy, 35 Gy) or whether the motion of the tissue will result in a lower received dose. Non-invasive targeting methods can be used to report the region of the heart for targeting, but are not yet sufficiently precise to use to create targets on their own.

1.3.3 Organs at risk

Organ at risk definitions and tolerances have been drawn from a number of sources for planning studies in STAR.

- RTOG 0915 lung SABR guidance, prescribed 30 Gy in 1# (Ipsen et al.[48])
- AAPM (American Association of Physicists in Medicine) TG101 guidance, prescribed 25 Gy in 1# (Jumeau et al.[7], Wang et al.[64])
- Combination of sources[65][66], prescribed 25 Gy in 1# (Blanck et al.[27])
- RTOG 0813 lung SABR guidance, prescribed 50 Gy in 5# (Xia et al.[67], Lydiard et al.[33])

There is no clear consensus on what values to use for planning these patients which is a consequence of the short term follow up experienced by the patients who have yet been treated and the relatively little single-fraction data available in all thorax and abdominal radiotherapy settings. OAR tolerances are usually defined to reduce the chance of a certain side effect to a particular likelihood and will depend on a number of factors including the general health of the patient group and the treatment effect being aimed for. There are too many unknowns at this stage in the development of this treatment to be definitive about what dose limits are appropriate. For the stomach, a structure found to be difficult to keep in tolerance in the UK experience, dose limits are found in trial protocols in 2 places: 22 Gy max (17.4 Gy $<$ 5 cc) (ENCORE)[42] and 12.4 Gy (11.2 Gy $<$ 10 cc)[68]. The latter reference is a 34 Gy single fraction lung trial and perhaps limits the stomach to a lower dose as it may be more achievable when planning to lung volumes which will typically be further from the stomach than the heart.

In addition to healthy organs near the target, low dose to the heart itself (1 to 3 Gy mean dose) is known to cause future heart disease at a time scale of typically years if not decades later. The lifetime excess relative risk is reported to be 7.4% per Gy mean heart dose[69 70].

From the small amount of clinical data now being reported, it is apparent that injury from STAR is possible but uncommon. Jumeau et al.[53] summarise the most recently reported data and show that where injury does occur, radiation pericarditis and pneumonitis are the most frequent side effects; both can be managed and are not likely to cause long-term damage. They cite one group's data of 10 patients including 4 cases of nausea. To date, only one case of a grade 4 toxicity to the stomach has been reported[45].

1.3.4 Discussion and conclusions

Several studies have reported that clinically acceptable plans from a target coverage and organ at risk sparing point of view are not difficult to construct[5,12,64], but the challenge might come both when it is better understood which cardiac structures suffer in the short term most from high or low dose radiation exposure (Blanck et al.[27] considered it necessary to include a departmental limit to coronary arteries as no guidance could be found). There is general concern for gastro-intestinal structures (oesophagus, stomach, bowel) and keeping dose as low as possible, even at the expense of target coverage, may be a sensible approach. Future trials must aim at better reporting of a wide range of structures which could link to SAEs. Both CyberKnife and c-arm linacs have been demonstrated to capably deliver high doses while sparing organs at risk for this purpose.

The differences in single fraction stomach doses found in trial protocols indicates the lack of certainty around organ at risk effects at high doses in single fractions. The impact of aiming to treat to 12.4 Gy max instead of 22 Gy max might be a loss of 5 mm or more of the PTV near the stomach. It is also unclear exactly how to report the maximum doses where trials specify different methods of outlining the organ itself. ENCORE-VT specifies planning on a free-breathe CT, but RTOG-0915 does not, leaving the planning team to decide whether to outline the full motion of the stomach or just during one phase of breathing. This is a point where reporting can be improved and this thesis aims to contribute to that goal.

Target volumes are not uniformly produced among centres performing STAR and should be a product of the regions of heart being targeted, the degree of motion (cardiac and respiratory) seen and the equipment used to deliver the radiation (dose rates, whether tracking is performed and what set up devices and tolerances are used). The current working assumption is that total target coverage is required to produce the desired clinical effect, rather than being able to target only a portion of the scar for example. However, as noted, it might not be overly important *where* in the VT sub-

strate the radiation is delivered, but simply that some part of the tissue is sufficiently modified to redirect the electrical signal. Crucially, wherever radiation is used to treat any disease, risk is incurred and so it must be well established that the treatment will be effective: ensuring precise targeting methods must therefore continue to be an avenue of research and trials should aim to be as prescriptive as possible in this regard. The limit on PTV volumes (200 cc) is a point of interest[54] and should be taken into consideration when planning STAR treatments.

There are a large range of approaches being adopted for STAR with treated volumes ranging from 3 to nearly 300 cc (although, as noted, larger volumes should be avoided). Detailed recording of target definition and dose distributions will significantly improve the understanding of how these treatments are being effective. In acknowledgement of all of these uncertainties, the issue of patient selection continues to be important: only those most in need of STAR should receive it, others should continue with more conventional treatments.

1.4 Motion modelling and tracking

All external radiotherapy approaches, whether robotic arm mounted or c-arm style, rely on the idea of the patient being fixed in space with some compensatory method of ensuring that displacement from the point of origin (isocentre) is accounted for. To acknowledge and compensate for known displacements during the radiotherapy process, the relevant question is: "How much variation in the position of an object (tumour) would be expected over a timeframe relevant to treatment?". This is a well researched question with general guidance to its solution provided by several references including ICRU (International Commission on Radiation Units and Measurement) report 62[71] which recommends the use of different rind volumes to compensate for positional errors due to motion. Analytical approaches to calculating appropriate dimensions of these volumes have also been studied[72].

Two broad aspects of motion need to be considered:

- Internal motion of the target - e.g. respiratory motion, organ filling, cardiac motion

- Patient external motion - voluntary or involuntary movement during treatment

In brief, the relevant volumes which are considered here are the gross target volume (GTV), internal target volume (ITV) and the planning target volume (PTV). The ITV builds on the the GTV by observing the range of positions that the GTV occupies and growing the target volume accordingly. The PTV acknowledges the errors in matching the patient position at treatment to the position they were in at planning. Use of tracking or patient control methods during treatment can be used to reduce the rind volumes: for STAR, respiratory motion might be removed or significantly reduced in the ITV leaving just cardiac motion as a factor to consider.

In this section, cardiac motion is first described and the literature is subsequently presented to provide baseline data on the degree of motion expected in patients' hearts. Finally, methods used for measuring and controlling motion in STAR and other relevant forms of radiotherapy are considered. Unfortunately, from a cardiology perspective, the question of the degree of motion at a single part of the heart *relative to some fixed point in space* is not one of routine interest and the sparsity of references with numerical values indicating cardiac motion reflects this.

1.4.1 Cardiac motion

Cardiac wall motion is far from simplistic, but is a complex interaction of 2 sets of fibres (endo- and epi-cardial): the base and apex rotate in opposite directions to each other, creating motion which minimises transmural stress on the LV muscle[73]. "Cardiac motion itself does not result in significant translational movement, ... contraction occurs in a "wringing" motion"[14]. From the perspective of the radiotherapy planning problem, total translation in 3 axes (sup-inf (SI), left-right (LR), ant-post (AP)) are the desirable data points for understanding how best to compensate for motion: such

data can inform ITV generation. Simplification of 'true' motion of the heart wall is therefore needed for use in radiotherapy planning.

Importantly, different regions of the myocardium move in different directions at different velocities[51]. As well, it is acknowledged that most patients who might be appropriate for STAR would have reduced heart motion in line with reduced LVEF[7 23 13]: "Larger regions of existing scar reduce the contractility of the heart" [51].

1.4.2 Motion reported in the literature

The results from a literature search investigating reported motion in segments of the LV are reported here.

Cardiac motion has been studied for hundreds of years, with some early publications even referencing notes by Leonardo Da Vinci[74]. A fundamental point is made by this reference that is picked up in various other publications who had the benefit of more modern imaging techniques: the apex hardly moves at all[75 76]. Between end-diastole and end-systole, the plane between the atria and ventricle (atrioventricular (AV)) moves towards the apex which is relatively stable. Some published data is noted here, included primarily in order to provide some baseline data for comparison with measurement made in this thesis.

Slager et al.[75] aimed to determine endocardial wall motion from anatomic landmarks which they demonstrated in pig hearts. Hearts of 23 patients, included because of suspected heart disease, were then imaged for these landmarks with the patients asked to suspend breathing during imaging to remove respiratory consideration. Hearts were imaged using "left ventricular cine-angiography" which, this author assumes, is performed using an ant-post arrangement of x-ray source and imager. Detected motion is reported using a coordinate system that relates to the heart at end-diastole and, due to the imaging orientation, does not include any ant-post motion. The y-axis is aligned with the long-axis of the heart (essentially LR), with the x-axis (SI) perpendicular to it. Results showed progressively less motion towards the apex with around 10 mm

of motion between end-systole and end-diastole near the mitral valve. On the x-axis, motion between cardiac phases was between 5 mm (mitral valve end) and 13 mm (near the centre).

Slager et al.'s results were reinforced by an MRI study[76] in which it was shown that long-axis shortening at end-systole compared with end-diastole was around 13 mm at the base, 7 mm at the mid-point and 1.6 mm at the apex.

Another study which aimed to highlight changes in motion due to myocardial infarction (MI) was performed around the same time but used ultrasound (US)[77]. The study looked at the displacement of the AV plane for 40 patients and 19 healthy volunteers using US. They compared septal, anterior, lateral and posterior positions and demonstrated significance in the difference between motion with and without MI in each location. For patients with an anterior MI, the difference in displacement was greatest at the septum (8 mm MI vs 15 mm normal) while the posterior edge was least impacted (12 mm MI vs 15 mm normal). For patients with posterior MI, the posterior position was most different (8 mm MI vs 15 mm normal).

1.4.3 Cardiac and respiratory motion during radiotherapy delivery

Publications relating to the application of motion data in STAR and related radiotherapy processes are presented here.

Fahimian et al.[52] considered the accuracy of the CyberKnife tracking system based on stereoscopic image pairs of a fiducial implanted in the ventricular apex (VA). Their results showed that 90% of the delivered radiation had radial deviations of less than 5.5 mm and they concluded that a minimum of a 5 mm margin should always be used for planning. Note that this is in the CyberKnife setting with tracking enabled; for non-tracked deliveries, one would expect that this margin may need to be even greater.

Lydiard et al.[33] aimed to demonstrate feasibility of MLC tracking for motion compensation of AF treatments. Using 4D US, they measured motion in 3 healthy male subjects' hearts near the pulmonary vein antra. Using Fourier analysis, cardiac mo-

tion was separated from respiratory motion and was found to be "1.8 ± 1 mm in the left-right direction, 3.6 ± 3 mm in the superior–inferior direction, and 3 ± 2 mm in the anterior-posterior direction". Total motion with respiratory motion included was 7.7 ± 3 mm, 15.6 ± 3 mm and 11.7 ± 2 mm respectively. This data was used to inform an MLC tracking algorithm that was then tested against 5 AF treatment plans. Results showed improvements in delivered dose distributions according to gamma analysis (for 2 mm, 2% gamma, the percentage of failed points were 13.1% without tracking and 5.9% with tracking). It is unclear as to whether these differences would be clinically significant but the principle of MLC tracking for STAR has been demonstrated to quantitatively improve delivered dose distributions.

A master's thesis from 2018[78] and a subsequent technical note[35] demonstrated the feasibility of cardiac synchronised VMAT delivery by splitting up a treatment plan into 3 'interleaved' plans which are all synchronised with the same part of the heart's rhythm when the heart is moving least: diastole. Plans therefore take much longer to deliver but are focused on treating a practically static target. This technique potentially allows for target volume reduction and reduces uncertainties in the planning process as the target motion is significantly reduced although breathing motion is not yet compensated for. The authors comment that a next step would be to compare dose distributions with their technique against 'conventional' approaches which would certainly allow for a more detailed analysis of the benefits of cardiac phased delivery of treatment. As a proof of principle, cardiac synchronised treatment delivery has been shown to be possible. There are many steps before such a technique could work for a patient; motion based phantom deliveries and accounting for breathing motion would be important next steps in that process. Consideration also needs to be given for the linac on which treatment is being delivered. Elekta units typically have beam on latency times of around 300 ms[79] which is a considerable portion of the cardiac cycle (750 ms for an 80 bpm rhythm), making this approach less achievable.

Another interesting piece of work has demonstrated the potential for acquiring

images from the Elekta XVI system which are both cardiac and respiratory gated[80]. By using the electrocardiogram (ECG) and breathing trace for the patient, the linac gantry was controlled to move at a rate that ensured image capture during specified parts of the breathing and cardiac cycles, resulting in a sharper image, primarily aimed at reducing noise for imaging thoracic tumours. While not directly a solution for managing cardiac motion in the STAR setting, the concept of a linac gantry being controlled for both cardiac and respiratory motion is certainly of interest in this field.

1.4.4 Diaphragm motion alone

A simpler question than motion in specific points in the myocardium is that of diaphragm motion which is often directly related to lung tumour motion (depending on the position of the tumour) and may similarly be useful for predicting motion of cardiac targets. As noted in several references in this section, respiratory motion is named as the largest contributor to intra-fraction motion in the cardiac SABR literature and is largest in the SI direction[14].

Edmunds et al.[81] used a neural-net approach to detecting the diaphragm position in cone-beam CT (CBCT) images on an Elekta linac using the XVI system with the aim of predicting diaphragm position during radiation delivery. They had good success rates with diaphragm positions tracked in 87.3% of images and a mean diaphragm apex prediction error of 4.4 mm when compared to a manually identified "ground truth". The authors comment that with coding improvements for speed and some extrapolation to 'fill in' frames where prediction failed, their process could be used to determine diaphragm position during treatment for lung tumour tracking.

In another study aiming to track tumour motion in lung radiotherapy, Wei and Chao[82] demonstrated the use of a parabolic curve fitting algorithm to track diaphragm motion in cone-beam CT images. They had a similar degree of tracking success (between 81 and 96% of projections across 6 patients had the diaphragm successfully detected) but a lower error of 0.8 mm mean positional error and 0.6 mm standard

deviation.

Hindley et al.[83] propose a potential method for real time diaphragm tracking with a methodology including the building of a model based on 4D images before it is applied to the planar images, in this case from the Varian kV imager. They reported 95th percentile errors of 0.5-3.1 mm in LR, 1.6-6.7 mm in SI and 1.2-4.0 mm in AP directions.

For c-arm linacs, delivery times are typically greater than 5 minutes: too long for a patient to hold their breath. However, some centres are able to deliver STAR in a sequence of short 'deep inspiration' breath holds (DIBH) in order to reduce respiratory motion[44] and planning studies have been carried out with DIBH in mind[67]. DIBH is often achieved by monitoring the patient with a surface guidance radiotherapy (SGRT) system such as AlignRT (VisionRT, UK) or Catalyst (C-RAD, Sweden)[84].

Controlling respiratory motion is also possible with abdominal compression: a device that pushes down on the patient's abdomen to restrict motion of the diaphragm. This approach was used in the original 5-man series[13] and the ENCORE-VT trial[42].

1.4.5 External patient motion

As well as respiratory and cardiac motion, the whole patient may move during treatment. Various studies on the degree of motion during treatment have been performed with CBCT verification imaging used at the start and end of treatment to compare differences in patient positioning. Case et al.[85] showed that for 29 patients each receiving 6 fractions of radiotherapy to the liver, the mean intrafraction positional differences were 1.3 mm, 1.6 mm and 1.5 mm in LR, AP and SI respectively. 90th percentile values were reported closer to 3 mm in each direction. A study of a new plastic shell to restrict patient motion in the lung SABR setting reported mean intrafraction motion of 0.05 mm, 0.44 mm and 1.44 mm in LR, AP and SI.

In the single fraction setting, STAR for example, external motion should be appreciated as the entire delivery will be offset by the average motion during the delivery.

Fiducial tracking, as per the CyberKnife system, promotes itself as an important tool in this context. SGRT systems are also a useful tool for monitoring patient position and can be set to restrict radiation delivery in the event that the patient moves more than by a pre-set amount.

1.4.6 Motion tracking and research aims

Motion tracking approaches for radiotherapy include fluoroscopy with implanted gold seeds[86], implantable electro-magnetic (EM) devices tracked using RF fields[87], ultrasound[88] and kilovoltage intrafraction monitoring (KIM)[89]. These approaches have been reported for use in prostate, lung and liver, among others. The KIM approach in particular suggests itself as widely accessible; it operates by detecting the location of an implantable fiducial in the patient's tumour and uses precalculated probability densities to predict the position of the object in 3D space. Other publications have also exploited kV planar images to track objects in the pancreas[90] and gastro-oesophageal junction and lung[91]. However, other than with the CyberKnife platform, fiducials have not been reportedly used for tracking areas of the heart.

At the time of writing, the field of STAR is such that it is being used only as a 'last resort' for patients: all other avenues of treatment have typically already been attempted. In the large majority, if not every patient, an ICD will be present with a lead running into the heart, with a distal electrode, or 'lead tip', embedded in or near the septal wall. This research hypothesises that the lead tip might be a relevant and accessible fiducial which could be tracked using kV planar images, as in KIM and other systems. The approach taken here is to extract the fiducial data off-line (when the patient is not present) to provide measurements of the motion in the heart which could inform planning and possibly provide quality assurance at the point of delivery. As in other publications[89 91], this concept may prove itself to be applicable during treatment, but this research study is a feasibility study only and does not attempt to be used in a 'live' environment.

The position of the lead tip is a better surrogate for the target in some cases than in others, depending on the area of the ventricle in which the VT is generated. Each patient undergoing STAR has different ventricular function depending on the damaged region and the extent of the damage. In the 'worst case' where the targeted myocardium is on the anterior wall, the motion and position of the lead tip may not be representative of target motion, but may still be able to act as a trackable point which can be used to quality assure patient set up and cardiac motion at different time points in their treatment pathway. Other surrogates, such as calcifications or sensing leads may also be present in some patients and might present other potential surrogates which could be used in the same way. No literature was found to show how the lead tip moves with regard to the tissue in which it is embedded. An extension to this work would be the use of ultrasound imaging to quantify lead tip motion against the tissue in which it resides.

An advantage of using the kV planar images to acquire measurement of cardiac motion is that the patient is in the treatment room and the correct position: measurements are directly relatable to planning considerations. Additionally, it carries no equipment costs as kV panels are standard on c-arm linear accelerators. Finally, as noted, other points in the images such as the diaphragm can also be tracked, meaning that organs at risk, such as the stomach, can also be considered using the same data sets.

1.4.7 Discussion and conclusions

Cardiac motion is complex and should not be underestimated for radiotherapy delivery with reported motion of up to 15 mm in parts of the myocardium. There are some references to baseline values for healthy hearts presented here, but the data presented by Höglund et al.[77] backs up the intuitive fact that diseased regions of the heart move differently to healthy regions. As STAR typically targets areas of scarred tissue and nearby circuit entrance or exit points, it is likely that in many cases, observed cardiac

motion will be less than or equal to those values presented here. In addition, each patient is physiologically unique and, in the modern era, it is appropriate to aim for personalised medicine: motion from the individual's heart should be used to prepare their own treatment plan.

Respiratory motion is an important factor for both targets and organs at risk, particularly the stomach, in the STAR setting. Various methods of controlling it have been used (DIBH, abdominal compression) in treating STAR and it is known to make a significant difference to the amount of motion in the target[33]. Various methods for accounting for respiratory motion during treatment are also used: CyberKnife's synchrony system, MLC tracking, and respiratory gating. Respiratory motion is well assessed and controlled in the radiotherapy setting: cardiac motion is a relatively new aspect of radiotherapy treatment with many avenues of research open to it.

Motion data is captured for patients receiving STAR with ultrasound, MRI, CT and other modalities potentially giving the users the ability to observe displacement ranges of the myocardium across the full treatment volume. No cardiac motion data has yet been presented for the patient in the treatment position or assessed changes in cardiac motion data at different points in the STAR process (assessment, planning, treatment delivery). The ability to capture motion data on-set has been demonstrated by a number of authors focusing on the motion of the diaphragm. Fiducials have been previously mentioned (sections 1.2 & 1.3) and are used to track points in the myocardium for CyberKnife deliveries. A convenient traceable point in the hearts of many STAR patients is the tip of the pacing lead. In this work, the use of x-ray imaging tools on-board the Elekta Versa linac is proposed to capture motion in the hearts of STAR patients at the position of the pacing lead tip. The reported data from this work should contribute to the growing body of data relating to cardiac motion and help improve the planning and reporting of STAR treatments.

1.5 Conclusions and research aims

Over the last decade, an entirely new paradigm in treating arrhythmias in the heart has been proposed and investigated by a number of authors. The Washington University in St. Louis group has been instrumental in informing the community, initiating trials and bringing oncology and cardiology teams together at SNORAD conferences. There has been significant global interest in the technique which may have the ability to open up new avenues of treatment for patients who have exhausted all other treatment options and suffer from significant physiological and social problems in their daily lives.

Target definition is quite different to general oncology practice in which tumours are usually visible or defined according to best practice. Tools being investigated for use in targeting such as non-invasive cardiac mapping 'vests' or similar tend to have large positional uncertainties which do not map well with the high precision techniques in modern radiotherapy practice. However, it has been shown that *where* the treatment goes might matter less than the fact that it is delivered at all. The previous statement must be followed by acknowledging that the data is too sparse and too early to make any definitive points along those lines. A natural consequence of the modernity of the field is that the effectiveness of the different approaches are not yet known: there is a general trend towards smaller target volumes which better spare organs at risk but which also, non-intuitively, appear to be delivering treatments just as effectively as larger targets. Indeed, larger targets have been associated with poorer patient outcomes and potentially should be avoided.

Different treatment platforms and techniques are being used to optimise treatments: maximising dose to the target and reducing dose to organs at risk. There is interest in, and a focus on controlling the motion both from the diaphragm and the myocardium. Several authors have published data on methods to measure organ displacements, but as yet none with the patient in the treatment position on a c-arm linac. Optimal methods for target and organ at risk definition have not been agreed on. Clinically, organ at risk tolerances have yet to be developed with much certainty and there are

technical aspects to how organs should be defined under the impact of respiratory and cardiac motion which have yet to be resolved. As trials continue into the next decade, dose reporting should be improved to enable high quality data comparison and guidance on the technical aspects of STAR to emerge.

1.5.1 Aims of this work

This project primarily aims to create and validate a method for characterising cardiac and respiratory motion in patients undergoing STAR treatment. The data acquisition and analysis methods are directed at modern radiotherapy centres with standard equipment: linear accelerators fitted with kV imaging panels. This approach is taken because the observation of cardiac motion on a linear accelerator is practical and potentially widely applicable, as well as novel. Using the linear accelerator to determine motion also ensures the patient is in the treatment position making measured data directly applicable to radiotherapy plans. The project also aims to apply the measured data from a small patient sample to treatment planning considerations: target sizes and control of dose to organs at risk.

This thesis presents two papers. The first describes the methodology for characterising motion at the point of the pacing lead tip and diaphragm using a novel geometric approach which includes manual selection of the pacing lead tip and section of the diaphragm. This methodology required the development of a novel data processing toolkit to identify the object of interest in each frame of an imaging sequence and return a displacement offset in physical distance units. It was validated by imaging a ball bearing in motion on a controllable platform and motorised arm. The first paper concludes that it is feasible to characterise cardiac motion at a point using the proposed methodology. It also contributes to the extant literature with a novel method for identifying diaphragm position in planar kV images from a linear accelerator.

The second paper aims to apply the methodology developed above to patient data at multiple time points in the patient journey. It discusses the implications of having

access to this information and how it could be applied in the clinic. The paper also addresses the topics of applying the data to target definition and organ at risk positioning, and concludes that this work opens up multiple avenues of research. While the small patient sample prohibits making broad statements about how to treat STAR patients, the measured data serves to illustrate the benefits of having access to such information throughout the treatment planning and delivery processes. This work aims to progress the discussion about targeting and dose restriction in STAR and does so from the current standard practice position in which STAR targets are treated in a similar way to oncological targets in radiotherapy. It is hoped that extensions of this research may contribute to the discussion on whether that is a clinically useful approach.

2 Measuring cardiac and respiratory motion with linear accelerator acquired kV planar images

Authors

James Daniel[*][1], Kevin Burke[£][1], Philip Whitehurst[£][2]

* - Project concept, design, data measurements, data analysis, critical analysis and writing

£ - Project concept, design and supervision

[1] - *South Tees Hospitals NHS Foundation Trust, Middlesbrough*

[2] - *The Christie NHS Foundation Trust, Manchester*

2.1 Abstract

Purpose: STereotactic Arrhythmia Radioablation (STAR) is a novel indication for radiotherapy in treating ventricular tachycardia (VT). Planning and delivering radiotherapy to a target displaced by both cardiac and respiratory motion is challenging and is being addressed in a number of different ways. We propose a method to capture both elements of motion using the kV imaging panel found on most linear accelerators (linac).

Methods: Rotational planar images, used to create 3D and 4D images for positional verification, were captured on an Elekta Versa HD linac. The pacing lead tip embedded in the septal wall was tracked using an algorithm written in Python which also tracks the position of the left diaphragm. Novel geometric methods were used to translate image positions in the 2D images into distance from a fixed centre of displacement (CoD) for each object and Fourier transforms were used to separate cardiac and respiratory motion. Validation of this approach was carried out by imaging a ball bearing in motion about a point in space at various frequencies and amplitudes. Image sequences

from patients treated at our centre were analysed using this technique and their cardiac and respiratory displacement data are reported.

Results: Validation showed that the process produced accurate results to within 0.5 mm for frequencies up to 120 cycles per minute (cpm) and amplitudes up to 17.5 mm covering all likely cardiac and respiratory motion. Lead tip displacement was on average (± standard deviation) 9.5 ± 2.1 mm (left-right), 9.7 ± 1.8 mm (ant-post) and 12.9 ± 2.7 mm (sup-inf) for the 3 patients; cardiac displacement alone was lower. Diaphragm displacement was between 11 and 19 mm measured as average peak-to-trough values across the image sequences. Accurate tracking of the lead tip was found in 84.9%, 82.9% and 92.6% of frames and of the diaphragm in 99.7%, 96.9% and 94.4% of frames, for each patient respectively.

Conclusions: Accurate tracking of a point in the heart and diaphragm has been demonstrated using Elekta XVI kV planar images. Results from a 3 patient sample show similar degrees of motion to other published data. The results from this work will be applied to technical aspects of treatment planning in the future.

2.2 Introduction

Ventricular tachycardia (VT) is a condition which can significantly decrease patients' quality of life[6] by causing chest pain, fainting, dizziness and can ultimately lead to cardiac arrest and death. Patients are commonly fitted with implantable cardioverter devices (ICDs) which are effective at keeping the patient alive during VT episodes but the shocks patients receive from them can be highly unpleasant and distressing[5]. Ongoing VT episodes lead to deteriorating left ventricle (LV) function and a greater risk of sudden cardiac death (SCD) which is a primary reason for also making use of other treatments aimed at reducing the number of VT episodes experienced by the patient[1]. Treatments include anti-arrhythmic drugs (AADs) and catheter ablation (heating of the heart muscle to disrupt errant pathways which lead to VT) among

others[4], although current treatments often have low rates of success[7,8].

A novel approach to treating VT is to use radiotherapy to disrupt conduction pathways in the parts of the myocardium which allow VT circuits to occur[13]: STereotactic Arrhythmia Radioablation (STAR)[12]. Since the first recorded treatment of a patient with STAR[14] and a publication of a 5-man case series in the New England Journal of Medicine[13], approximately 100 patients have been treated worldwide with both CyberKnife (Accuray, CA) (robotic-arm mounted linear accelerator) and conventional radiotherapy treatment units (linacs: c-arm style linear accelerators). The interest in using radiotherapy is clear: it can ablate more deeply than catheter procedures and, at the point of treatment delivery, is essentially non-invasive, therefore carrying less (obvious) acute risk to the patient.

2.2.1 Cardiac and respiratory motion

One of the challenges in treating areas of the heart with STAR is motion dually produced by the heart and diaphragm, the combination of which has been rarely considered when planning and delivering radiotherapy treatments. Motion in radiotherapy can cause regions in the target to be under-treated, and nearby healthy tissues, or organs at risk (OARs), to be overdosed, and so motion compensation is commonly used for tumours near the diaphragm which move as the patient breathes; lung and liver[9,2] for example.

Managing motion in radiotherapy relies firstly on knowing the precise distance from a fixed point in space (isocentre) to the region targeted for treatment, and how it varies over time[71]. For radiotherapy to the thorax or abdomen, when motion is known to be significant, planning is frequently carried out using respiratory gated 4D CT which reflects internal motion as linked to the breathing cycle. Cardiac frequencies are typically 4 to 5 times higher than respiratory frequencies however, meaning that the traditional radiotherapy 4D CT imaging can under-represent cardiac wall displacement. Alternative methods of acquiring cardiac motion data are therefore needed to characterise

it fully such as ultrasound, 4D MRI and the work presented here. Once the motion is measured, its management during treatment can be achieved in a number of ways: extra margins are commonly added to treatment plans to ensure the motion does not adversely affect the target or OARs[71], CyberKnife's Synchrony technology allows for respiratory motion compensation using fiducials during treatment[14], respiratory gating systems are available for linac deliveries[93], surface guided radiotherapy (SGRT) is frequently used for maintaining breath hold during delivery[84] and even gating for cardiac motion has been experimentally demonstrated on a linac[35].

It is relevant to acquire motion data with the patient in the treatment position as varying patient position might change the observed motion. It is also preferential to acquire such data in the treatment room as the physiological effect of lying on the treatment couch on a linac can be significant[94]: hypothetically, breathing and heart rates might be affected by the position and environment the patient is in. For reference, there are relatively few publications reporting the amount of motion seen in the myocardium for radiotherapy purposes[95 33]. There are a greater number of publications which include data on respiratory motion[96 82 81] which has been studied for radiotherapy for a longer period of time.

Linacs are commonly equipped with kV planar imaging panels and x-ray sources which are used to image patients prior to treatment to ensure geographical set up is accurate. A sequence of several hundred images is acquired while the x-ray source and panel rotate about the patient (see figure 3 for a graphical representation). A 3D, or 4D respiratory-gated, cone-beam CT (CBCT) dataset is then reconstructed. Reynolds *et al.* used this technology experimentally to acquire images which could be simultaneously cardiac- and respiratory-gated in order to improve treatment of thoracic tumours[80].

High density objects are relatively easy to identify in kV planar images of human anatomy. Under current normal practice, most patients receiving STAR will have ICDs fitted which include a metal tip embedded in the septal wall between ventricles:

the lead tip (distal electrode) which is usually around 6 to 8 mm long and 1 mm in diameter. Treatment volumes for some patients are in close proximity to this point: several centimeters along the wall from the apex. By measuring the degree of motion of the lead tip in these image sequences, information about the motion of the cardiac muscle at that point can be inferred and then potentially related to motion at other points[75]. The diaphragm can also be identified in these kV planar images[82 96 97].

Patients attending for STAR at our centre undergo pre-planning assessment using kV planar imaging sequences and the same imaging sequences are used immediately prior to treatment for geographical verification of the treatment volume. We hypothesise that it may be possible to track both cardiac and respiratory motion in these images and use the measured data to inform the planning and treatment process.

2.2.2 Aims

This paper describes a toolkit for measuring motion amplitudes and frequencies at the position of the pacing lead tip embedded in the myocardium and the apex of the left diaphragm. It makes use of planar kV images captured on a linear accelerator and tracks the position of the lead tip and the diaphragm. Motion components are separated using Fourier analysis and are reported as displacement magnitudes of the lead tip and the average magnitude of travel of the diaphragm (peak-to-trough measurement). Images acquired during the treatment of 3 patients were analysed for lead tip displacement in 3 axes and respiratory motion in the sup-inf axis. Validation of the toolkit was carried out by imaging a ball bearing in motion on motorised platforms.

This work is a first step towards optimal, patient-specific, treatment techniques.

2.3 Materials and Methods

2.3.1 Workflow

All image acquisition was carried out using the XVI imaging system on Elekta Versa HD linear accelerators (Elekta, Stockholm). Image processing and data analysis was

performed using custom-built code written in Python 3.6 and 3.8 using the Spyder version 4 front-end. Specific packages and function used are mentioned where relevant.

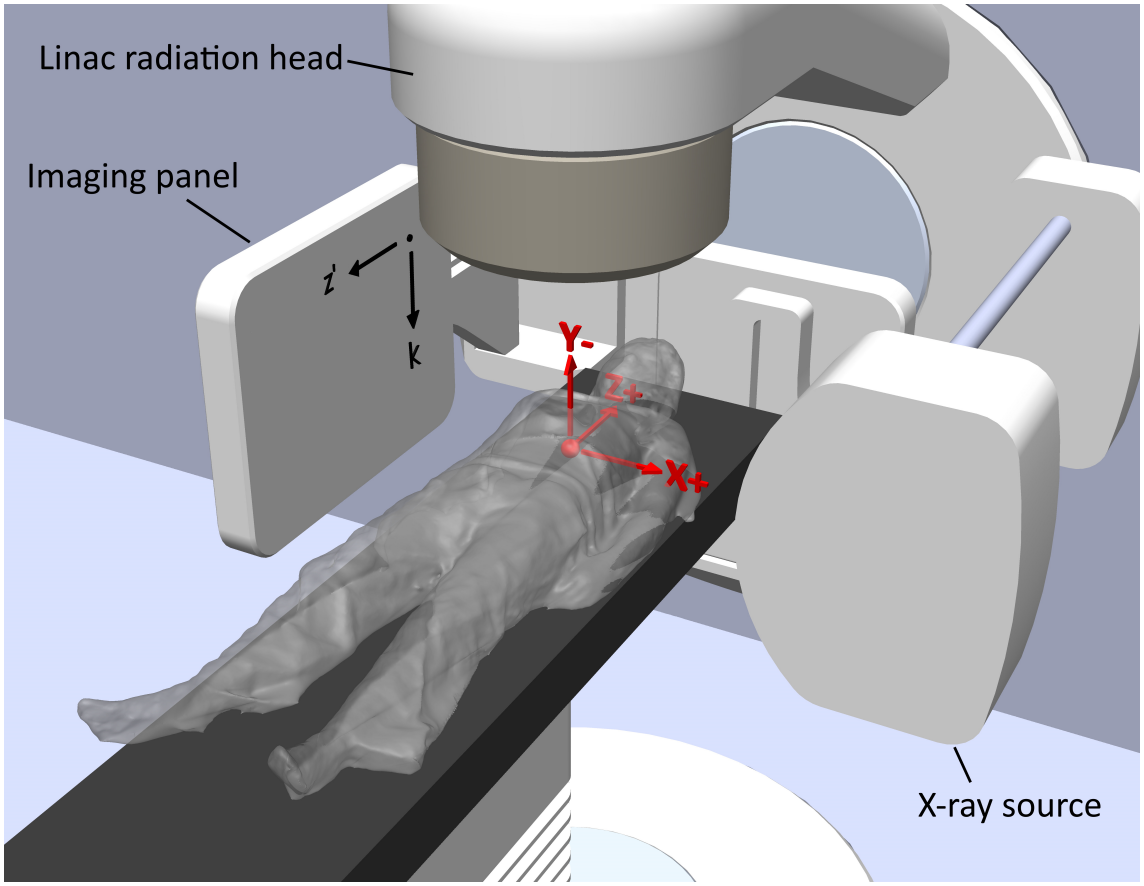

Figure 3: Representation of a patient on a linac couch. DICOM coordinates represented in red (note the negative y-axis projection) and imaging panel coordinates displayed on the imaging panel in black. The gantry angle is 0 in this image; the angle increments positively as the gantry rotates clockwise.

Figure 3 shows the XVI set up with coordinate system used in this work. The patient coordinate system accords with the DICOM 3.0 standard and is used as an input to the code. Figure 4 shows the identification of the lead tip in a CBCT image; the 3D position of the lead tip must be read by a human operator using software capable of displaying DICOM coordinates and manually entered into a python console running the code. The coordinate system in the panel aligns with patient coordinate system along Z (-Z'), but requires a new axis to describe the convolution of displacement along

X and Y axes in the patient: K.

Images are acquired through angles -180 to 20 (the gantry rotates clockwise) with a spacing of approximately 0.2 degrees. Images are taken 0.182s apart (5.5Hz); each series of 1000 $\pm$ 20 images took approximately 3 minutes to acquire. For reference, normal ICDs operate at between 128 to 256 Hz, completely sampling the cardiac frequencies[98].

Image data was transferred from the XVI control terminal on an Elekta Versa HD to a PC for analysis. Relevant data included were the ($\approx$ 1000) imaging files ('.HIS' format) and a file describing each image on a frame-by-frame basis ('_FRAMES.xml'). Each dataset comprised $\approx$0.5 Gb of storage. The '.HIS' format contained sufficient information in the header to allow the use of the NUMPY.FROMFILE (a file reading package which requires file-type inputs and returns human readable data) to interpret images correctly (NUMPY v. 1.18.4+mkl).

There were 6 steps involved in producing the displacement data for pacing lead tip and diaphragm:

1. Reconstructed DICOM images from the planar image sequence are used for a human operator to identify an approximate centre of displacement (CoD) of the lead tip and diaphragm apex. In the future, these positions may be automatically detected

2. The 3D positions are projected onto each 2D planar image to identify the approximate expected location of each object in each frame (see appendix 2.7.1)

3. The planar images are processed to highlight relevant features

4. The lead tip and the diaphragm apex are located in each image based on the expected position

5. Geometric corrections, including compensation for the effect of gravity on the linac gantry, are applied to the traces and units are transformed from pixels to mm using a conversion factor calculated at the point of the object

6. Fourier analysis is used to separate different components of the displacement

2.3.1.1 Identifying the CoD in DICOM coordinates

Figure 4: A slice from the cone beam CT reconstruction of the XVI imaging sequence for a patient. The tip position is identified with the red marker.

3D reconstructed images were used to locate an approximate CoD of the tip (shown in red in figure 4). The diaphragm apex position in X and Y was located in the same way.

2.3.1.2 Projection of the CoD onto planar images

The geometric method to acquire the projection of the CoD into the panel coordinate system is described in appendix 2.7.1. As an overview of the process, the x-ray source, CoD and panel are modelled by points and planes in 3D space. A line projected from the position of the x-ray source at each gantry angle through the CoD and into

the plane is constructed. The intersection of the constructed line and the plane is calculated and is related to the coordinate system of the panel. The algorithm returns the K and Z' coordinates for the CoD at each gantry angle along with a factor to transform pixel values into distance at the position of the CoD in space.

2.3.1.3 Image Processing

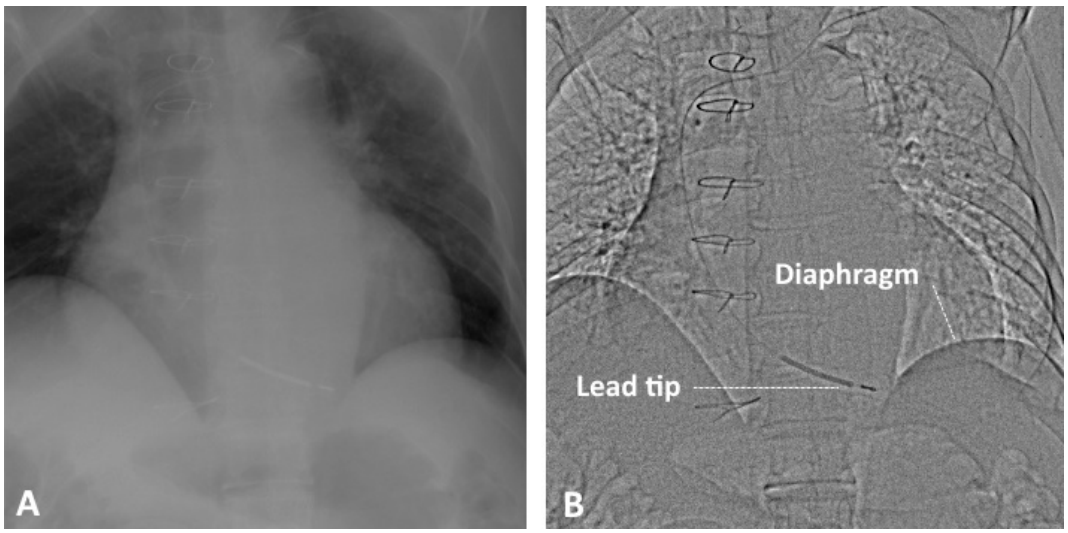

Figure 5: A - An unprocessed .HIS file image from the XVI system: the pacing lead tip is barely visible. B - the processed image clearly displaying the pacing lead tip for locating.

While often clearly visible, the lead tip cannot be assigned a common image pixel value in each frame due to variable path lengths through the patient depending on source angle, relative position of the tip to the imaging panel and changes in scattering contributions. Images were therefore processed prior to the tracking algorithm being used.

Image processing depended on the object of interest: lead tip or diaphragm. Initial processing steps were the same for both: taking the base 10 logarithm of each image in line with the commercially used method for respiratory binning on the XVI system: the "Amsterdam Shroud" technique[96]. Subsequent steps were based on stan-

dard image processing techniques with an element of trial and error, starting with filter sizes based on observed image dimensions. For the lead tip, a ten pixel wide median filter was created and convolved with the images using OPENCV.FILTER2D (4.3.0.36). The logarithmic image divided by the convolved image to highlight the relevant features (see figure 5). For the diaphragm, a Z' oriented edge enhancing Sobel filter (OPENCV.SOBEL v 4.3.0.36) was used, also with a ten pixel wide kernel.

2.3.1.4 Location of the lead tip and diaphragm

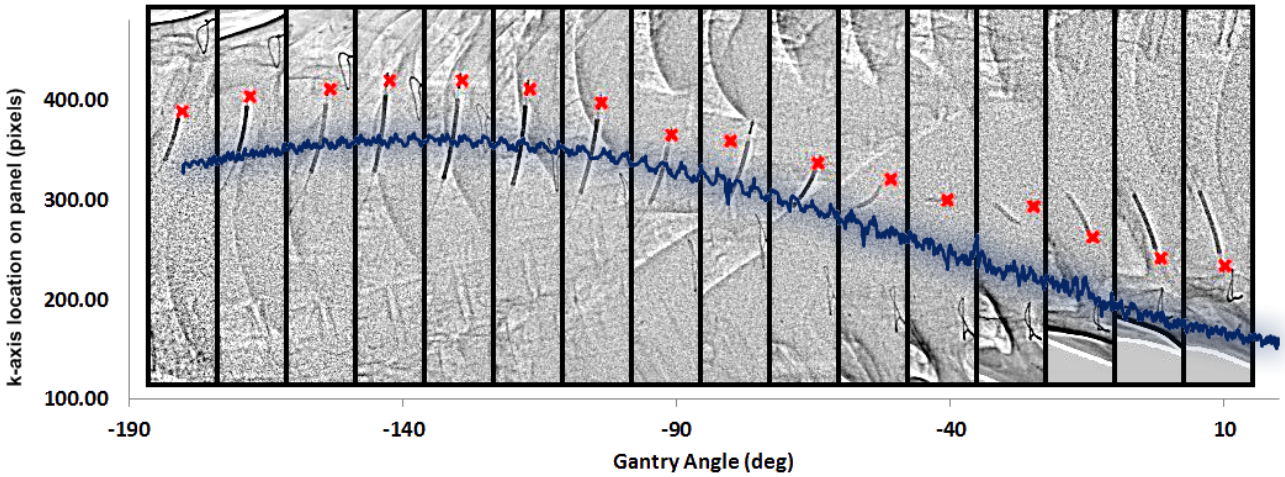

Figure 6: 16 cropped and rotated images from a patient dataset with the lead tip identified with a red cross. The dark blue line is the location of the tip on all 1000 images and has been offset slightly from the red crosses for visibility.

The pacing lead tip location was identified through a combination of edge detection and by selecting pixel groups with relevant image values. For the diaphragm, the expected panel location of the point in the image was used as the centre of a 20 pixel wide region which was then averaged along the K axis in order to reduce noise in the measurement. Gradients were then used to identify the most superior edge as the surrogate for the diaphragm apex.

Figure 6 shows the identification of the lead tip across a sequence of patient images

and the corresponding data trace.

2.3.1.5 Signal processing

Signals returned from this process were K and Z' tip locations and Z' locations for the diaphragm. The aim of this work was to provide data to aid the radiotherapy treatment planning process which is fundamentally about relating targets and risk areas to a fixed isocentre (centre of motion of the linear accelerator). The signals contained components of K-geometry (the effect of the rotating gantry on the projection of the object onto the panel), respiratory displacement, cardiac displacement, patient motion, mechanical sag of the panel and linac arm, and noise.

Mechanical sag of the panel was accounted for using the manufacturer's proprietary methods (previously measured gantry and panel sag[v] data recorded in the FRAMES.XML file). Fourier analysis was used to separate the components of displacement:

- Low frequencies (< 6 cpm) including residual K-geometry and patient motion
- Respiratory frequencies (between 6 and 30 cpm)
- Cardiac frequencies (> 30 cpm)

Note that the unit 'cycles per minute' (cpm) is applied in this paper to both respiratory and cardiac motion.

The NUMPY implementation of the fast Fourier transform (FFT) was used to extract the frequency domain of each trace. Bandstop and bandpass filters were created with the SCIPY.SIGNAL package (version 1.4.1) and applied using the limits set out above to extract each component of motion. Frequencies reported by the FFT were quantised to the sampling frequency in Hz divided by the number of measured points in the trace (∼1000 in each case): approximately 0.33 cpm.

[v]The gantry weighs over 3 tonnes and moves as it rotates meaning that the isocentre is not a single point in space, but rather a small volume. At each gantry angle, the relative position of the panel and radiation source is specified to correct images at the end of acquisition and is known as flexmap data.

K-geometry was conflated with patient motion in the low frequency range of the signals. In order to present the patient motion as a separate component, K-geometry needed to be minimised. This was achieved for the lead tip by iterating in 2D space to find the position with the least residual low frequency components in the Fourier spectrum. When the minimal position was found, new K and Z' expected positions were found and used to process the signals before Fourier analysis was performed. Any variation in the CoD was accepted in reporting the full displacement of the lead tip but was removed in the fourier analysis of the cardiac motion alone.

2.3.2 Patient data

3 patients who were treated with STAR at our centre contributed the data from their treatment to this study. A subset of their data is presented here in order to demonstrate the efficacy of this toolkit.

Full magnitude displacements of the lead tip and average peak-to-trough diaphragm position are presented in the results. X and Y axis data are retrieved from the K-signal by selecting regions of the signal ($\pm 10^{\circ}$) around gantry angles of 180 and 0 (AP, Y-axis) and -90 (LR, X-axis). For angles not precisely orthogonal to the direction of motion, the detected displacement is not entirely dependent on the desired axis alone. Geometric analysis shows that over a 10° range the error caused by this approach will be 4.4% at most and will give an average of approximately 1.6% (see appendix 2.7.2). Considering displacements up to 1 cm, that is a maximum error of 0.16 mm.

2.3.3 Toolkit validation

Validation was performed to ensure and characterise accurate performance of the algorithms.

As a first pass approach, visualising traces plotted with gantry angle on the X-axis and displacement on the Y-axis (see figure 8 as an example) was sufficient to identify that reasonable amplitudes and frequencies were acquired and frames where

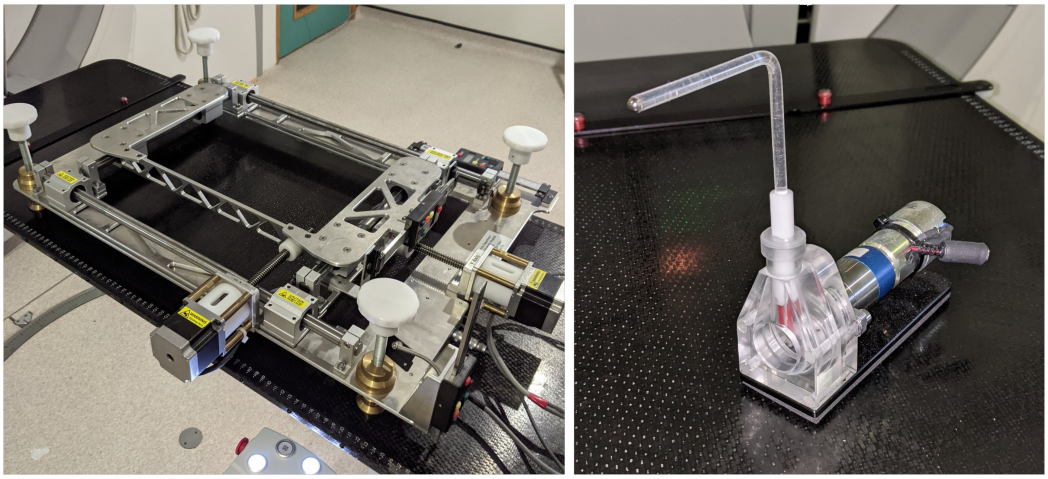

Figure 7: Validation phantoms used. Left - moving platform, Right - motorised arm

the algorithm had failed to adequately detect the objects of interest. Images were also written out to file with the lead tip and diaphragm points identified on them (figures 5 & 6, for example) to enable visual assessment of the detected positions. Complete imaging datasets were loaded into imageJ which allowed a 'cine'-like visualisation of the data.

Frame-by-frame analysis of the data was performed for 3 of the patient data sets. Frames where the lead tip was incorrectly identified by the code were labelled and a reason assigned to why the code had failed to properly identify the tip. Results were compiled as percentage rates in which the tip was correctly identified and were compared with a visual inspection of the lead and tip on each frame. Where the human eye failed to distinguish between the two objects, the frame was labelled as such.

For the dataset for patient 1, manual detection of the lead tip and the diaphragm at the selected X and Y coordinates was performed by eye: each image was presented to the user in sequence and a mouse click recorded the position of the coordinates to an array. Identification of the lead tip was performed as close as possible to the last pixel which was clearly part of the tip, and the diaphragm was identified at the most superior edge. Manually identified positions were then compared with automatically generated

values to determine the inherent error in the positions reported by the toolkit.

A piece of validation work was performed to demonstrate that known displacements and speeds in all three axes were correctly reported by the coding toolkit, regardless of the shape and size of the object being tracked. A 5mm diameter ball bearing was carried on a moving platform and motorised arm (see figure 7). The arm was capable of moving with an amplitude of 123 mm and frequencies of 41.3, 58.4, 76.4, 103.6, 112.1 and 162.4 cpm. The moving platform[99] was designed for precise motion over distances up to several centimetres, but was limited to moving at rates under approximately 5 cpm. The combination of the platform moving in X and Z and the motorised arm moving in Y allowed for a set of images with a ball bearing moving at relevant frequencies and amplitudes in the 3 axes. However, images of the ball bearing, acquired using the same XVI imaging sequence as for the patients, were fundamentally different to those of the lead tip meaning that extra code was needed to identify the centre of the ball bearing; a simple coding task which was easily validated by inspection. A range of frequencies and amplitudes were selected to represent normal cardiac and respiratory motion. The ball bearing was imaged moving in each axis separately and in combination. The toolkit, with the additional module to detect the ball bearing, was used to analyse the traces and compare frequency and amplitudes with the physically measured values.

2.4 Results

2.4.1 Phantom validation measurements

Table 1 shows the results from the validation testing performed using the motorised arm and moving platform. The maximum error in amplitude was seen in the Z axis only testing (0.5 mm) and in X for the combined motion tests (0.4 mm). All measurements reported amplitudes within 0.5 mm. Frequencies were all within 6% of the periodicity of the phantom and the average deviation was -0.5%.

Axis in motion			Frequency (cpm)			Amplitude (mm)		
			Phantom	*Measured*	*Deviation*(%)	*Phantom*	*Measured*	*Deviation*(%)
X only			18.0	18.0	0.0	5	5.1	0.1
			13.1	13.0	-0.8	10	10.1	0.1
			10.6	10.6	0.0	15	15.2	0.2
Y only			61.9	59.7	-3.5	6.2	6.2	0
			78.6	78.8	0.1	6.2	6.1	-0.1
			103.6	96.9	-6.5	6.2	6.1	-0.1
			112.1	118.3	5.6	6.2	6.1	-0.1
Z only			18.0	17.9	-0.6	5	5.1	0.1
			13.1	12.8	-2.3	10	10.3	0.3
			10.6	10.4	-1.9	15	15.5	0.5
All (set 1)	-	X	8.4	8.6	2.4	5	5.4	0.4
		Y	41.3	42.7	3.4	6.2	5.9	-0.3
		Z	11.2	11.0	-1.8	7.5	7.6	0.1
All (set 2)	-	X	6.1	6.3	3.3	7.5	7.8	0.3
		Y	61.9	58.4	-5.7	6.2	5.9	-0.3
		Z	6.1	6.1	0.0	12.5	12.7	0.2
All (set 3)	-	X	6.1	6.1	0	10	10.3	0.3
		Y	78.6	78.9	0.4	6.2	6.1	-0.1
		Z	4.9	4.8	-2.0	17.5	17.9	0.4

Table 1: Frequency and amplitude measurements made using the moving platform and mechanical arm.

2.4.2 Patient data

Figure 8 and tables 2 and 3 present the results from the patient image sequences. Points of error in the data were identified by inspection and were removed from the data traces.

Figure 8 shows the complete data trace for one of the patients. Where frames had been identified as not having tracked the pacing lead tip sufficiently well to be included, the background is set to grey. X and Y, and Z displacement traces clearly show the range of displacement of the pacing lead tip over the course of 3 minutes, when breathing and average positional changes have been removed. Figures for the displacement values for all patient traces are provided in tables 2 & 3. The diaphragm displacement trace is also shown.

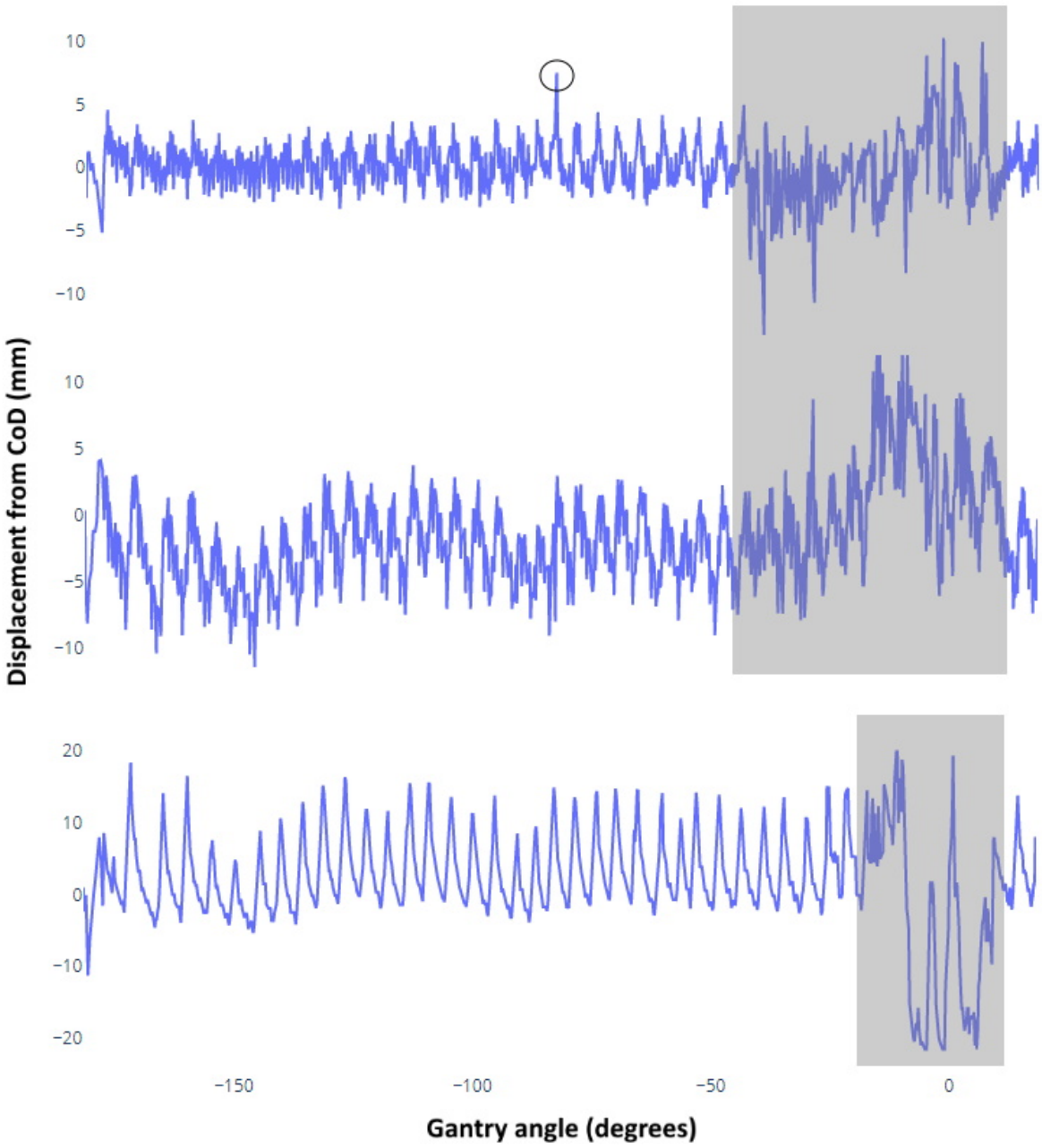

Figure 8: Top - displacement of the lead tip in the X and Y axes (detected in the K-axis on the panel), Middle - displacement of the lead tip in the Z axis, Bottom - displacement of the diaphragm from its own centre of motion. Grey shaded areas and circled point indicate data removed from analysis. Note the different y-scale on the diaphragm trace. Each trace is taken from a full imaging sequence acquired over approximately 3 minutes.

	Full trace (mm)			Cardiac only (mm)			
Patient	*LR*	*AP*	*SI*	*LR*	*AP*	*SI*	*Rate* (*cpm*)
1	10.9	8.0	13.0	6.6	7.1	8.3	60-84
2	10.6	9.7	15.5	6.7	7.4	9.5	69.8
3	7.1	11.5	10.1	6.4	7.8	8.8	54.7

Table 2: Lead tip displacement in full and for cardiac motion only for 3 patients. Cardiac frequency also reported.

Patient	*SI* (*mm*)	*Rate* (*cpm*)
1	19.0	20
2	15.5	15
3	11.3	19-22

Table 3: Diaphragm sup-inf (SI) displacement and frequencies for 3 patients. Displacement is the average peak-to-trough measurement.

2.4.3 Patient data validation

Results from frame-by-frame inspection of 3 patient datasets showed that the code accurately located the tip of the pacing lead in 84.9%, 82.9% and 92.6% of the images. Visually, it was impossible to either see the tip or distinguish it from the lead in 14.5%, 7.9% and 0% of the images respectively. Failure to detect the tip therefore occurred for coding or image processing reasons in 0.6% (6 frames), 9.2% (92 frames) and 7.4% (74 frames) of the images for each patient respectively. These failures to detect are likely to be correctable with improved image processing to enhance the edges of the lead tip or by modifying the code to account for unusual angles and positions of the lead tip. Machine learning might be another approach to improving detection rates.

From the combined 3 datasets with a total of 3030 frames, the reasons for the error in detection were: end of the lead, rather than the lead tip detected (190 frames), lead

tip not distinguishable from the lead (180 frames), lead tip near anatomical structure (3 frames), start-up issues (4 frames) and unknown reasons (3 frames).

The diaphragm was accurately located in 99.7%, 96.9% and 94.4% of frames. Reasons for failure to detect the diaphragm were: identification of a mechanical structure (25 frames), wrong side of the diaphragm detected (25 frames), other interfering object (ribs for example) (10 frames), unknown issues (19 frames).

For the ground truth measurements, the average positional error in the lead tip was -1.0 $\pm$ 2.9 mm in the transverse plane (LR, AP) and -1.3 $\pm$ 2.5 mm in SI. From observation of the detected positions of the lead tip, it was clear that the code was identifying a position approximately 2.5 mm back from the tip end (ground truth) positions. Accounting for that positional error and excluding all frames identified in which the tip was incorrectly located by the code (as above), the average positional errors for the lead tip were 0 $\pm$ 0.9 mm in the transverse plane (LR, AP) and -0.7 $\pm$ 0.4 mm in SI. For the diaphragm, the positional error was 0.8 $\pm$ 0.6 mm (SI only) over all frames.

2.5 Discussion

Table 1 shows that the geometric approach used to interpret information detected on the XVI imaging panel produces spatial results accurate to within 0.5 mm over the range of amplitudes measured (up to 17.5 mm). Amplitude in the Y-axis (AP) was on average reported as slightly lower than that of the phantom while in the X-axis (LR), displacement is reported higher. This effect might be due to the higher frequency of motion in Y, or might relate to small errors in the coding to identify the centre of the image of the ball bearing. In either case, it is a small effect and within the error margins reported in appendix 2.7.2. Measured frequencies were on average 0.5 $\pm$ 3 cpm of the known periodicity of the verification jig. This validation approach demonstrates the methods used to extract spatial and temporal information from XVI image sequences works with high precision. The geometrical methods used to both construct orthogonal

axis displacement from a rotational image set, and translate pixel to physical distances at the point of the object, are effective.

In the clinical data, identification of the pacing lead tip and diaphragm was successful in 83.5% and 97% of frames respectively. Diaphragm tracking rates can be compared against 87.3% of frames (Edmunds et al.[81]) and 81 to 96% (Wei and Chao[82]). The accuracy of the diaphragm tracking in this toolkit matches the smallest reported tracking errors found elsewhere: 0.8 mm ± 0.6 mm[82]. The novel aspect of this work is the pre-selection of the point about which the diaphragm is tracked which allows for a very simple approach to determining the superior edge using line profiles. A possibility for improving the method would be to adapt some of the principles from other work by tracking several points on the diaphragm and fitting a parabola to them. There are no other published papers to directly compare the lead tip tracking accuracy with, but as the lead tip was misidentified in a number of frames in two of the datasets even when it was visually identifiable, it is reasonable to assert that it would also be possible to improve lead tip tracking. Alternative image processing approaches might improve the visibility of the lead tip in frames where it was not identifiable by eye.

Average full displacement magnitudes for the lead tip were 9.5 ± 2.1 mm LR, 9.7 ± 1.8 mm AP and 12.9 ± 2.7 mm SI. Displacement magnitudes for the cardiac motion separated from diaphragm motion were 6.6 ± 0.2 mm LR, 7.4 ± 0.4 mm AP and 8.9 ± 0.6 mm SI. The displacements measured at the lead tip for the patients in this study are similar with those reported at various points in the left ventricles of healthy volunteers[75 33] and patients with VT[95]. The full detected range of motion is reported here which is strongly influenced by breathing patterns; note that SI lead tip motion for patient 2 is identical to the average peak-to-trough diaphragm displacement range.

Frequency identification in the datasets worked well. Patient 2 was paced at 70 cpm while the other patient rhythms were not controlled by their ICDs and this is evident in table 2. Breathing rates were also identifiable from the FFT for each patient but were generally less regular (FFT peaks were more spread out) than the cardiac rates.

With the code tested in this paper, frames in which the lead tip and diaphragm were misidentified had to be rejected manually from the results; this is an aspect that would need to be automated or made redundant through better tracking if this technique was to be adapted for use in a 'live' environment to inform patient treatment at the time of acquisition. Tracking times would also need to be improved for live use: without being optimised for speed, it takes approximately 3 minutes for both lead tip and diaphragm to be tracked in a full 1000 image set.

The most significant way to optimise for speed would be the use of multi-processing. Currently, Python uses a single core to run processes in code. Parallel processing of images on multiple cores or the graphics processing unit (GPU) would diminish the time needed to track the pacing lead tip across an image set. For example, a 4 core processor could run the code in one quarter of the time, closer to 45 seconds than 3 minutes. Another time saving method would be to automatically estimate the initial position of the lead tip CoD which might be achieved by making an intelligent guess based on previous datasets and refining it using the iterative approach described earlier.

When the work has been done to improve reliability of lead tip and diaphragm detection, and multi-processing is used to reduce the time to trace positions over the whole image set, the code would need to be packaged and made usable by radiographers. This would involve making the data readily accessible, creating a graphical user interface and training the radiographers to be able to rapidly interpret the data presented to them.

The novelty in this work is the use of on-board imaging data from linear accelerators to detect cardiac frequency motion and report it in a way that can be directly related to planning system data. It has the potential to present motion data live to the operator of the linac, to enable in-situ quality assurance of the internal motion relevant for delivery of radiotherapy to the heart without the use of extra imaging equipment. It is also a solution potentially accessible to all users of conventional linear accelerators which are fitted with kV imaging panels.

2.6 Conclusions

It has been shown that it is possible to use imaging data, acquired as part of a normal patient pathway for treating ventricular tachycardia with radiotherapy, to characterise motion in the patient's heart near the treatment volume. By separating out breathing and cardiac displacement, it is possible to compare this data with published data from other sources which show similar amounts of motion.

Further work should include the application of the data found in this study to the concept of optimising treatment technique for STAR. Consideration should be given to the need to sufficiently treat the volume outlined for ablation and sparing nearby organs at risk. This work also has potential to be used to quality assure patient set-up and may have application as part of post-treatment dosimetric audit.

2.7 Appendices

2.7.1 Appendix A: Geometric method

The geometric method to acquire the projection of the object into the panel coordinate system is described here:

1. Assign coordinates to the x-ray source and centre of panel based on the angle they are at for each position and the distance they are from the isocentre. The x-ray source is 1000 mm from the isocentre, the panel is located 536 mm from the isocentre (total distance 1536 mm from each other).

2. Create vectors for a point at the centre of the panel, $\vec{P}0$ = [Px, Py, Pz], where Px, Py, Pz are the panel coordinates, the source position, $\vec{S}0$ = [Sx, Sy, Sz] where Sx, Sy, Sz are the source coordinates and the normal to the plane, $\vec{n}$

$$\vec{n} = \begin{pmatrix} sx - Px \\ sy - Py \\ sz - Pz \end{pmatrix} \tag{1}$$

3. Define a vector through the x-ray source and the object

$$\vec{u} = \begin{pmatrix} Ox - Sx \\ Oy - Sy \\ Oz - Sz \end{pmatrix} \tag{2}$$

where Ox, Oy, Oz are the object coordinates (CoD, not inlcuding motion), and define the relationship that Op, the position of the object projected to the plane, is

$$\vec{Op} = \vec{S0} + r \times \vec{u} \tag{3}$$

will result in a point in the plane when r is solved for the point where the line and plane intersect.

4. By introducing a vector $\vec{w}$ = S0 - P0, the resolution of r can be expressed as:

$$r = \frac{-\vec{n} \cdot \vec{w}}{\vec{n} \cdot \vec{u}} \tag{4}$$

5. The position of the point in space described by $\vec{Op} = \vec{S0} + r \times \vec{u}$ can then be related back to P0, the centre of the panel to return K and Z' values in the

coordinate space of the panel.

6. Additionally, for each position reported, the conversion from coordinates on the panel into physical distance at the CoD for the object are calculated as:

$$pix2mm = F \times \frac{\|\vec{Op} - \vec{S0}\|}{\|\vec{u}\|} \tag{5}$$

where F is the physical size of a pixel in mm. Note that this can be reduced to $F \times r$.

2.7.2 Appendix B: Error analysis

An estimate of the error contributions for lead tip and diaphragm positions is made here.

Contributions of error:

- Detection of the object of interest by the code
  - For the lead tip, this is 0 ± 0.9 mm in LR and AP and 0.7 ± 0.4 mm in SI
  - For the diaphragm, this is 0.8 ± 0.6 mm in SI
- Relating the detected positions in 3D space to the object's CoD
  - Considering cardiac and respiratory motion: any residual error from the CoD being inaccurately located is negated when Fourier analysis is applied to remove low frequency elements so this error is effectively 0. The same applies where the CoD translates during imaging.
  - Considering patient voluntary / involuntary motion during imaging: error in CoD location or translation can dominate measurement.
- Conversion from pixels to mm distances

- This depends on knowledge of several distances: the length of the imaging area on the panel, the x-ray source to CoD position distance, the x-ray source to the projection of the CoD on the imaging panel, the x-ray source to isocentre position, and the isocentre to imaging panel centre distance (see equation 5 in appendix 2.7.1)
- Assuming an error of 2 cm in the x-ray source to isocentre, isocentre to panel position, and length of imaging panel area, and offsetting the CoD coordinates by 1 cm in X, Y and Z for a CoD which is 5 cm off axis in all the axes, the difference in the conversion is around 1.5%. Given a maximum displacement from the CoD of 2 cm, the error in this step is approximately 0.3 mm.

- Fourier analysis to extract the separate components of motion
  - Quantisation of the fast Fourier transform returns frequency intervals of 0.3 Hz
  - Choice of frequencies at which to split signals is unlikely to result in unwanted combination of cardiac / respiratory / low frequency components.

- Using a 10° symmetric range to select the data for each axis
  - The shape of the pathway over which the lead tip moves is unknown so an assumption is made that it moves on an ellipse
  - The largest observable ratio between LR and AP motion is assumed to be 2. A model of the motion of the lead tip is therefore constructed as an ellipse with the major axis twice the length of the minor axis
  - Diameters taken at 10° from the major and minor axes can be shown to be no more than 4.4% different to the lengths of the nearest axis
  - Averaging the error over the range of angles (-10° to +10° around the axis) results in a maximum error of 1.6%

- For displacement of <1 cm, this translates into a maximum error of 0.16 mm and is only applicable to the LR and AP measurements for the lead tip.

Combining the errors in quadrature and not considering the measured offsets, the total error in positions reported for the lead tip and diaphragm are:

- Lead tip LR, AP: ±0.96 mm
- Lead tip SI: ±0.50 mm
- Diaphragm SI: ±0.67 mm

The error in low frequency motion of the patient is unquantified and may be dominated by the error in CoD location.

The error in the reporting of frequencies for cardiac and respiratory motion is: ±0.3 Hz.

3 On the subject of measurement based target and organ at risk definition for stereotactic arrhythmia radioablation

Authors

James Daniel[*][1], Kevin Burke[£][1], Philip Whitehurst[£][2]

* - Project concept, design, data measurements, data analysis, critical analysis and writing

£ - Project concept, design and supervision

[1] - *South Tees Hospitals NHS Foundation Trust, Middlesbrough*

[2] - *The Christie NHS Foundation Trust, Manchester*

3.1 Abstract

Purpose: A new approach to treating ventricular tachycardia (VT), STereotactic Arrhythmia Radioablation (STAR), has been set up at a number of centres globally. A previously described toolkit for measuring cardiac and respiratory motion in STAR patients has been used to retrospectively analyse a 3 patient sample at a number of points in their treatment. The data from these patients is presented and discussed here with implications for STAR planning methods.

Methods: Patient workflows and technical aspects of treatment are described. Left-right (LR), ant-post (AP) and sup-inf (SI) motion for the pacing lead tips embedded in patients' septal walls was extracted for cardiac motion with and without respiratory motion combined. Target volumes were created to ensure total dose coverage using the measured motion and were compared with the clinically used targets. Stomach positions were measured on 4D CT and related to diaphragm positions in order to enable the use of diaphragm tracking data for the assessment of stomach dose.

Results: Motion of the lead tip and diaphragm are presented for 11 image sets (8 pre-planning and 3 at the point of delivery). On average, approximately 30% of the motion of the lead tip could be apportioned to respiratory motion. Targets which ensured total dose coverage required volumes between 1.5 and 1.8 times greater than those developed clinically for these patients. It was shown that for 2 of the patients, the edge of the visible stomach on the 4D CT average dataset was closely equivalent to the level at which occupancy fell below 25%. Considering the errors involved, it might be possible to maintain low risk of toxicity in the stomach without adding a rind around it. The most relevant way to use the measured data was found to be in the quality assurance of treatment plans, rather than as a forward predictor of necessary treatment volumes.

Conclusions: Measured data for 11 image sequences for 3 patients have been analysed to extract cardiac and respiratory motion traces from on-board imaging systems on radiotherapy treatment units. Analysis of the data has provided insights into treatment planning margins and optimisation processes and suggests potential avenues for future research.

3.2 Introduction

Radiotherapy delivered in a single fraction was originally used as an experimental substitute for surgery in the early years of the 20th century[100]. While the majority of modern radiotherapy is delivered in 15 fractions or more, single fraction treatments have found common use in the palliative setting for those patients who need quick reduction in swelling from tumours compressing the spinal cord and other such acute issues[101]. An aim of radiotherapy in the 21st century has been to reduce the number of treatment fractions; recent approaches include short course ($< 5\#$) and single fraction treatments to treat oligometastases in the spine[102], brain[103], liver[104] and primary tumours in the lung[105].

The cardiology and oncology communities have proposed a novel use of single fraction radiotherapy to treat ventricular tachycardia (VT)[13]: STereotactic Arrythmia Radioablation (STAR). Both CyberKnife[22,12] and linear accelerators[28,38] (linacs) have been used to deliver STAR using different approaches to ensuring radiation dose encompasses the target without adversely affecting adjacent healthy organs[31]. The premise for STAR has coincided with a growing interest in, and the technical abilities required for, delivering thorax treatment in few or single fractions[53]; the novel element for radiotherapy planning and delivery is in directing the radiation beam towards, rather than away from, the heart with its own unique time dependent displacement.

Technical issues in treating STAR mostly come from the various components of patient motion involved: respiratory, cardiac, and voluntary and involuntary patient movement. Other difficulties arise from the relatively poor understanding of the treatment mechanisms in STAR[7] and the normal uncertainty issues involved in delivering radiotherapy. Common approaches to addressing these issues include reducing the motion, tracking the motion and mitigating uncertainty through margins: specifying larger volumes of tissue to treat in order to ensure that the intended treatment volume is dosed, or that the intended avoidance volume is avoided[71].

The application of abdominal compression has been shown to reduce lower lung and liver tumours in all three axes[106], sup-inf motion being notably greater without compression, and more affected by compression, than ant-post or left-right. For STAR, the reduction in diaphragmatic motion also impacts on the heart's motion within the thorax; there is no expectation that abdominal compression should reduce the heart's own pumping motion.

3.2.1 Targets

As yet, there is limited evidence as to how much of the substrate needs to be treated for the desired therapeutic effect in STAR. Whether the effect-causing dose is as low as 20 Gy or as high as 35 Gy[21] and whether that dose is needed to the whole treatment region

or any nearby part of the myocardium[107] are both important questions to answer. While fractionated treatments allow the use of probabilistic approaches to creating planning volumes in which, for example, tumour cells will receive at least 95% of the prescribed dose for 90% of the patients treated[72], STAR targets are currently being created with an approach which translates clinical experience with catheter ablation into the radiotherapy setting. Until more evidence is available, this is likely to be the only way to plan STAR treatments.

Little work has yet been done to provide guidance on how to create target volumes in STAR. It is known that targets over 200 ml are associated with increased mortality[54]. Some treatments have used zero margins[7] while compensating for breathing motion and others have taken a pragmatic approach, treating STAR like other radiotherapy targets[42].

3.2.2 Organs at risk

Critical structures near the target must also be considered in order to safely deliver radiotherapy: treatment aims must be balanced against the potential to harm. Poorly designed treatments can undermine the clinical effort to treat the patient by, for example, destroying the optic nerve so the patient loses their sight[108] or causing fistulae to form in gastro-intestinal organs[53]. In the STAR setting, the stomach is a critical and mobile organ to deal with; in particular the fundus of the stomach moves mostly in accordance with the diaphragm which can be into, and out of, the treatment field over time. At least one patient treated is known to have needed surgery to repair a fistula[53].

In typical radiotherapy cancer treatments, organs at risk which are prone to movement, or for which a small positional offset could result in significant damage, are considered using planning organ at risk volumes (PORV): growing the delineated organ by several millimetres. This ensures that dose constraints such as point maxima are accurate with a high probability, or that they act as upper bounds on the dose

received by the actual organ during radiotherapy. For the stomach in STAR, the same approach can be taken, but doing so can lead to potentially unnecessary restrictions on the dose to the target in order to spare the stomach even in cases in which the stomach dose is not likely to be particularly high. A small number of studies have focused on cardiac motion impacting OAR positioning[109 80] but there is a dearth of dose reporting studies on organs at risk under motion for the kinds of dose constraints considered in STAR (point dose maxima, limiting volumes receiving more than a specific dose).

3.2.3 Paper aims

A number of researchers have applied cardiac and respiratory gating techniques in order to image[82 81 80], plan and treat[33 35] more accurately and with smaller fields. Our centre has demonstrated the use of the Elekta XVI imaging system to track points in treatment verification images for STAR patients (see previous chapter): specifically cardiac displacement at the point of the pacing lead tip and on the diaphragm. Use of the XVI system to track motion was motivated by the possibility of under-sampling cardiac motion in respiratory gated 4D CT scans. We hypothesise that these tracking data can be used to improve target coverage and organ at risk avoidance in STAR.

In this paper, data from 3 patients treated at our centre between July 2019 and November 2020 are presented and analysed to critically appraise our current planning processes. The XVI data allowed characterisation of the displacement in the myocardium at the point of the pacing lead tip and at a point on the diaphragm representative of the stomach. Each of these motion traces is referenced to its own centre of displacement (CoD) and with Fourier analysis, cardiac and respiratory motion were separable at the point of the lead tip. The diaphragm tracking data is assessed as a useful surrogate for the position of the stomach and a classical planning organ at risk volume (PORV) margin is compared against a phase-averaged structure adjusted for the location probability density.

The aims of this work were (1) to examine the adequacy of the cardiac motion

data for the purpose of ensuring target coverage (2) to use the diaphragm motion data to best spare the stomach while not being overly aggressive in avoiding it and (3) to validate our current workflows and propose any relevant changes to workflows for subsequent patients being treated at our centre.

3.3 Materials and Methods

3.3.1 Planning data and patient workflows

Patients attended the radiotherapy department at 3 points in time: pre-treatment motion assessment carried out on a linac with the XVI cone-beam CT (CBCT) system (see previous chapter for detail), 4D CT planning scan acquisition, and treatment. Patients were set up in BodyFIX (Elekta, Stockholm) 'vacbags' at every point in the process.

Motion assessment examined the effect of applying pressure to the abdomen. Compression was applied with the BodyFIX compression system (compression bar) and 4D imaging datasets were acquired with and without the compression bar in place. Motion of the diaphragm and heart were observed over a range of imaging slices and axes, typically using points like the pacing lead tip as helpful reference markers. Separation between the diaphragm and heart was observed, along with any significant bowel or stomach gas that might be forced into difficult planning positions when compression is applied.

Subsequently, 4D respiratory gated CT images were acquired from which averaged 4D images were calculated for treatment planning. Targets were drawn in ProSoma (MedCom, Darmstadt) and Oncentra (Elekta, Stockholm) planning software, the latter being used because of its facility to contour on anatomical slices through short and long axis views of the heart. Targets were made up by combining visible myocardium on various phases of the respiratory gated 4D CT. In one case, a 'target' was drawn on a single respiratory phase before being grown to the equivalent of an 'internal target volume'[71] using other phases, while in the other two cases an ITV was created by the

clinicians in a single step looking at multiple respiratory phases simultaneously. A number of additional diagnostic modalities were used to aid targeting (ECG, invasive and non-invasive cardiac imaging techniques, fast CT, MRI) depending on aspects of the patient's previous treatment. A consultant clinical oncologist was present to aid targeting throughout and advice was sought from specialist imaging cardiologists.

For treatment, patients were imaged before beam on with 3D and 4D CBCT and afterwards using 3D CBCT. During treatment, the surface guidance system, Catalyst (C-RAD, Sweden), was used to monitor patient position. 3D XVI imaging included 360 degrees of gantry rotation with images acquired at approximately every degree ($\sim$ 400 images). 4D XVI imaging included 200 degrees of gantry rotation with images acquired every 0.2 degrees ($\sim$ 1000 images) with a larger field of view. Both imaging sets were acquired at 5.5Hz. Only results from 4D image sets are presented in this work.

The data analysis in this paper is retrospective: decisions about treatment were not made on the basis of the data presented here. Patients 1 and 3 were compressed while patient 2 was not: these decisions were based on the visual interpretation of the images by the clinicians, radiographers and physicists involved, and not a quantitative approach. The decisions made in treating these patients were also peer reviewed by the other national centres treating STAR and the group at Washington University in St. Louis who have provided mentorship throughout the introduction of this novel technique to the UK centres.

3.3.2 Data analysis

Data traces were extracted and analysed according to the methods in the previous chapter for each of the patients. Parameters of interest were the displacement ranges and CoD for the lead tip and diaphragm, the cardiac motion separated from respiratory components, and the frequencies for both respiratory and cardiac motion. A rationale for the reporting methods is presented in appendix 3.7.1. An example of the measured

distribution of lead tip positions in the LR axis is shown in figure 10. Imaging sequences analysed were: the motion assessment scans taken approximately 2 to 3 weeks before treatment both with and without compression applied, and the 4D imaging sequence taken immediately prior to treatment.

Several approaches were then used to process the data as described here.

3.3.3 Tracking point data analysis

In order to present motion from each motion component separately, cardiac motion at the point of the lead tip was assessed both in its unprocessed form and having removed frequencies using the Fourier transform which corresponded to breathing frequencies and below (everything below 30 cpm): everything not overlapping with cardiac frequencies (typically above 60 cpm).

Figure 9 shows the separation of cardiac and respiratory signals graphically. Figure 9:A shows the frequency spectrum for the motion of the lead tip in blue; respiratory frequencies are then removed leaving the orange spectrum which is dominated by cardiac motion frequencies. Figures 9:B and 9:C show the displacement traces: blue for the measured displacement, orange for the Fourier transformed cardiac frequency data only. Both figures 9:B and 9:C show the same data, 9:C is a subset of the data, enlarged to demonstrate the different frequency components.

Figure 10 shows the distribution of positional displacement from the CoD for the lead tip. As in figure 9, blue shows the full displacement and orange shows the cardiac displacement alone. The data represented in figure 10 can be used to determine probabilities with which the lead tip would be within set distances of the CoD. However, this work consistently reports the full displacement trace (table 5 for example): see appendix 3.7.1 for the rationale behind presenting the data in this way.

Displacements in orthogonal axes of motion (LR, AP) were measured by selecting data from gantry angles within 10 degrees of the cardinal angle of interest (-180, 0 for AP and -90 for LR). Displacements in SI used the entire imaging sequence. Frames in

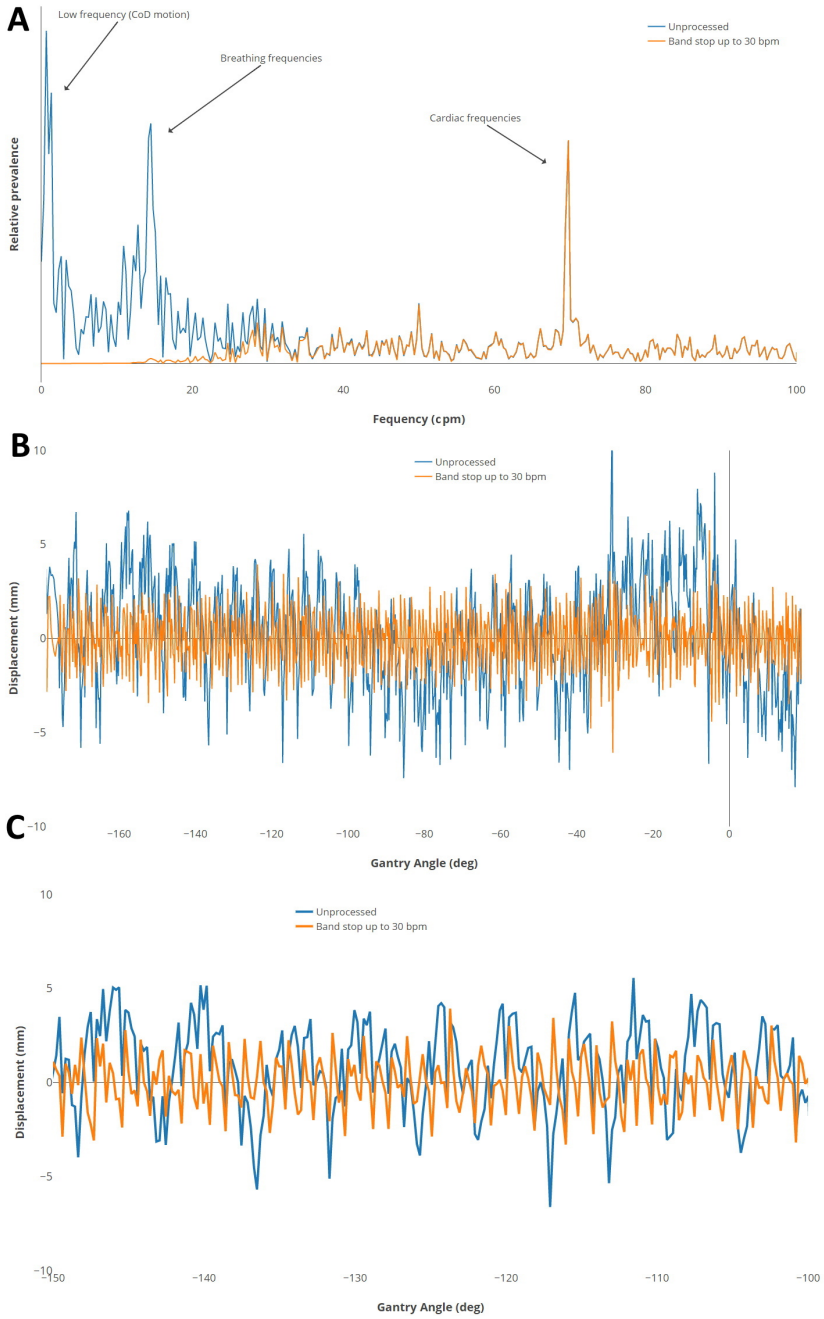

Figure 9: Separation of the cardiac and respiratory signals for a SI data trace. A - the Fourier transform of the original trace seen in blue in B. B - the original trace and its reconstructed counterpart with frequencies below 30 cpm removed. C - a highlighted section of B making it easier to see the respiratory signal in the blue trace and its absence in the orange trace.

which the lead tip were not correctly identified were rejected. To report displacement of the pacing lead tip in the ant-post axis, approximately 150 measured positions of the lead tip were used: 50 from gantry angles around 180 degrees and 100 from gantry angles around 0 degrees (note that these gantry angles are reported in the standard way and refer to the position of the radiation head, but the XVI system is fixed orthogonally to these positions). To report lead tip displacement in the left-right axis, approximately 100 measured positions of the lead tip were used from around gantry angles of 270 degrees. Maximum and minimum positions were then identified to report the full range of displacement of the lead tip. Outlying values created by coding errors, identified by eye and confirmed by comparison with the original images, were removed from the analysis.

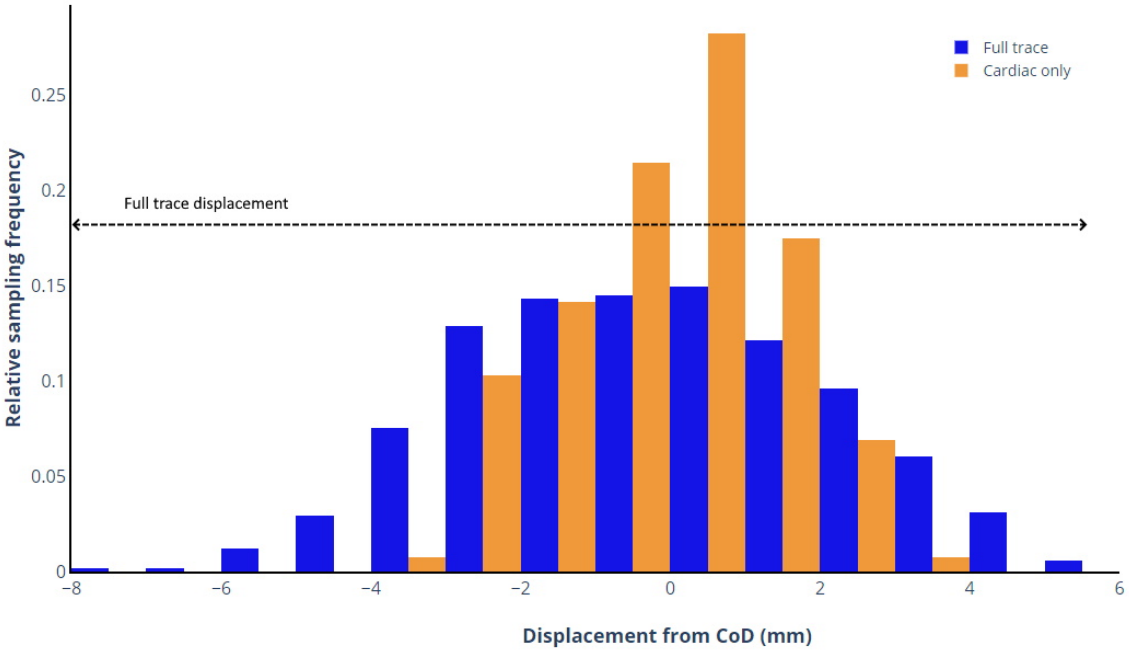

Figure 10: Distribution and reported range for lead tip displacement. Y-axis represents the frequency with which the lead tip displacement was sampled in 1 mm bins, normalised to sum to 1. Blue is the original tracked displacement (cardiac and respiratory), orange is the cardiac motion alone. Indicated reporting range is for the original tracked displacement. See appendix 3.7.1 for further detail.

The absolute position of the CoD for the lead tip in DICOM coordinates (relative to

the imaging isocentre) was found using the iterative method discussed in the previous chapter while the centre of the diaphragm motion was found by taking the median SI position of the diaphragm trace. Maxima and minima values corresponding to inhalation and exhalation positions of the diaphragm were identified using the PEAKS function from the SCIPY.SIGNAL package (version 1.4.1) (see figure 11). Depending on the specific patient signal, different parameters in the SCIPY.SIGNAL package were used to optimise the result, for example a threshold value above which peaks should be identified.

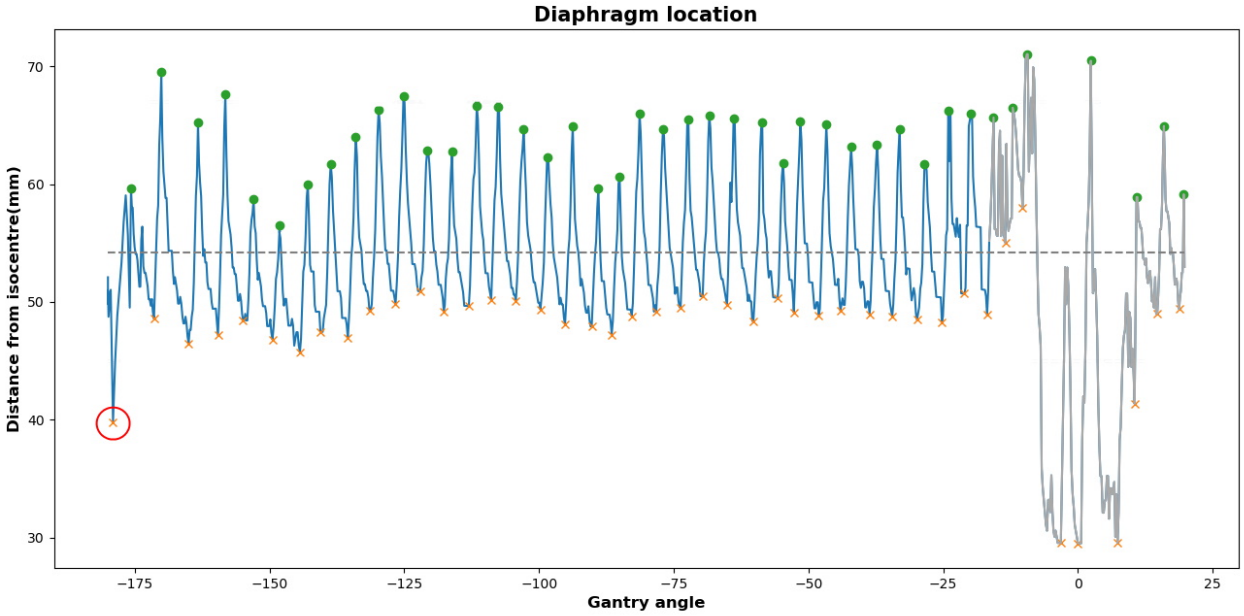

Figure 11: Diaphragm trace (SI) for patient 2. Red circle indicates rejected data points. Grey region beyond gantry = -20 was poorly tracked and not included. Green circles and orange crosses indicate points identified for peak to trough analysis. Dotted line indicates the median value. Note that this is in the coordinate system of the XVI panel meaning that greater positive distances are more inferior in the patient.

3.3.4 Target assessment

To ensure that the myocardium tissue intended for treatment is always inside the treatment field, detected lead tip motion should be considered. In order to illustrate the

increase in ITV and PTV volumes potentially needed to achieve this, new targets were delineated in the planning system using the following method. The 2 phases of 4DCT showing the most extreme myocardial positions were found. Target areas (GTVs) based on the clinical targets were drawn on both of these phases. The GTVs were then expanded by the measured cardiac displacement for each patient and summed to give an ITV. The ITV was then expanded by 3 mm to give an equivalent PTV for the new target, as per clinical protocol. The clinical and modified ITV and PTV volumes were then compared in absolute terms and using ratios. The discussion section describes this approach under the heading 'proposition 1'. The results of these comparisons are shown in table 4 and are illustrated in figure 13. They can be seen as an upper limit on the use of lead tip measurement data to ensure target coverage using the methods proposed in this paper.

3.3.5 Stomach and diaphragm positions

The most superior points on the diaphragm and the fundus of the stomach were recorded on each phase of the 4DCT images for each patient and the range and offset of the positions for each organ were compared.

An estimate of the lead tip CoD was made in the planning CT. Using the XVI measured relationship between lead tip and diaphragm CoDs, the corresponding SI maximum, minimum and CoD positions for the diaphragm in the planning CT were found. The most superior, 25th percentile and median positions of the stomach were identified and compared with the structure drawn on the planning average 4D CT for the stomach and its PORV.

Figure 12 shows the relationship between the cardiac CoD and diaphragm range in each image set. The stomach is visible in figure 12.B as a lighter shade of grey beneath the left side diaphragm.

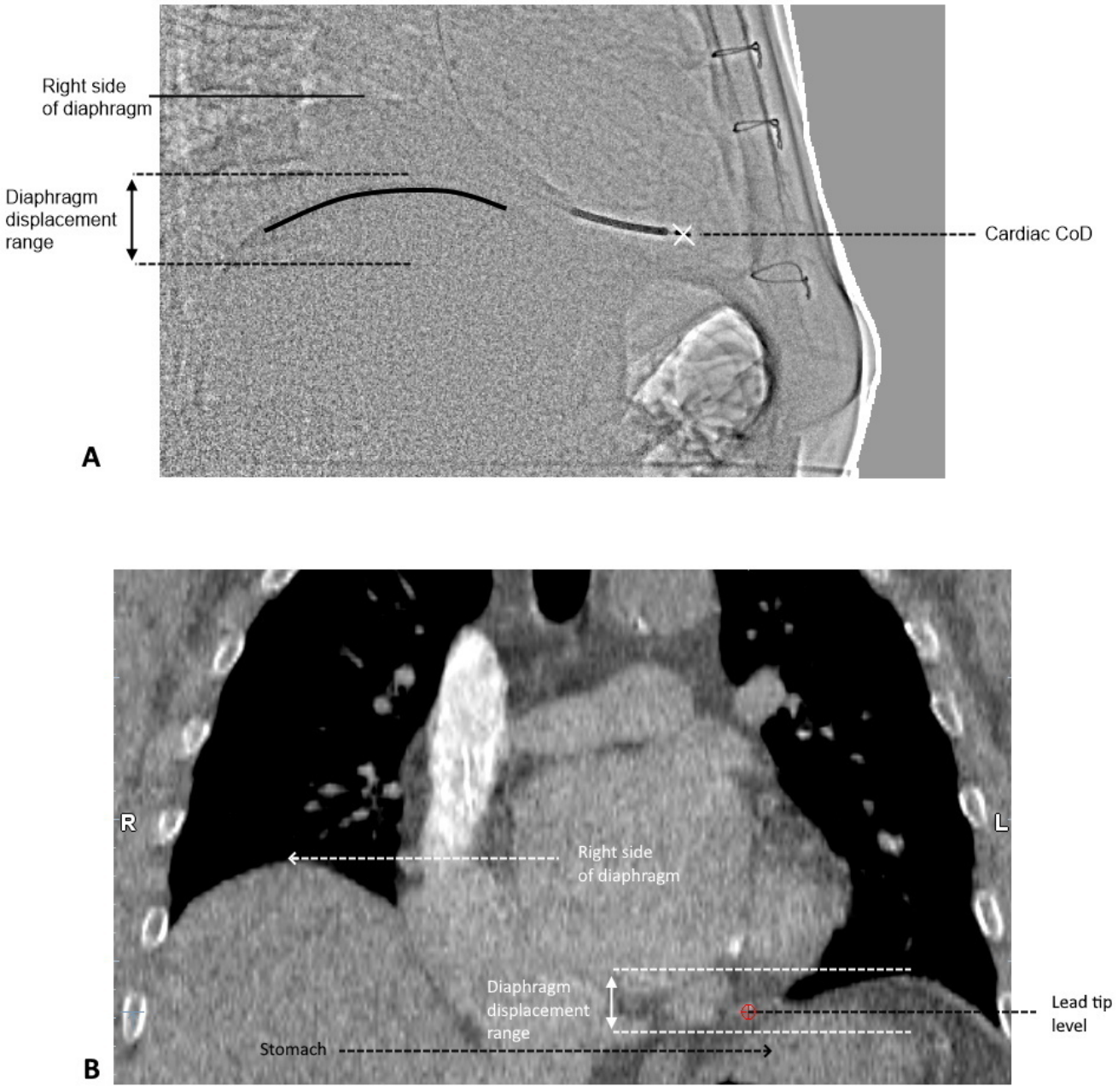

Figure 12: Position of the lead tip CoD and diaphragm range in planar XVI images (A) and from a phase in the 4DCT (B).

3.4 Results

Tabulated values for each data extraction and analysis task are presented here. Errors associated with each measured point are 0.96 mm for LR and AP displacement, 0.50 mm for SI displacement of the lead tip and 0.67 mm for the diaphragm.

Table 4 compares ITV and PTV volumes produced for the clinical plans given to the patients and the volumes produced by including the measured displacement.

	ITV (cc)			PTV (cc)		
Patient	Clinical	Modified	Ratio	Clinical	Modified	Ratio
1	61.2	159.6	2.6	139.2	253.2	1.8
2	31.9	60.9	1.9	75.1	109.4	1.5
3	23.3	51.2	2.2	62.8	94.5	1.5

Table 4: Comparison of ITV and PTV volumes created for the clinical plans and using the cardiac displacement data to expand the ITV (modified).

Table 5 presents the total displacement and cardiac only displacement for the assessment and treatment verification scans for each patient. Patient 3 had 2 assessment sessions 6 months apart and so has 4 assessment measurements. Patients 1 and 3 were compressed for treatment and patient 2 was uncompressed for treatment. Average total displacement measurements for the lead tip across all datasets were: 7.7 $\pm$ 1.4 mm, 9.7 $\pm$ 1.9 mm and 11.8 $\pm$ 2.3 mm in LR, AP and SI axes respectively. Cardiac only displacement was: 5.9 $\pm$ 1.0 mm, 7.0 $\pm$ 0.6 mm and 8.2 $\pm$ 0.8 mm in LR, AP and SI.

Tables 6 and 7 include the data relevant to identifying the stomach in the kV images.

Patient	*Image sequence*	Frequency (cpm)		Full trace			Cardiac			Diaphragm
		Cardiac	*Respiratory*	*LR*	*AP*	*SI*	*LR*	*AP*	*SI*	*SI*
	Assessment: Compressed	60-84	20	10.9	8.0	10.4	6.6	7.1	8.3	19.0
1	Assessment: Uncompressed	57-82	16	9.3	10.7	10.2	7.2	6.8	9.4	22.3
	Pre-treat 4D	60-86	15	8.4	7.7	8.8	5.8	6.0	7.2	15.3
	Assessment: Compressed	70	15	6.1	10.8	14.5	4.3	6.5	7.4	8.5
2	Assessment: Uncompressed	70	15	7.0	9.7	15.5	6.7	7.4	9.5	15.5
	Pre-treat 4D	72	16	7.9	6.7	12.9	5.7	6.3	8.0	14.9
	Assessment: Compressed (1)	55	22	7.6	9.2	9.7	7.1	7.2	8.6	11.9
	Assessment: Uncompressed (1)	55	14	7.6	8.5	14.2	6.0	6.4	8.2	22.2
3	Assessment: Compressed (2)	50	19-22	7.1	11.5	10.1	6.4	7.8	8.8	11.3
	Assessment: Uncompressed (2)	48	11-14	6.2	12.5	13.2	5.4	7.8	7.5	14.7
	Pre-treat 4D	54	15-21	6.4	11.8	10.6	4.1	7.3	7.4	14.7

Table 5: Total and cardiac only displacements measured for each patient. Diaphragm displacement is presented in the SI direction. All values in mm.

Patient	Mean (mm)	St dev (mm)
1	14.8	0.9
2	8.0	1.9
3	9.4	1.5

Table 6: Mean and standard deviation of the distance from the diaphragm crest to the most superior edge of the fundus of the stomach measured on 8 phases of 4DCT.

	Planar images (mm)		Planning CT (mm)	
Patient	Max	25th pctl	PORV	Visible
1	5.4	3.2	5.3	3.3
2	4.4	2.4	-4.9	-8.9
3	6.3	2.4	4.5	2.5

Table 7: Distances from the median position of the stomach as detected in planar images: 'max' at maximum exhale, and '25th pctl' is the point above which the stomach resides for 25% of the time. Comparison with positions from 4D CT also referenced to the median position of the stomach.

3.5 Discussion

Implications of the lead tip displacement on targeting are discussed here, as well as the effects of abdominal compression and the differences between pre-planning and treatment. Note that given the inherent uncertainties in the data extraction process, any displacement or difference less than 1 mm is ignored in this analysis. The small patient numbers must be considered; this analysis has been performed in order to examine the utility and potential of the information retrieved, not to make broad generalisations.

3.5.1 Implications for targets

Before applying the measured data to the targets, the limitations of the datasets are discussed: there are 2 main difficulties in using the data from table 5.

Firstly, the displacement relates only to a single point in the ventricular wall and cannot be simply applied across the whole ventricle as if it contracted identically. Secondly, 4D CT data does not contain images of the heart in all phases of its contraction.

The first point cannot be addressed by tracking a single point in the heart. It is possible to modify the displacement seen at the lead tip using published data for motions of the cardiac wall in healthy volunteers[75], but this is a crude model and would need development and testing to use clinically. Other points of interest in the heart might be traceable: calcification and other ICD leads for example. Future studies will aim to track more of the myocardium using the same images.

The second point describes the challenge in imaging the heart with technology that has been developed over time to control for respiratory motion only. This presents a fundamental challenge to the delineation of structures in the heart for planning as well as making it problematic to locate the lead tip CoD in 4D CT images. For the cases reported in table 5, there is asynchrony between cardiac and respiratory frequencies meaning that there will be some undefined amount of cardiac positional data missing in the 4D CT. If the heart rate for a patient was an exact multiple of the

breathing rate during imaging, one might expect that the heart would move in the 4D CT with respiratory motion only: the same cardiac phase would be captured for every respiratory phase. As a basic comparison, the lead tip was identified in each phase of 4D CT images and was found to exhibit approximately 50% of the motion seen in the XVI data.

A partial solution to both of these issues is suggested here, with the underlying assumed principle that STAR should be treated as per oncological targets in which coverage of the whole target is aimed for.

Proposition 1: Identify the phases which show the extremes of cardiac positions in the 4D CT data. Contour the target on each of these, expand these targets in each axis by the measured displacements (values from table 5, "Full trace" column), scaled according to published data[75], and add them together. This approach should provide a final ITV in which the cardiac tissue for treatment will always exist, provided the measured displacement represents the full range of motion at all points in the target.

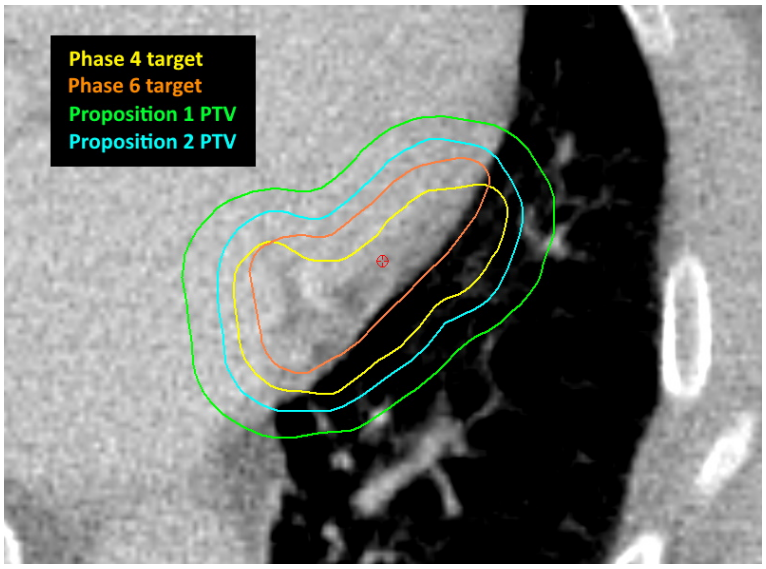

Figure 13: ITVs created from 2 phases of the 4DCT for patient 1 at a point on the anterior wall of the left ventricle. PTVs created for each of the propositions suggested here are displayed.

Proposition 1 appears to create an ITV larger than necessary. However, without cardiac gated imaging with the patient in the treatment position, it is not possible to know that the full range of cardiac motion has been captured for treatment planning and so reliance on a process like proposal 1 would be appropriate. Note that only one PTV was made larger than 200 cc using proposition 1 in this small patient sample. However, it must be recognised that larger treatment volumes do not lead to improved outcomes: the exact opposite is true in fact[54].

A second proposition is therefore suggested which aims to ensure that *some* of the target is consistently within the ITV.

Proposition 2: Targets should be delineated as suggested in proposal 1 by looking for extremes of motion in the respiratory phases. These targets on different phases should be summed into an ITV which can then be quality assured by checking for minimum thicknesses corresponding to the displacement measures from the lead tip. Where the total width of the ITV is less than measured displacement, it should be expanded.

Proposition 2 represents clinical practice much more closely than proposition 1. For the patients in this study, this approach would have suggested broadening the ITVs by a relatively small amount in comparison to proposition 1: up to 3.5 mm for patient 2 in the SI direction (12 mm target thickness and 15.5 mm displacement of the lead tip). For both proposition 1 and 2 however, a targeting approach based on respiratory gated information does not necessarily include the range of motion seen in motion at points in the myocardium.

The information missing from this discussion is knowledge of how much tissue needs to be treated in order to achieve a treatment effect: a reduction in VT burden and fewer ICD shocks. Proposition 1 ensures coverage of the target, as much as is possible, while proposition 2 is focused more on ensuring that some of the tissue is treated to the prescription dose. Following the experience of catheter ablation for treating VT, the key aim of treatment is to 'cut' across errant circuits in the myocardium. Given

a high fidelity knowledge of the location of those circuits, it might be possible and preferable to create plans aimed at treating just the minimum of tissue. If the data shows a specific minimum dose level at which 'cutting' effects occur, then by including the quality assurance from knowing cardiac wall displacements as described above, it would be possible to prescribe the minimum necessary treatment volume (MNTV) to ensure success. Achieving the MNTV should be one of the goals of further research in this field. Most importantly, the principles laid out here by measurement must absolutely be balanced against the need to treat patients in such a way that life is preserved as a priority and ensuring that numerical approaches do not interfere with good clinical outcomes[54].

3.5.2 Effects of abdominal compression

The effect of abdominal compression is discussed here: firstly with regard to the diaphragm motion and secondly with regard to the lead tip displacement. Only the assessment scans are discussed; differences between assessment and treatment are presented in the next section.

Respiration depth measured as the average peak-to-trough distance changed when compression was applied, but the difference was not consistent for all patients. Patient 1 showed a 3.3 mm (15%) decrease in respiration depth with compression. Patient 2 showed a more dramatic 7 mm (45%) decrease in breathing depth with compression. Patient 3 had 2 assessments 6 months apart; their breathing depth under compression was consistent (between 11 and 12 mm) and less so without (between 14 and 22 mm).

Respiration rate can also be considered. Patients 1 and 3 showed an inverse relationship between breathing rate and depth: faster breathing was associated with shallower breaths. The dramatic change in respiration depth for patient 2 was not associated with a change in their breathing rate.

Considering the displacement of the lead tip, compression had a limited and unpredictable impact. Patient 3 demonstrated the most intuitive change: SI motion was

suppressed under compression in each of their assessment sessions (3.8 mm average reduction in SI motion). Patient 1 experienced increased displacement in LR (10.9 mm with compression vs 9.3 mm without), suggesting that the compression was pushing the diaphragm against the heart and forcing it outward with each breath. Taking the cardiac motion separated from the respiratory components (see figure 9:C for comparative reference), there were no significant differences between the axes with and without compression for patients 1 and 3. Patient 2 showed reduced LR and SI motion for cardiac motion alone under compression.

In the sample of 3 patients in this study, abdominal compression was able to suppress diaphragm motion but had limited effect on the motion at the position of the lead tip. For the purpose of controlling target motion, there was limited application for abdominal compression in these patients. Abdominal compression generally reduced diaphragm motion providing improved control over the position of nearby organs at risk.

3.5.3 Assessment compared with pre-treatment scans

Firstly correlation between SI displacement of the lead tip and breathing depth at all points in the patient pathway is discussed before differences observed between assessment and treatment for each patient are analysed.

Full trace SI displacement at the point of the lead tip correlated with breathing depth to some degree for each patient. r^2 values for least squares regression for patients 1 and 3 were both 0.7. For patient 2 however, there was no correlation seen between breathing depth and SI motion at the lead tip ($r^2 = 0$). This can be explained by the patient's inconsistent breathing patterns. While the breathing depth for patient 2 under compression was relatively low, the average position of the diaphragm varied considerably as did the average position of the lead tip making the actual displacement as large as it was without compression. The patient did not report discomfort but abdominal compression clearly had some negative impact on their breathing. Erratic

breathing under compression was also observed visually and contributed to the decision to treat patient 2 without compression. Given that the cardiac motion itself was affected by compression, the decision not to compress the patient appears validated.

When attending for treatment (compression applied) patient 1's breathing rate was lower (15 vs 20 bpm) and their depth of breathing was also reduced (15 versus 19 mm). Their LR and SI lead tip displacements were significantly reduced while cardiac displacement alone was affected less between assessment and treatment. The main difference for patient 1 at treatment was reduced diaphragm motion resulting in reduced motion at the lead tip. The patient may have been more anxious at their assessment scan and more relaxed at treatment, possibly through greater familiarity with the process and environment of the linac bunker.

Patient 2 had a breathing rate and depth similar at both assessment and treatment; AP and SI axes showed lower lead tip displacement at treatment compared with assessment.

Patient 3 showed an increased breathing depth and a decreased breathing rate at treatment compared with both their 'compressed' assessments. This difference did not translate into differences in lead tip displacement except in LR where the displacement was reduced.

These data demonstrate the potential for the use of this measurement and analysis toolkit to quality assure patient set up by comparing values from pre-planning with pre-treatment before initiating the treatment beam. In the case of all of the patients, it would have been notable that motion was reduced. The increased breathing depth seen for patient 3 may have been interpreted as an issue. A greater number of data points may help draw out any trends between these observations.

3.5.4 Organs at risk

Table 7 shows that by considering the lead tip CoD as a fixed point in the patient and applying the relationship between tip CoD and diaphragm CoD found in the XVI

image sequences, it is possible to predict CT slice positions for which the apex of the fundus of the stomach is likely to be present for a set percentage of time. If 25% and 50% are chosen, patients 1 and 3 show that the practice of outlining the stomach on the 4DCT and growing it by 3 mm gives remarkably close agreement between the visible stomach and the 25th percentile, while the maximum position of the stomach is close to the PORV location.

Using patient specific occupancy positions measured using data over tens of respiratory cycles at high frequency, as in the XVI datasets in this study, a more patient-specific and slightly less conservative approach may be feasible. Instead of applying the tolerances to the PORV, if one uses the occupancy factors of 0.25 and 0.5 for the newly defined regions, one can apply the same tolerances multiplied by 4 and 2 accordingly. Note that 2×17.5 Gy[42] is 35 Gy: a dose level not usually encountered in these plans which suggests that one could apply no tolerances above the slice representing the 50% occupancy of the stomach (see figure 14).

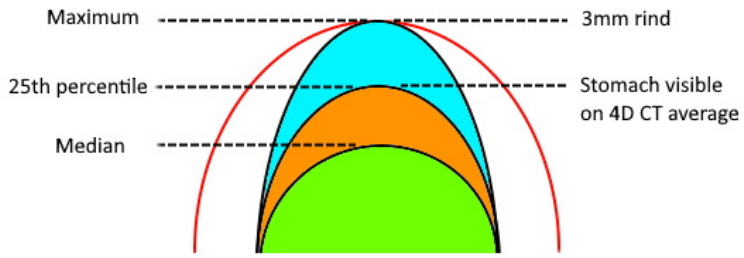

Figure 14: Schematic of the measured stomach positions compared with those delineated on the planning average 4DCT images for patient 1. Green represents 100%, orange is 50% and light blue is 25% occupancy. The red line indicates the original 3 mm PORV around the original delineated stomach (middle black line).

Two issues must be considered. Firstly, the errors associated with locating the point of 50% occupancy for the stomach and secondly the reproducibility of this point between planning and treatment. The error analysis is presented in Appendix 3.7.2: the

estimated error in finding the 50% occupancy position is 3.4 mm. Reproducibility can be assessed by comparing cardiac CoD to diaphragm CoD distances against the same distances measured at pre-treatment: 3.6, 1.3 and 0.9 mm for each patient respectively.

Adding the 3.4 mm error onto the SI position of the stomach's 50% occupancy position results in approximately the 25% occupancy position which correlates with the superior edge of the stomach as defined on the averaged 4D CT scan (see figure 14). The implication for treatment planning would then be to treat the 4D CT average definition of superior stomach edge as the 50th percentile position: at most, one would expect for that edge to receive 50% of the dose observed in the treatment plan at that position. Under such conditions, stringent planning requirements to maintain maximum doses of less than 22 Gy to the stomach PRV (3 mm beyond that edge) might be relaxed leading to more optimal coverage of the myocardium if near the stomach.

Table 7 shows this to be an effective strategy for patients 1 and 3 but not for patient 2 where approximately 1 cm of difference is seen between stomach positions predicted using the XVI data and 4D CT. As previously noted, patient 2 was observably less stable than the other patients: they were not compressed for treatment and their breathing patterns were erratic.

There is insufficient data here to determine whether this approach would work for the majority of patients, but it raises relevant questions about how reproducible critical structure locations in STAR patients are. Using this data toolkit at the point of treatment would allow one to determine the distance from the heart to the stomach (diaphragm surrogate): quality assuring the abdominal compression. This opens up strategic possibilities such as repositioning the compression or preparing multiple plans assuming different relational positions of the structures and selecting the optimal plan on the basis of the measurement.

This analysis also highlights the need for planning data to be motion based and not captured at a single point in the respiratory cycle. A free-breathe CT scan might

select a stomach position at peak inhale: up to 1 cm from its median position which could lead to an underestimation of the dose it will receive at treatment.

Even when 4D data is used as the input for treatment planning, most modern planning systems and workflows are not equipped to efficiently provide motion-based OAR dose reporting which means there is limited data on the effect of motion, cardiac, respiratory or otherwise. While this should not limit progress for STAR at this stage in its development, it may impact on a centre's confidence or ability to completely treat target volumes when the stomach, oesophagus or other OAR is close by. With developing technologies and techniques, it is conceivable that OAR motion will be "built-in" for future radiotherapy endeavours, at which time it may be possible to review and refine the treatment approaches in the ways proposed in this paper in a more routine manner.

3.5.5 Further work

This is a preliminary piece of work intended to explore the utility and potential for a toolkit which can measure displacement and CoDs for the lead tip and diaphragm / stomach in STAR patients. Various avenues for future work are opened up and a few are discussed briefly here.

3.5.5.1 Quality assurance process

Quality assurance of the treatment planning and delivery process for STAR has been discussed previously in this work. An overview of a potential quality assurance process and the requirements for its implementation are laid out here.

Primary data is acquired prior to treatment planning on the linear accelerator and includes the displacement of the pacing lead tip in all three axes, the displacement of the diaphragm and the relative distance between both CoDs. At the point of treatment, secondary data is captured, remeasuring the same displacements and distances.

These data are valuable at different moments during the patient pathway. At the point of treatment delivery, a comparison of primary and secondary data would allow the opportunity to quantitatively assess patient set up in terms of abdominal compression reproducibility and patient breathing patterns. At the point of treatment planning, decisions could be made about whether motion is large enough to warrant the use of multiple plans which are either more accepting of dose close to organs or restrict dose to the target to protect organs at risk. When the secondary data points are compared to the primary at the point of treatment, the most appropriate plan given the patient set up would be selected for treatment. The same principle is used for various treatment sites (bladder as an example[110]) and is usually referred to as 'plan of the day'.

In order to make this process feasible, speed would be the critical element to improve on. Currently, data must be taken from the XVI servers which takes a few minutes to copy, then the code is run which takes several minutes more. In total, the process might take 10 minutes to run. The code is also in an experimental state and can only be run by the author of this work. It would need to be made accessible for multiple users with due consideration for regulatory needs if this procedure results in decisions about irradiating the patient being made on its results.

3.5.5.2 Vector modelling and other points in the images

Significant amounts of data are discarded by this work: approximately a quarter of the images in a 4D XVI imaging sequence are useful for determining the displacement of the lead tip at cardinal angles. Assuming perfectly periodic motion, the captured data could be applied to developing a motion model, rather than simple displacements which would refine the information regarding target definition.

Additionally, some patients have multiple sensing leads and calcification in areas of myocardium that would be useful to track and model and this toolkit can be modified

to do so.

3.5.5.3 Velocity considerations

Considering the total displacement seen in table 5 and assuming no deformation of the tissue in the septal wall, the measured frequencies can be used to show that parts of the heart are moving between 6 and 21 mm/s.

Time dependent factors in delivering STAR are: motion of the MLC, motion of the gantry, dose rate, and the periodicity (if any) of these. A comparison of the velocities encountered in STAR plans against the velocities and vectors of motion encountered here would be beneficial to demonstrate the impact of cardiac and respiratory motion on the intended dose distributions. Lydiard et al.[33] have demonstrated the benefit of MLC tracking for STAR treatments, measurement data from this work can contribute to that avenue of research.

3.5.5.4 Deep inspiration breath hold

An extension to the use of abdominal compression for STAR would be a 'deep inspiration breath hold' technique, commonly used for breast treatments[111] albeit typically to reduce dose to the heart. Such a technique is capable of reducing diaphragmatic motion, taking a significant component of motion out of consideration.

There is at least one centre delivering STAR using a deep inspiration breath hold (DIBH) technique. Such a technique largely removes the respiratory element of motion from the patient. A useful piece of work for technique validation would be to compare patient traces using this toolkit in DIBH versus a free-breathing set up.

3.5.5.5 Gating

This toolkit provides a retrospective method for acquiring motion data during STAR

imaging. It is possible to acquire kV planar images during treatment. A future project might look at acquiring that data 'live' during treatment and using the diaphragm and cardiac data to gate the treatment.

3.6 Conclusions

A point-based tracking system has been applied to on-set imaging of patients receiving STAR treatment. The data measured at the point of the lead tip and diaphragm has highlighted that motion data additional to respiratory gated 4D CT images can significantly alter the observable motion in both the target and organs at risk for STAR patients.

Our centre is planning these patients in accordance with a UK national group of centres aiming, in the first instance, to provide another line of treatment to patients who otherwise have exhausted their treatment options. As the target is not cancerous, the normal principles of treatment planning do not necessarily apply meaning that an under-treatment of the target may not be an issue if the relevant parts of the heart are receiving a sufficiently high dose; the problem being that it is clear neither which parts of the tissue need to be dosed nor what the relevant dose is.

As this work continues in clinical trials, it must take an approach with unifies the planning approaches in order to make reasonable sense of the outcomes, both in producing a clinically desired effect and restricting any negative outcomes associated with the use of radiotherapy in the thorax and abdomen. In the short term, on the basis of these results, we aim to quality assure our planning volumes using the measurement approach described in this paper and to work towards using this tool to ensure patients' cardiac and respiratory motion is the same at treatment delivery as it was at planning.

3.7 Appendices

3.7.1 Appendix A: Notes on data reporting

Throughout this paper, the full displacement of the lead tip is reported (see figure 10) and the peak-to-trough diaphragm displacements are reported. The rationale for this is presented here.

The lead tip displacement includes cardiac motion, respiratory motion and any external patient motion and represents the 'real' values that are relevant when considering *where* the lead tip will be over a 3 minute period. Another way to present the data would be the average distance travelled during one heartbeat, but the sampling frequency of 5.5 Hz is too low to do so and preserve the integrity of the data and this can be demonstrated by considering a simple sinusoid.

For a sampling frequency of 5.5 Hz, a 60 cpm signal (cardiac) has 5.5 samples per cycle. For a sinusoid sampled at 5.5 samples per cycle, the observed peak-to-trough differences are approximately 90% of the expected amplitude on average. Over 10 cycles, the average peak-to-trough differences are approximately 98.5% of the expected amplitude. Over more cycles, the effect is essentially negated. Presenting the data as the full displacement therefore means that one can make the statement: "the lead tip did not move outside of a region X mm wide during the imaging sequence". This approach presents the data in a clear way, but also one in which the displacement is maximally reported.

For the same sampling frequency, a 15 cpm signal (respiratory) has 22 samples per cycle and the effect is barely apparent even over a single cycle. When the data is presented as peak-to-trough distances, it is less affected by, for example, a very deep breath which would extend the range of displacement.

3.7.2 Appendix B: Error analysis

Measurement of the distance between the heart and the diaphragm in the planar images is subject to the error analysis from the previous chapter. Given a 0.5 mm error in both SI positions, the distance to the diaphragm 50% occupancy position should be cited as 0.7 mm.

High quality 4D planning images are then required to estimate the distance from the diaphragm to the stomach which is estimated to have an error of 2 mm (1 CT slice width). Note that the stomach-to-diaphragm distance varies across phases; the average distance was used in this analysis.

Finally, the error in estimating the lead tip position in the 4D dataset must be addressed. The maximum travel from the CoD seen in this study was 15.5 mm; assuming a normal distribution of possible CoD locations, 1 standard deviation from the CoD would be around 2.6 mm which we use here as an estimated error in locating the lead tip CoD.

Combining these errors in quadrature results in an error estimate of 3.4 mm.

If a registration point is created for the patient at the assessment scan and used again at planning, the largest error (2.6 mm) would be mostly negated. Total error would then be 2.1 mm.

4 Critical analysis

4.1 Introduction

This work has demonstrated the feasibility of characterising cardiac motion in radiotherapy patients on conventional linear accelerators. The required images can be captured during routine preparation for radiotherapy and the output data can be included in treatment planning workflows and referred to at the point of delivery to ensure reproducibility. The methodology for capturing this motion data uniquely ensures that the patient is both in the treatment position *and* is under treatment conditions: they are in the environment in which treatment will take place. This gives the best opportunity to measure cardiac and respiratory motion under similar stress conditions to those the patient will experience again when they return for treatment. While this work is inconclusive with regards to the full applicability of the data, it has begun to show how it might form part of organ at risk delineation and can contribute to ensuring that treatment volumes are of sufficiently large dimensions.

This section presents a critical analysis of the methods used to measure and analyse the data in this thesis. Areas of interest are highlighted and a concluding section reflects on the project in its entirety.

4.2 Use of XVI data

Firstly, the concept of using XVI data for this project was a positive development. The imaging data was incidentally acquired as part of the 'normal' work up for these patients meaning that there was no extra radiation dose given to them for this research project and no extra complications for the patients during their treatment. Pacing lead tips and diaphragms were clearly visible in nearly all the captured images making this project feasible. STAR is too nascent for commercial systems to have yet been developed for this purpose but if the field becomes large enough, one might expect to see such systems become available.

The primary benefit of using this data was that the patients were in the treatment position for radiotherapy. Several other imaging approaches for gathering motion data in the heart and lungs of patients are available such as ultrasound, MRI, fast CT and others. Measurements made with these other modalities can be accessed and would be useful and problematic in their own ways. Ultrasound has the benefit of extremely high temporal imaging frequency, typically in the kHz range, meaning that temporal aliasing problems would be negated but it can produce artefacts around pacing lead wires which would need to be accounted for. 4D MRI is also capable of capturing images at a higher rate than 5.5 Hz in this study, but often suffers from artefacts generated by the pace maker. Fast CT scanners can produce exquisite images of the heart with contrast, but usually have gantries too small and incompatible couches to accommodate radiotherapy immobilisation devices. The XVI system has the advantage of being in the treatment room and truly represents the patients in the environment and position ready for treatment, and uses low energy x-rays which are preferentially absorbed by the lead tip material, creating good amounts of contrast across a large number of angles.

The main issues with using XVI data to track the pacing lead tip are (1) the limited positional range it represents: a single point in the myocardium and (2) the relatively low frequency of image acquisition. It has been mentioned several times in the text that the heart moves in a wringing motion and a single point cannot fully represent it. However, the single point has utility in being measurable at multiple points in time, making it a viable quality assurance tool for treatment. From the imaging parameter aspect, changes to the parameters for XVI (frequency, kV, mAs) have not yet been investigated and it may be possible to improve the utility of the processes defined for this work by doing so.

A number of extensions to this work would be useful. Firstly, the use of the Clarity (Elekta, Stockholm) ultrasound system, which is used for prostate positioning and tracking in radiotherapy, to supplement the data measured on XVI. For no extra ra-

diation dose to the patient, Clarity, or some other ultrasound system, might be able to measure displacement ranges at multiple points in the heart. Secondly, more of the data gathered by XVI might be used. A large quantity of data is wasted in restricting the gantry angles around the angle of interest to $\pm$ 10°. Some work was put into modelling the motion of the lead tip to produce a full motion trace in 3D but the work had to be stopped because of time limitations. One problem with this side project was an assumption that every heartbeat was identical, but it is possible that an approach could be found to producing 3D motion traces from the XVI measured data. Thirdly, other points might be tracked in patients' hearts. Sensing leads, calcification and other high density regions were visible in the images captured for the 3 patients in this study which might all be used to track different areas of the heart and add to the planning information on a patient-by-patient basis.

4.3 Image processing

The image processing techniques that were used to highlight the lead tip and diaphragm were successful but could be improved. This work was essentially a feasibility study and the measured data corroborates the hypothesis that it is possible to retrieve cardiac and respiratory motion from XVI data. The image processing approaches, however effective, were fairly simplistic. Artificial intelligence approaches might be trained to highlight objects in these images more successfully and increase the rate of frames without detection errors. A simple first approach might be to track the angle of the lead tip and generate edge detection kernels using those angles. Additionally, diaphragm-shaped (parabolic) kernels may help to increase the detection rate of the diaphragm.

Lead tip detection rates were reasonably high, but could be improved. The main issue was a loss of contrast at angles where the lead tip and lead were in a direct line with the x-ray source and panel; the tip 'disappeared' into the lead. Not much could be done to recover those angular data, but where that issue occurred at cardinal gantry angles (which were always chosen to measured displacement in DICOM axes), an

alternative approach might have been chosen. For example, gantry angles offset from cardinal positions in orthogonal pairs could be used to improve the amount of data available. As noted above, a side project to use more of the acquired data had to be stopped because of time limitations and may be continued in the future. Another route to improve detection rates would be to adjust the imaging parameters to specifically improve contrast in the lead tip and diaphragm.

More robust methods for tracking the diaphragm are in common use: the XVI system uses the 'Amsterdam Shroud' techniques (compressing images into a single column of data) to track the breathing phase of the images. However, the disadvantage of that technique is that it is ignorant of the geographical point at which the data is acquired and cannot be immediately translated into distances between heart and diaphragm, for example. Other authors also present different methods for diaphragm tracking which produce more robust traces[112].

The advantage of the process in this study was the ability to position the point of diaphragm tracking at any location. If the location was anywhere other than near the most superior point, it would suffer from being obscured at different gantry angles, but this is a surmountable problem and opens possibilities of tracking any internal location in the patient.

4.4 3D geometric approach

The approach used in this study was to select objects in 3D DICOM sets and then track them in 2D kV planar images. There are doubtlessly many ways in which 3D objects can be tracked in 2D images (the computer games industry is entirely focused on translating between 3D and 2D as an example) but this specific approach for linac point tracking has not yet been exploited. There are, however, many examples of other, similar pieces of work for tracking tumours in the lung[113], using kV-MV image pairs to track fiducials[114], and other applications for object tracking with kV images in the literature[115].

The downside of this approach is the requirement for 3D datasets to be constructed and examined by a human operator prior to tracking being performed. An extension to this would be to allow an iterative approach to finding the diaphragm and lead tip which could speed up the process and make it more viable for quality assurance prior to treatment, for example. Template approaches to fiducial tracking for example remove the need for this step.

The main error introduced by this approach is that pixel to mm conversion of distance is always performed at the position of the centre of displacement (CoD) and not the current tracked point in 3D space. This results in an error in the conversion of approximately 1% per cm distance from the CoD which is negligible (<0.5 mm) over distances up to 3 cm displacement. For the purpose of diaphragm and cardiac motion tracking, it is sufficiently accurate.

4.5 Application of data to patient anatomy

As noted, tracking motion at a single point has the problem that it cannot fully represent the motion of the myocardium. It has been used in this study both to suggest a method for fully covering targets, by using some model of cardiac motion to scale by the detected motion, and to quality assure volumes: to check that volume dimensions at least take into consideration displacement at some defined position. The latter approach is more likely to be successfully adopted into clinical practice than the first given the large scale expansion of treatment volumes needed to cover the target presented in this work. Doing so is not in line with good radiotherapy practice: positive outcomes have been observed without applying such large expansions to volumes. It is also much more likely, according to the various publications on the subject, that target sizes will become smaller in the course of time: cutting through errant circuits, rather than ablating large volumes of cardiac tissue.

The proposal for applying occupancy-based tolerances to the stomach sparing is potentially applicable with the caveat that it must be done carefully on a patient-

by-patient basis. Our centre has removed sections of target volumes in order to keep the dose low in the stomach PORV. By applying a measurement based approach to stomach location occupancy, that might be avoided. Whether this has any impact on the effectiveness of treatment is another question which cannot be answered without trial data.

The stomach is the obvious organ to observe using the methods in this work: its radio-sensitivity, proximity to the treatment site and motion in line with the observable diaphragm all make it a worthwhile target for tracking. Other organs could also be considered such as the oesophagus. Some method for improving the contrast of other organs at risk would be required such as implanting a metal fiducial or having the patient swallow some radio-contrast agent. In theory, it would be possible to track multiple points in the patient near the target to ensure control over the target and organs at risk for STAR treatment.

4.6 Conclusions

This work contributes to the field of cardiac SABR in a number of ways: demonstrating the feasibility of the service in a modern radiotherapy centre, progressing the aim of quality assurance for cardiac radiotherapy treatments from planning to delivery, and developing the reporting of doses to targets and organs at risk in motion in the single fraction setting. It has created opportunities for further work in both cardiac and lung treatments and has developed understanding of the applicability of abdominal compression in this field.

As the field of STAR progresses and targets become more refined, motion of the cardiac wall will become more important. Techniques like the one presented in this thesis must be available to centres wishing to deliver STAR and should be included in trials to ensure the best quality targeting and dosimetric data possible. Doing so will enable treatments to be more precise, irradiating less tissue and maximising patients' chances of a successful treatment with minimal negative side effects.

References

[1] Tang, P. T., Shenasa, M., and Boyle, N. G. Ventricular arrhythmias and sudden cardiac death. *Cardiac electrophysiology clinics*, 9(4):693–708, 2017.

[2] British Heart Foundation. Heart & circulatory disease statistics 2020, 2020. Available at: https://www.bhf.org.uk/what-we-do/our-research/heart-statistics/heart-statistics-publications/cardiovascular-disease-statistics-2020 (Accessed: 17th November 2020).

[3] Gaztañaga, L., Marchlinski, F. E., and Betensky, B. P. Mechanisms of cardiac arrhythmias. *Revista Española de Cardiología (English Edition)*, 65(2):174–185, 2012.

[4] G, S., Blomström-Lundqvist, C., Mazzanti, A., Blom, N., Borggrefe, M., Camm, J., Elliott, P. M., Fitzsimons, D., Hatala, R., et al. 2015 esc guidelines for the management of patients with ventricular arrhythmias and the prevention of sudden cardiac death: The task force for the management of patients with ventricular arrhythmias and the prevention of sudden cardiac death of the european society of cardiology (ESC) endorsed by: Association for european paediatric and congenital cardiology (AEPC). *Ep Europace*, 17(11):1601–1687, 2015.

[5] Robinson, C. G., Samson, P. P., Moore, K. M., Hugo, G. D., Knutson, N., Mutic, S., Goddu, S. M., Lang, A., Cooper, D. H., Faddis, M., et al. Phase I/II trial of electrophysiology-guided noninvasive cardiac radioablation for ventricular tachycardia. *Circulation*, 139(3):313–321, 2019.

[6] Francis, J., Johnson, B., and Niehaus, M. Quality of life in patients with implantable cardioverter defibrillators. *Indian pacing and electrophysiology journal*, 6(3):173, 2006.

[7] Jumeau, R., Ozsahin, M., Schwitter, J., Vallet, V., Duclos, F., Zeverino, M., Moeckli, R., Pruvot, E., and Bourhis, J. Rescue procedure for an electrical storm using robotic non-invasive cardiac radio-ablation. *Radiotherapy and Oncology*, 128(2):189–191, 2018.

[8] Sapp, J. L., Wells, G. A., Parkash, R., Stevenson, W. G., Blier, L., Sarrazin, J.-F., Thibault, B., Rivard, L., Gula, L., Leong-Sit, P., et al. Ventricular tachycardia ablation versus escalation of antiarrhythmic drugs. *New England Journal of Medicine*, 375(2):111–121, 2016.

[9] Kim, E.-J., Davogustto, G., Stevenson, W. G., and John, R. M. Non-invasive cardiac radiation for ablation of ventricular tachycardia: a new therapeutic paradigm in electrophysiology. *Arrhythmia & electrophysiology review*, 7(1):8, 2018.

[10] Private communication. Bates, M (South Tees Hospitals NHS Foundation Trust) and Lee, G (Royal Melbourne Hospital), 2021.

[11] Martin, R., Hocini, M., Haïsaguerre, M., Jaïs, P., and Sacher, F. Ventricular tachycardia isthmus characteristics: insights from high-density mapping. *Arrhythmia & electrophysiology review*, 8(1):54, 2019.

[12] Loo, B. W., Soltys, S. G., Wang, L., Lo, A., Fahimian, B. P., Iagaru, A., Norton, L., Shan, X., Gardner, E., Fogarty, T., et al. Stereotactic ablative radiotherapy for the treatment of refractory cardiac ventricular arrhythmia. *Circulation: Arrhythmia and Electrophysiology*, 8(3):748–750, 2015.

[13] Cuculich, P. S., Schill, M. R., Kashani, R., Mutic, S., Lang, A., Cooper, D., Faddis, M., Gleva, M., Noheria, A., Smith, T. W., et al. Noninvasive cardiac radiation for ablation of ventricular tachycardia. *New England Journal of Medicine*, 377(24):2325–2336, 2017.

[14] Zei, P. C. and Soltys, S. Ablative radiotherapy as a noninvasive alternative to catheter ablation for cardiac arrhythmias. *Current cardiology reports*, 19(9):79, 2017.

[15] Nguyen-Ho, P., Kaluza, G. L., Zymek, P. T., and Raizner, A. E. Intracoronary brachytherapy. *Catheterization and cardiovascular interventions*, 56(2):281–288, 2002.

[16] Taylor, C. W., Nisbet, A., McGale, P., and Darby, S. C. Cardiac exposures in breast cancer radiotherapy: 1950s–1990s. *International Journal of Radiation Oncology* Biology* Physics*, 69(5):1484–1495, 2007.

[17] Lydiard, S., Hugo, G., O'Brien, R., Blanck, O., and Keall, P. A review of cardiac radioablation (cr) for arrhythmias: procedures, technology and future opportunities. *International Journal of Radiation Oncology* Biology* Physics*, 2020.

[18] Scholz, E. P., Seidensaal, K., Naumann, P., André, F., Katus, H. A., and Debus, J. Risen from the dead: Cardiac stereotactic ablative radiotherapy as last rescue in a patient with refractory ventricular fibrillation storm. *HeartRhythm case reports*, 5(6):329–332, 2019.

[19] Sharma, A., Wong, D., Weidlich, G., Fogarty, T., Jack, A., Sumanaweera, T., and Maguire, P. Noninvasive stereotactic radiosurgery (cyberheart) for creation of ablation lesions in the atrium. *Heart Rhythm*, 7(6):802–810, 2010.

[20] Blanck, O., Bode, F., Gebhard, M., Hunold, P., Brandt, S., Bruder, R., Grossherr, M., Vonthein, R., Rades, D., and Dunst, J. Dose-escalation study for cardiac radiosurgery in a porcine model. *International Journal of Radiation Oncology* Biology* Physics*, 89(3):590–598, 2014.

[21] Refaat, M. M., Ballout, J. A., Zakka, P., Hotait, M., Al Feghali, K. A., Gheida, I. A., Saade, C., Hourani, M., Geara, F., Tabbal, M., et al. Swine atrioventricular node ablation using stereotactic radiosurgery: Methods and in vivo feasibility investigation for catheter-free ablation of cardiac arrhythmias. *Journal of the American Heart Association*, 6(11):e007193, 2017.

[22] Zei, P., Soltys, S., Loo, B., Norton, L., Al-Ahmed, A., Gardner, E., and Maguire, P. First-in-man treatment of arrhythmia (ventricular tachycardia) using stereotactic radiosurgery. *Heart Rhythm*, 10:1–554, 2013.

[23] Cvek, J., Neuwirth, R., Knybel, L., Molenda, L., Otahal, B., Pindor, J., Murárová, M., Kodaj, M., Fiala, M., Branny, M., et al. Cardiac radiosurgery for malignant ventricular tachycardia. *Cureus*, 6(7):e190, 2014.

[24] Varian. Varian acquires cyberheart (company adds technology for cardiac radioablation to its radiation medicine portfolio), 2019. Available at: https://www.prnewswire.com/news-releases/varian-acquires-cyberheart-300847090.html (Accessed: 28th Feb 2020).

[25] Maguire, P., Cardonna, C., De La Pena, C., Hinojosa, M., Assad, J., Azpiri, J., Gardner, E., Wong, D., and Zei, P. First-in-man cardiac radiosurgery for atrial arrhythmia. *International Journal of Radiation Oncology• Biology• Physics*, 96 (2):E504–E505, 2016.

[26] Zei, P., Gardner, E., Fogarty, T., and Maguire, P. Noninvasive cardiac radiosurgery: current clinical experience for treatment of refractory arrhythmias. *EP Europace*, 19(Supplement 3):iii402–iii402, 2017.

[27] Blanck, O., Ipsen, S., Chan, M. K., Bauer, R., Kerl, M., Hunold, P., Jacobi, V., Bruder, R., Schweikard, A., Rades, D., et al. Treatment planning considerations for robotic guided cardiac radiosurgery for atrial fibrillation. *Cureus*, 8(7):e705, 2016.

[28] Krug, D., Blanck, O., Demming, T., Dottermusch, M., Koch, K., Hirt, M., Kotzott, L., Zaman, A., Eidinger, L., Siebert, F.-A., et al. Stereotactic body radiotherapy for ventricular tachycardia (cardiac radiosurgery). *Strahlentherapie und Onkologie*, 196(1):23–30, 2020.

[29] Buergy, D., Rudic, B., Tueluemen, E., Gauter-Fleckenstein, B., Borggrefe, M., and Wenz, F. Fallserie zur SBRT bei ventrikulärer tachykardie zeigt beeindruckenden therapieeffekt. *Strahlentherapie und Onkologie*, 194(5):462–464, 2018.

[30] Fernandez-Ruiz, I. Noninvasive radioablation for vt. *Nature Reviews Cardiology*, 15(3):133, 2018.

[31] Sharp, A. J., Mak, R., and Zei, P. C. Noninvasive cardiac radioablation for ventricular arrhythmias. *Current Cardiovascular Risk Reports*, 13(1):1, 2019.

[32] Kautzner, J., Calkins, H., and Steffel, J. The year in cardiology 2018: arrhythmias and cardiac devices. *European Heart Journal*, 40:803–808, 2019.

[33] Lydiard, S., Caillet, V., Ipsen, S., O'Brien, R., Blanck, O., Poulsen, P. R., Booth, J., and Keall, P. Investigating multi-leaf collimator tracking in stereotactic arrhythmic radioablation (star) treatments for atrial fibrillation. *Physics in Medicine & Biology*, 63(19):195008, 2018.

[34] Bhaskaran, A., Nayyar, S., Porta-Sánchez, A., Haldar, S., Bokhari, M., Massé, S., Liang, T., Zehra, N., Farid, T., Downar, E., et al. Exit sites on the epicardium rarely subtend critical diastolic path of ischemic vt on the endocardium: implications for noninvasive ablation. *Journal of cardiovascular electrophysiology*, 30 (4):520–527, 2019.

[35] Poon, J., Kohli, K., Deyell, M. W., Schellenberg, D., Reinsberg, S., Teke, T., and Thomas, S. Cardiac synchronized volumetric modulated arc therapy for stereotactic arrhythmia radioablation—proof of principle. *Medical physics*, 47 (8):3567–3572, 2020.

[36] Markman, T. M. and Nazarian, S. Treatment of ventricular arrhythmias: What's new? *Trends in cardiovascular medicine*, 29(5):249–261, 2019.

[37] Fajardo, L. and Stewart, J. Experimental radiation-induced heart disease. I. Light microscopic studies. *The American journal of pathology*, 59(2):299, 1970.

[38] Pilling, K., Wilkinson, M., Richmond, N., Walker, C., McQuillan, L., Brooks, R., Ogilvie, A., Shepherd, E., McStay, R., Greenhalgh, D., et al. Non-invasive cardiac radioablation for ventricular tachycardia. *Radiography*, 26:S7, 2020.

[39] Lee, J., Bates, M., Shepherd, E., Thornley, A., Kelland, N., Greenhalgh, D., Atherton, P., Peedell, C., and Hatton, M. P1115 Cardiac SABR for ventricular tachycardia-initial uk experience. *EP Europace*, 22(Supplement 1):162–236, 2020.

[40] Zeng, L.-J., Huang, L.-H., Tan, H., Zhang, H.-C., Mei, J., Shi, H.-F., Jiang, C.-Y., Tan, C., Zheng, J.-W., and Liu, X.-P. Stereotactic body radiation therapy for refractory ventricular tachycardia secondary to cardiac lipoma: A case report. *Pacing and Clinical Electrophysiology*, 42(9):1276–1279, 2019.

[41] CyberHeart. CyberHeart's Cardiac Arrhythmia Ablation Treatment: Patients With Refractory Ventricular Tachycardia, 2016. Available at: https://clinicaltrials.gov/ct2/show/NCT02661048 (Accessed: 25th March 2019).

[42] Cuculich, P. and Robinson, C. Phase I/II study of ep-guided noninvasive cardiac radioablation (ENCORE) for treatment of ventricular tachycardia protocol: 5.0 version date: 09/26/2018 principal investigators Phillip Cuculich, MD and Clifford Robinson, MD. 2018. Available at: https://www.clinicaltrials.gov/ProvidedDocs/18/NCT02919618/Prot_SAP_000.pdf (Accessed: 23rd Nov 2020).

[43] UCLA. Clinical trials: Cardiac SABR, 2018. Available at: https://www.uclahealth.org/radonc/cardiac-sabr (Accessed: 3rd Feb 2019).

[44] Blanck, O., Buergy, D., Vens, M., Eidinger, L., Zaman, A., Krug, D., Rudic, B., Boda-Heggemann, J., Giordano, F. A., Boldt, L.-H., et al. Radiosurgery for ventricular tachycardia: preclinical and clinical evidence and study design for a german multi-center multi-platform feasibility trial (RAVENTA). *Clinical Research in Cardiology*, 109(11):1319–1332, 2020.

[45] Robinson, C., Samson, P., Moore, K., Hugo, G., Knutson, N., Mutic, S., Goddu, S., Cooper, D., Faddis, M., Noheria, A., Smith, T., Woodard, P., Gropler, R., Hallahan, D., Rudy, Y., and Cuculich, P. Longer term results from a phase I/II study of EP-guided noninvasive cardiac radioablation for treatment of ventricular tachycardia (ENCORE-VT). *International Journal of Radiation Oncology• Biology• Physics*, 105(3):682, 2019.

[46] Cuculich, P. S. Heart rhythm society 2020: Longer term results from encore-vt study. 2020. Available at: https://www.youtube.com/watch?v=477icQI3WsE (Accessed: 23rd Nov 2020).

[47] Zei, P. C. and Mak, R. Noninvasive stereotactic radioablation for ventricular tachycardia: ENCORE-VT (EP-guided noninvasive cardiac radioablation): Is the sequel as good as the original? *Am Heart Assoc*, 139:322–324, 2019.

[48] Ipsen, S., Blanck, O., Oborn, B., Bode, F., Liney, G., Hunold, P., Rades, D., Schweikard, A., and Keall, P. Radiotherapy beyond cancer: Target localization in real-time MRI and treatment planning for cardiac radiosurgery. *Medical physics*, 41(12), 2014.

[49] Constantinescu, A., Lehmann, H. I., Packer, D. L., Bert, C., Durante, M., and Graeff, C. Treatment planning studies in patient data with scanned carbon ion beams for catheter-free ablation of atrial fibrillation. *Journal of cardiovascular electrophysiology*, 27(3):335–344, 2016.

[50] Hohmann, S., Deisher, A. J., Suzuki, A., Konishi, H., Rettmann, M. E., Merrell, K. W., Kruse, J. J., Newman, L. K., Parker, K. D., Monahan, K. H., et al. Left ventricular function after noninvasive cardiac ablation using proton beam therapy in a porcine model. *Heart rhythm*, 16(11):1710–1719, 2019.

[51] Weidlich, G. A., Hacker, F., Bellezza, D., Maguire, P., and Gardner, E. A. Ventricular tachycardia: a treatment comparison study of the cyberknife with conventional linear accelerators. *Cureus*, 10(10):e3445, 2018.

[52] Fahimian, B., Loo, B., Soltys, S., Zei, P., Lo, A., Maguire, P., Gardner, E., and Wang, L. First in-human stereotactic arrhythmia radioablation (star) of ventricular tachycardia: dynamic tracking delivery analysis and implications. *International Journal of Radiation Oncology• Biology• Physics*, 93(3):E466–E467, 2015.

[53] Jumeau, R., Ozsahin, M., Schwitter, J., Elicin, O., Reichlin, T., Roten, L., Andratschke, N., Mayinger, M., Saguner, A. M., Steffel, J., et al. Stereotactic radiotherapy for the management of refractory ventricular tachycardia: Promise and future directions. *Frontiers in cardiovascular medicine*, 7(108), 2020.

[54] Samson, P., Wan, L., Moore, K., Cuculich, P., and Robinson, C. Large ablation volume is associated with lower survival in patients treated with noninvasive cardiac radioablation. *Heart Rhythm*, 16(5, Supplement):S93 – S141, 2019. ISSN 1547-5271. Heart Rhythm 40th Scientific Sessions May 8-11, 2019, San Francisco.

[55] Cuculich, P. S., Zhang, J., Wang, Y., Desouza, K. A., Vijayakumar, R., Woodard, P. K., and Rudy, Y. The electrophysiological cardiac ventricular substrate in patients after myocardial infarction: noninvasive characterization with electrocardiographic imaging. *Journal of the American College of Cardiology*, 58(18): 1893–1902, 2011.

[56] Dubois, R., Shah, A. J., Hocini, M., Denis, A., Derval, N., Cochet, H., Sacher, F., Bear, L., Duchateau, J., Jais, P., et al. Non-invasive cardiac mapping in clinical practice: Application to the ablation of cardiac arrhythmias. *Journal of electrocardiology*, 48(6):966–974, 2015.

[57] Cluitmans, M. J. M., Peeters, R., Westra, R., and Volders, P. Noninvasive reconstruction of cardiac electrical activity: update on current methods, applications and challenges. *Netherlands Heart Journal*, 23(6):301–311, 2015.

[58] Milanič, M., Jazbinšek, V., MacLeod, R. S., Brooks, D. H., et al. Assessment of regularization techniques for electrocardiographic imaging. *Journal of electrocardiology*, 47(1):20–28, 2014.

[59] Wang, Y., Cuculich, P. S., Zhang, J., Desouza, K. A., Vijayakumar, R., Chen, J., Faddis, M. N., Lindsay, B. D., Smith, T. W., and Rudy, Y. Noninvasive electroanatomic mapping of human ventricular arrhythmias with electrocardiographic imaging. *Science translational medicine*, 3(98):98ra84–98ra84, 2011.

[60] Jamil-Copley, S., Bokan, R., Kojodjojo, P., Qureshi, N., Koa-Wing, M., Hayat, S., Kyriacou, A., Sandler, B., Sohaib, A., Wright, I., et al. Noninvasive electrocardiographic mapping to guide ablation of outflow tract ventricular arrhythmias. *Heart Rhythm*, 11(4):587–594, 2014.

[61] Zhang, J., Cooper, D. H., Desouza, K. A., Cuculich, P. S., Woodard, P. K., Smith, T. W., and Rudy, Y. Electrophysiologic scar substrate in relation to vt: Noninvasive high-resolution mapping and risk assessment with ecgi. *Pacing and Clinical Electrophysiology*, 39(8):781–791, 2016.

[62] Zhou, S., Sapp, J. L., AbdelWahab, A., Šťovíček, P., and Horáček, B. M. Localization of ventricular activation origin using patient-specific geometry: Preliminary results. *Journal of Cardiovascular Electrophysiology*, 29(7):979–986, 2018.

[63] Carbucicchio, C., Jereczek-Fossa, B., Andreini, D., Catto, V., Piperno, G., Conte, E., Cattani, F., Rondi, E., Vigorito, S., Piccolo, C., et al. Stra-mi-vt (stereotactic radioablation by multimodal imaging for ventricular tachycardia): rationale and design of an italian experimental prospective study. *Journal of Interventional Cardiac Electrophysiology*, pages 1–11, 2020.

[64] Wang, L., Fahimian, B., Soltys, S. G., Zei, P., Lo, A., Gardner, E. A., Maguire, P. J., and Loo, B. W. Stereotactic arrhythmia radioablation (STAR) of ventricular tachycardia: A treatment planning study. *Cureus*, 8(7):e694, 2016.

[65] Grimm, J., LaCouture, T., Croce, R., Yeo, I., Zhu, Y., and Xue, J. Dose tolerance limits and dose volume histogram evaluation for stereotactic body radiotherapy. *Journal of applied clinical medical physics*, 12(2):267–292, 2011.

[66] Abelson, J., Murphy, J., Loo, B., Chang, D., Daly, M. E., Wiegner, E., Hancock, S., Chang, S., Le, Q.-T., Soltys, S., et al. Esophageal tolerance to high-dose stereotactic ablative radiotherapy. *Diseases of the Esophagus*, 25(7):623–629, 2012.

[67] Xia, P., Kotecha, R., Sharma, N., Andrews, M., Stephans, K. L., Oberti, C., Lin, S., Wazni, O., Tchou, P., Saliba, W. I., et al. A treatment planning study of stereotactic body radiotherapy for atrial fibrillation. *Cureus*, 8(7):e678, 2016.

[68] Videtic, G. M., Hu, C., Singh, A. K., Chang, J. Y., Parker, W., Olivier, K. R., Schild, S. E., Komaki, R., Urbanic, J. J., and Choy, H. NRG Oncology RTOG 0915 (NCCTG N0927): a randomized phase II study comparing 2 stereotactic body radiation therapy (SBRT) schedules for medically inoperable patients with stage I peripheral non-small cell lung cancer. *International journal of radiation oncology, biology, physics*, 93(4):757, 2015.

[69] van Nimwegen, F. A., Schaapveld, M., Cutter, D. J., Janus, C., Krol, A., Hauptmann, M., Kooijman, K., Roesink, J., van der Maazen, R., Darby, S. C., et al. Radiation dose-response relationship for risk of coronary heart disease in survivors of hodgkin lymphoma. *Journal of Clinical Oncology*, 34(3):235–246, 2015.

[70] Darby, S. C., Ewertz, M., McGale, P., Bennet, A. M., Blom-Goldman, U., Brønnum, D., Correa, C., Cutter, D., Gagliardi, G., Gigante, B., et al. Risk of ischemic heart disease in women after radiotherapy for breast cancer. *New England Journal of Medicine*, 368(11):987–998, 2013.

[71] Landberg, T., Chavaudra, J., Dobbs, J., Gerard, J. P., Hanks, G., Horiot, J. C., Johansson, K. A., Möller, T., Purdy, J., Suntharalingam, N., and Svensson, H. Report 62. *Journal of the International Commission on Radiation Units and Measurements*, os32(1):NP–NP, 04 1999.

[72] Van Herk, M., Remeijer, P., Rasch, C., and Lebesque, J. V. The probability of correct target dosage: dose-population histograms for deriving treatment margins in radiotherapy. *International Journal of Radiation Oncology* Biology* Physics*, 47(4):1121–1135, 2000.

[73] Stöhr, E. J., Shave, R. E., Baggish, A. L., and Weiner, R. B. Left ventricular twist mechanics in the context of normal physiology and cardiovascular disease: a review of studies using speckle tracking echocardiography. *American Journal of Physiology-Heart and Circulatory Physiology*, 311(3):H633–H644, 2016.

[74] Hamilton, W. and Rompf, J. Movements of the base of the ventricle and the relative constancy of the cardiac volume. *American Journal of Physiology-Legacy Content*, 102(3):559–565, 1932.

[75] Slager, C. J., Hooghoudt, T. E., Serruys, P. W., Schuurbiers, J. C., Reiber, J. H., Meester, G. T., Verdouw, P. D., and Hugenholtz, P. G. Quantitative assessment of regional left ventricular motion using endocardial landmarks. *Journal of the American College of Cardiology*, 7(2):317–326, 1986.

[76] Rogers Jr, W. J., Shapiro, E. P., Weiss, J. L., Buchalter, M. B., Rademakers, F. E., Weisfeldt, M. L., and Zerhouni, E. A. Quantification of and correction for left ventricular systolic long-axis shortening by magnetic resonance tissue tagging and slice isolation. *Circulation*, 84(2):721–731, 1991.

[77] Höglund, C., Alam, M., and Thorstrand, C. Effects of acute myocardial infarction on the displacement of the atrioventricular plane: an echocardiographic study. *Journal of internal medicine*, 226(4):251–256, 1989.

[78] Poon, J. *Cardiac synchronized volumetric modulated arc therapy.* PhD thesis, University of British Columbia, 2018.

[79] Saito, M., Sano, N., Ueda, K., Shibata, Y., Kuriyama, K., Komiyama, T., Marino, K., Aoki, S., and Onishi, H. Evaluation of the latency and the beam characteristics of a respiratory gating system using an elekta linear accelerator and a respiratory indicator device, abches. *Medical physics*, 45(1):74–80, 2018.

[80] Reynolds, T., Shieh, C.-C., Keall, P. J., and O'Brien, R. T. Dual cardiac and respiratory gated thoracic imaging via adaptive gantry velocity and projection rate modulation on a linear accelerator: A proof-of-concept simulation study. *Medical Physics*, 46(9):4116–4126, 2019.

[81] Edmunds, D., Sharp, G., and Winey, B. Automatic diaphragm segmentation for real-time lung tumor tracking on cone-beam ct projections: a convolutional neural network approach. *Biomedical Physics & Engineering Express*, 5(3):035005, 2019.

[82] Wei, J. and Chao, M. A constrained linear regression optimization algorithm for diaphragm motion tracking with cone beam ct projections. *Physica Medica*, 46: 7–15, 2018.

[83] Hindley, N., Keall, P., Booth, J., and Shieh, C.-C. Real-time direct diaphragm tracking using kV imaging on a standard linear accelerator. *Medical physics*, 46 (10):4481–4489, 2019.

[84] Bertholet, J., Knopf, A., Eiben, B., McClelland, J., Grimwood, A., Harris, E., Menten, M., Poulsen, P., Nguyen, D. T., Keall, P., et al. Real-time intrafraction motion monitoring in external beam radiotherapy. *Physics in Medicine & Biology*, 64(15):15TR01, 2019.

[85] Case, R. B., Sonke, J.-J., Moseley, D. J., Kim, J., Brock, K. K., and Dawson, L. A. Inter-and intrafraction variability in liver position in non–breath-hold stereotactic body radiotherapy. *International Journal of Radiation Oncology* Biology* Physics*, 75(1):302–308, 2009.

[86] Adamson, J. and Wu, Q. Prostate intrafraction motion evaluation using kV fluoroscopy during treatment delivery: a feasibility and accuracy study. *Medical physics*, 35(5):1793–1806, 2008.

[87] Balter, J., Wright, N., Dimmer, S., Friemel, B., Newell, J., Cheng, Y., and Mate, T. Demonstration of accurate localization and continuous tracking of implantable wireless electromagnetic transponders. *International Journal of Radiation Oncology* Biology* Physics*, 57(2):S264–S265, 2003.

[88] Richardson, A. and Jacobs, P. Intrafraction monitoring of prostate motion during radiotherapy using the Clarity® autoscan transperineal ultrasound (TPUS) system. *Radiography*, 23(4):310–313, 2017.

[89] Kim, J., Nguyen, D., Huang, C., Fuangrod, T., Caillet, V., O'Brien, R., Poulsen, P., Booth, J., and Keall, P. Quantifying the accuracy and precision of a novel real-time 6 degree-of-freedom kilovoltage intrafraction monitoring (KIM) target tracking system. *Physics in Medicine & Biology*, 62(14):5744, 2017.

[90] Campbell, W. G., Miften, M., and Jones, B. L. Automated target tracking in kilovoltage images using dynamic templates of fiducial marker clusters. *Medical physics*, 44(2):364–374, 2017.

[91] Regmi, R., Lovelock, D. M., Hunt, M., Zhang, P., Pham, H., Xiong, J., Yorke, E. D., Goodman, K. A., Rimner, A., Mostafavi, H., et al. Automatic tracking of arbitrarily shaped implanted markers in kilovoltage projection images: a feasibility study. *Medical Physics*, 41(7):071906, 2014.

[92] Guckenberger, M., Richter, A., Boda-Heggemann, J., and Lohr, F. Motion compensation in radiotherapy. *Critical Reviews™ in Biomedical Engineering*, 40(3): 187–197, 2012.

[93] Yoganathan, S., Das, K. M., Agarwal, A., and Kumar, S. Magnitude, impact, and management of respiration-induced target motion in radiotherapy treatment: a comprehensive review. *Journal of medical physics*, 42(3):101, 2017.

[94] Goldsworthy, S., Palmer, S., Latour, J., McNair, H., and Cramp, M. A systematic review of effectiveness of interventions applicable to radiotherapy that are administered to improve patient comfort, increase patient compliance, and reduce patient distress or anxiety. *Radiography*, 26:314–324, 2020.

[95] Roujol, S., Anter, E., Josephson, M. E., and Nezafat, R. Characterization of respiratory and cardiac motion from electro-anatomical mapping data for improved fusion of mri to left ventricular electrograms. *PloS one*, 8(11):e78852, 2013.

[96] Zijp, L., Sonke, J.-J., and van Herk, M. Extraction of the respiratory signal from sequential thorax cone-beam x-ray images. In *International conference on the use of computers in radiation therapy*, pages 507–509, 2004.

[97] Rit, S., van Herk, M., Zijp, L., and Sonke, J.-J. Quantification of the variability of diaphragm motion and implications for treatment margin construction. *International Journal of Radiation Oncology* Biology* Physics*, 82(3):e399–e407, 2012.

[98] Swerdlow, C. D., Asirvatham, S. J., Ellenbogen, K. A., and Friedman, P. A. Troubleshooting implanted cardioverter defibrillator sensing problems i. *Circulation: Arrhythmia and Electrophysiology*, 7(6):1237–1261, 2014.

[99] Thompson, D. and Burke, K. A plan-corrected alternative to couch translations in cranial stereotactic radiosurgery, 2015. Available at:

https://www.eposters.net/poster/a-plan-corrected-alternative-to-couch-translations-in-cranial-stereotactic-radiosurgery# (Accessed: 13th Dec 2020).

[100] Holsti, L. R. Development of clinical radiotherapy since 1896. *Acta Oncologica*, 34(8):995–1003, 1995.

[101] Sze, W., Shelley, M., Held, I., Wilt, T., and Mason, M. Palliation of metastatic bone pain: single fraction versus multifraction radiotherapy–a systematic review of randomised trials. *Clinical Oncology*, 15(6):345–352, 2003.

[102] Jin, R., Rock, J., Jin, J.-Y., Janakiraman, N., Kim, J. H., Movsas, B., and Ryu, S. Single fraction spine radiosurgery for myeloma epidural spinal cord compression. *Journal of experimental therapeutics & oncology*, 8(1):35–41, 2009.

[103] Leksell, L. The stereotaxic method and radiosurgery of the brain. *Acta Chirurgica Scandinavica*, 102(4):316–319, 1951.

[104] Schefter, T. E., Kavanagh, B. D., Timmerman, R. D., Cardenes, H. R., Baron, A., and Gaspar, L. E. A phase i trial of stereotactic body radiation therapy (sbrt) for liver metastases. *International Journal of Radiation Oncology* Biology* Physics*, 62(5):1371–1378, 2005.

[105] Hara, R., Itami, J., Kondo, T., Aruga, T., Uno, T., Sasano, N., Ohnishi, K., Kiyozuka, M., Fuse, M., Ito, M., et al. Clinical outcomes of single-fraction stereotactic radiation therapy of lung tumors. *Cancer: Interdisciplinary International Journal of the American Cancer Society*, 106(6):1347–1352, 2006.

[106] Heinzerling, J. H., Anderson, J. F., Papiez, L., Boike, T., Chien, S., Zhang, G., Abdulrahman, R., and Timmerman, R. Four-dimensional computed tomography scan analysis of tumor and organ motion at varying levels of abdominal compression during stereotactic treatment of lung and liver. *International Journal of Radiation Oncology* Biology* Physics*, 70(5):1571–1578, 2008.

[107] Bhaskaran, A., Downar, E., Chauhan, V. S., Lindsay, P., Nair, K., Ha, A., Hope, A., and Nanthakumar, K. Electroanatomical mapping–guided stereotactic radiotherapy for right ventricular tachycardia storm. *HeartRhythm Case Reports*, 5(12):590–592, 2019.

[108] Milano, M. T., Grimm, J., Soltys, S. G., Yorke, E., Moiseenko, V., Tomé, W. A., Sahgal, A., Xue, J., Ma, L., Solberg, T. D., et al. Single-and multi-fraction stereotactic radiosurgery dose tolerances of the optic pathways. *International Journal of Radiation Oncology* Biology* Physics*, 110(1):87—99, 2018.

[109] Palmer, J., Yang, J., Pan, T., and Court, L. E. Motion of the esophagus due to cardiac motion. *PloS one*, 9(2):e89126, 2014.

[110] Kibrom, A. Z. and Knight, K. A. Adaptive radiation therapy for bladder cancer: a review of adaptive techniques used in clinical practice. *Journal of medical radiation sciences*, 62(4):277–285, 2015.

[111] Bergom, C., Currey, A., Desai, N., Tai, A., and Strauss, J. B. Deep inspiration breath hold: techniques and advantages for cardiac sparing during breast cancer irradiation. *Frontiers in oncology*, 8:87, 2018.

[112] Chao, M., Wei, J., Li, T., Yuan, Y., Rosenzweig, K. E., and Lo, Y.-C. Robust breathing signal extraction from cone beam ct projections based on adaptive and global optimization techniques. *Physics in Medicine & Biology*, 61(8):3109, 2016.

[113] van Sörnsen de Koste, J. R., Dahele, M., Mostafavi, H., Sloutsky, A., Senan, S., Slotman, B. J., and Verbakel, W. F. Markerless tracking of small lung tumors for stereotactic radiotherapy. *Medical physics*, 42(4):1640–1652, 2015.

[114] Wiersma, R., Mao, W., and Xing, L. Combined kv and mv imaging for real-time tracking of implanted fiducial markers a. *Medical physics*, 35(4):1191–1198, 2008.

[115] Gehrke, C., Oates, R., Ramachandran, P., Deloar, H. M., Gill, S., and Kron, T. Automatic tracking of gold seed markers from cbct image projections in lung and prostate radiotherapy. *Physica Medica*, 31(2):185–191, 2015. ISSN 1120-1797. doi: https://doi.org/10.1016/j.ejmp.2015.01.002. URL https://www.sciencedirect.com/science/article/pii/S1120179715000046.

Appendices

A Code written by the author

This appendix includes a brief overview of the majority of the bespoke code written for the work in this thesis. Modules are presented with inputs, functionality and outputs. Number of lines of code are included to indicate the amount of processing performed by each module.

Estimated total lines of code in this "core" version of the data processing toolkit = **780**

A top level function (**fullProcess**) which calls the other modules in turn is first described

fullProcess module (~100 lines of code)

- Module runs by calling other functions taking inputs from the user in the console and outputting data to the screen and to file
- Inputs
    - File location for HIS files from XVI system
    - Tip and diaphragm coordinates as observed in CBCT reconstructions
- Functions
    - Calls the following modules in turn:
        - **Positions**
        - **DetectObjects**
        - *[Processes returned data traces geometrically]*
        - **Iterate**
- Outputs
    - Data traces produced in this process are stored in memory and further manipulated by either the user or the **Analyse** module

Modules listed below not included in the **fullProcess** module are called by other modules when needed

Modules

- ***hisFileTools*** (~80 lines of code)
    - Inputs – image filename
    - Functions –
        - Reads header and image data from XVI files (.HIS)
        - Processes image to create 2 output images
    - Outputs
        - Lead tip detection
        - Diaphragm detection
- ***xmlParse*** (~30 lines of code)
    - Inputs – name of xml file in XVI data store
    - Functions – parses the xml and creates an array containing the salient data for each frame: timestamp, gantry angle, flexmap data
    - Outputs – data array
- ***Positions*** (~100 lines of code)
    - Inputs – coordinates (x, y, z) and gantry angles for each image
    - Functions – applies geometric methods to create expected positions on the panel (k, z’ coordinates) from the original input coordinates
    - Outputs
        - List of k-coordinates at each gantry angle
        - List of z’-coordinates at each gantry angle
        - List of pixel to distance conversion factors

- ***DetectObjects*** (~250 lines of code)
    - Inputs – filenames for each frame, lists of k and z' coordinates
    - Functions –
        - Lead tip detection
            - *Starts at either the previous tip position in the image or the expected geometrical position*
            - *Searches for nearest similar pixel values to the previous tip value*
            - *Takes profiles around the most likely tip position*
            - *Categorises profiles and identifies the most likely position of the lead tip*
            - *Returns the position of the identified lead tip*
        - Diaphragm detection
            - *Starts at the geometric expectation of k position*
            - *Collapses a surrounding region to a column of data points along z'*
            - *Finds the position between maximum and minimum in this data column*
            - *"Sanity" checks the results by comparing to previous location and restricting amount of travel in a single frame*
    - Outputs –
        - Array of tip positions per gantry angle
        - Array of diaphragm levels per gantry angle
- ***Iterate*** *(~70 lines of code)*
    - Inputs –
        - Array of tip positions per gantry angle
        - Geometrically corrected array of tip positions per gantry angle
        - Range of positions in which to search
    - Functions –
        - *Use Fourier analysis to remove all frequencies above 1 cpm from the geometrically corrected trace [create baseline]*
        - *For each position in the search range, assume CoD at this location, geometrically process tip position array at this location and compare against baseline*
        - *Find the global minima of this process and repeat with a range one fifth the size*
    - Outputs –
        - Global minima positions in X and Y
- ***Analyse*** *(~150 lines of code)*
    - Inputs –
        - Geometrically processed data traces for tip and / or diaphragm
    - Functions –
        - Multiple use code
        - Fourier analysis using NUMPY package returns frequency spectra
        - Peak and trough searches using FINDPEAKS function from SCIPY
    - Outputs –
        - Produces graphs and numerical outputs to screen

B DClinSci modules

This thesis forms part of the work completed to gain the qualification of DClinSci. Taught modules have also contributed credits to this qualification and are listed on the following page.

DClinSci Appendix – List of AMBS A units and Medical Physics B units together with assignments

AMBS – A Units		
Unit title	**Credits**	**Assignment wordcount**
A1: Professionalism and professional development in the healthcare environment	30	Practice paper – 2000 words A1 – assignment 1 – 1500 words A1 – assignment 2 – 4000 words
A2: Theoretical foundations of leadership	20	A2 – assignment 1 – 3000 words A2 – assignment 2 – 3000 words
A3: Personal and professional development to enhance performance	30	A3 – assignment 1 – 1500 words A3 – assignment 2 – 4000 words
A4: Leadership and quality improvement in the clinical and scientific environment	20	A4 – assignment 1 – 3000 words A4 – assignment 2 – 3000 words
A5: Research and innovation in health and social care	20	A5 – assignment 1 – 3000 words A5 – assignment 2 – 3000 words
Medical Physics – B Units		
B1: Medical Equipment Management	10	2000 word assignment
B2: Clinical and Scientific Computing	10	2000 word assignment
B3: Dosimetry	10	Group presentation 1500 word assignment
B4: Optimisation in Radiotherapy and Imaging	10	Group presentation 1500 word assignment
B6: Medical statistics in medical physics	10	3000 word assignment
B8: Health technology assessment	10	3000 word assignment
B9: Clinical applications of medical imaging technologies in radiotherapy physics	20	Group presentation 2000 word assignment
B10a: Advanced Radiobiology	10	Virtual experiment + 1500 word report
B10c: Novel and specialised external beam radiotherapy	10	1500 word report/piece of evidence for portfolio
B10d: Advanced Brachytherapy	10	1500 word report/piece of evidence for portfolio
Generic B Units		
B5: Contemporary issues in healthcare science	20	1500 word assignment + creative project
B7: Teaching Learning Assessment	20	20 minute group presentation
Section C		
C1: Innovation Project	70	4000-5000 word Literature Review Lay Presentation